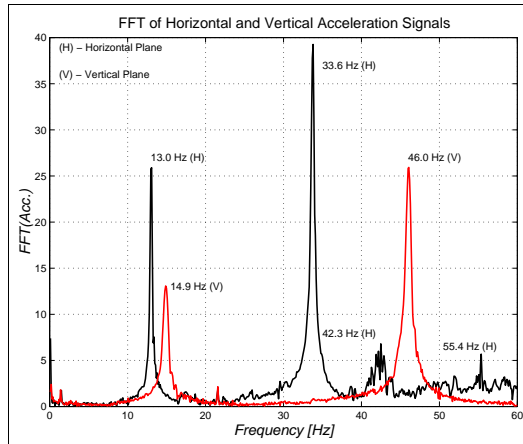
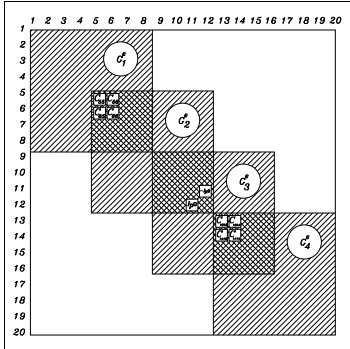
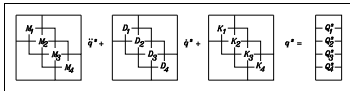
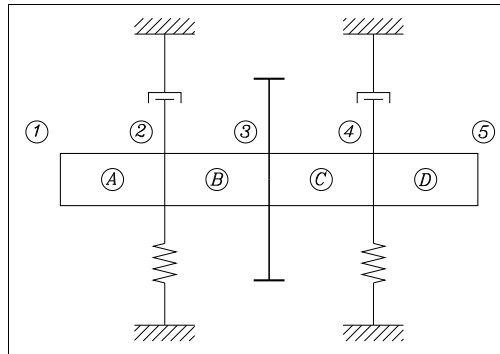
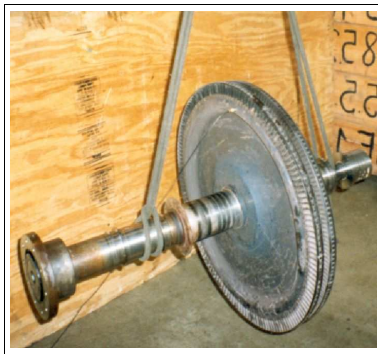


# VIBRATIONS IN ROTATING MACHINERY

## MODELLING, ANALYSIS, EXPERIMENTAL TESTS, VIBRATION MONITORING & DIAGNOSIS



Dr.-Ing. Ilmar Ferreira Santos, Associate Professor  
 Department of Mechanical Engineering  
 Technical University of Denmark  
 Building 358, Room 159  
 2800 Lyngby  
 Denmark  
 Phone: +45 45 25 62 69  
 Fax: +45 45 88 14 51  
 E-Mail: ifs@mek.dtu.dk

# Contents

<b>1</b>	<b>Dynamics of Rotating Machines - Finite Element Modelling, Simulation, Analysis and Experiments</b>	<b>4</b>
1.1	Introduction . . . . .	4
1.2	Mechanical Models of Rotating Machines . . . . .	4
1.3	Mathematical Model of Rotating Machine Elements – Kinematics . . . . .	5
1.3.1	Inertial and Moving Referential Frames and Transformation Matrices . . . . .	5
1.3.2	Absolute Angular Velocity . . . . .	6
1.4	Mathematical Model of the Rotating Machine Elements – Equations of Motion . . . . .	7
1.4.1	Rigid Discs – Gears, Impellers, etc. . . . .	7
1.4.2	Flexible Shaft Element . . . . .	9
1.4.3	Bearings . . . . .	16
1.4.4	Excitation Forces – Unbalance Mass on the Rigid Disc . . . . .	18
1.4.5	Excitation Forces – Distributed Unbalance along the Shaft Length . . . . .	19
1.5	Global Model and Equation of Motion . . . . .	20
1.6	Example of Rotor-Bearing System Modelling . . . . .	22
1.6.1	Rotor-Bearing Modelling using a MatLab Program . . . . .	23
1.6.2	Natural Frequencies and Mode Shapes - MatLab Program Results . . . . .	30
1.6.3	Validation of Rotor-Bearing System Modelling using Theoretical and Experimental Natural Frequencies . . . . .	37
1.6.4	Validation of Rotor-Bearing System Modelling – Experimental Transient Analysis . . . . .	38
1.6.5	Validation of Rotor-Bearing System Modelling – Theoretical Transient Analysis and MatLab Program . . . . .	42
1.6.6	Validation of Rotor-Bearing System Modelling – Theoretical Transient Analysis and MatLab Program Results in Time and Frequency Domains . . . . .	49
1.6.7	Campbell Diagram – MatLab Program and Theoretical Results . . . . .	50
1.7	Basic Phenomenology of Rotor-Bearing Systems . . . . .	57
1.7.1	Steady-State Response due to Unbalance Excitation - Forward and Backward Orbits . . . . .	57
1.7.2	Cross-Coupling Stiffness and Rotor-Bearing Stability Analysis . . . . .	58
1.8	Stability Analysis of Rotor-Journal Bearing Systems . . . . .	61
1.9	Further Bibliography related to Journal Bearing Properties – Research and Development . . . . .	71
1.9.1	On the Adjusting of the Dynamic Coefficients of Tilting-Pad Journal Bearings . . . . .	71
1.9.2	Tilting-Pad Journal Bearings with Electronic Radial Oil Injection . . . . .	72
1.10	Exercises using MatLab Program . . . . .	73
1.11	Project 3 – Rotor-Journal Bearing Stability - Lateral Dynamics . . . . .	78
<b>2</b>	<b>Diagnosis of Rotating Machinery Malfunctions &amp; Condition Monitoring</b>	<b>82</b>
2.1	Introduction . . . . .	82
2.2	Measurement Procedures and Locations . . . . .	82
2.3	Diagnostic Techniques . . . . .	82
2.3.1	Time-Domain or Waveform Analysis . . . . .	82
2.3.2	Orbital Analysis . . . . .	83
2.3.3	Spectrum Analysis . . . . .	84
2.3.4	Cepstrum Analysis . . . . .	85
2.4	Theoretical and Experimental Example . . . . .	85

2.4.1	Description of the Test Facilities . . . . .	85
2.4.2	Mechanical Model of the Rotor Test Rig . . . . .	86
2.4.3	Theoretical Natural Frequencies and Mode Shapes . . . . .	87
2.4.4	Experimental Natural Frequencies of the Rotating Components . . . . .	88
2.4.5	Measuring the Damping Factor ( $\xi$ ) and the Log Dec ( $\beta$ ) of the Rotor Kit. . . . .	88
2.4.6	Experimental Natural Frequencies taking into account the Foundation . . . . .	89
2.4.7	Experimental Forward and Backward Orbits . . . . .	90
2.4.8	Detecting Experimentally Super-Harmonic Vibrations . . . . .	92
2.5	Identification of Malfunctions . . . . .	92
2.6	Condition Monitoring – Steam Turbines <sup>1</sup> . . . . .	94
2.7	Research & Development – Bearings with Electronic Oil Injection . . . . .	96

# 1 Dynamics of Rotating Machines - Finite Element Modelling, Simulation, Analysis and Experiments

## 1.1 Introduction

The aim of this chapter is to introduce the basic phenomenology related to vibration and stability in rotating machines. The Finite Element Method is presented in order to achieve mathematical models for representing rotor-bearing lateral vibration. The dynamics of rigid and flexible rotating machines is illustrated. Comparison between theoretical and experimental results, obtained with help of small test rigs, elucidate the most important topics related to rotor dynamics.

## 1.2 Mechanical Models of Rotating Machines

The basic components of a rotating machines can be seen in figure 1 and listed above:

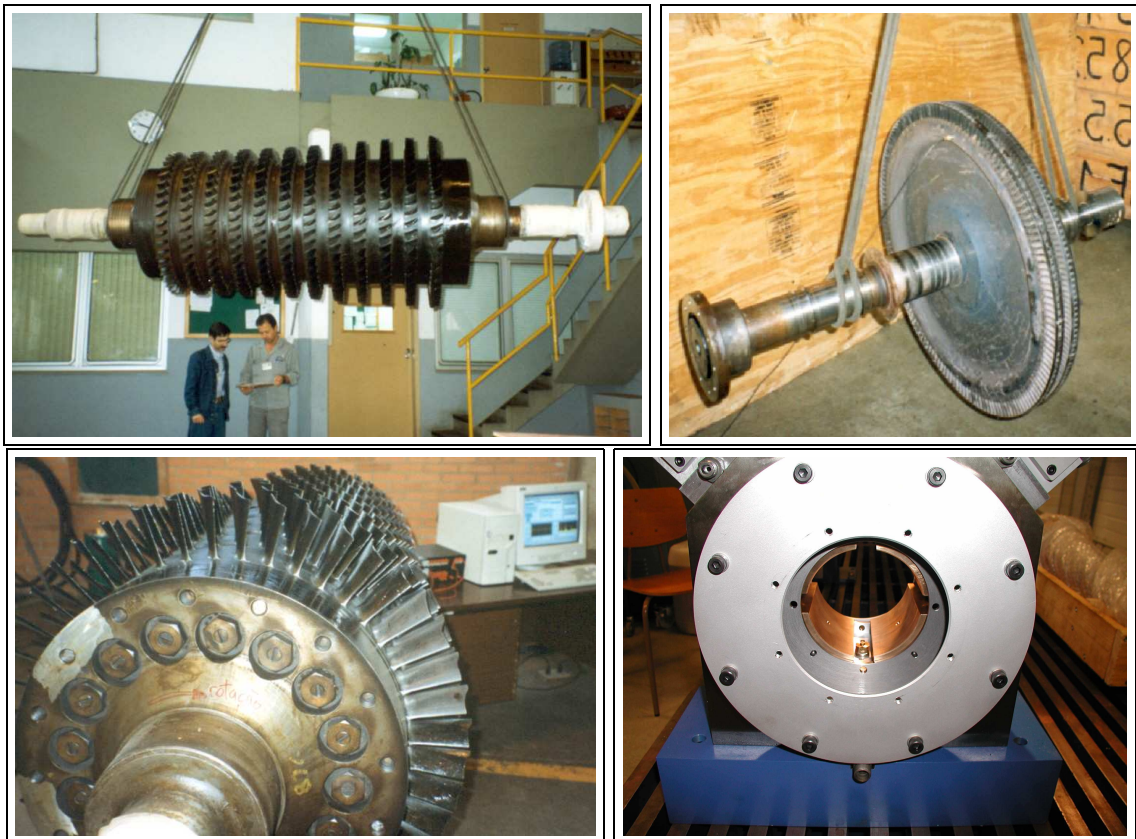


Figure 1: *Basic components of a rotating machine – Discs, shaft, blades, bearing.*

- Rigid Discs
- Shaft

- Bearings
- Blades

In the manuscript emphasis will be given to rigid discs, flexible shafts and journal bearings as you can see in figure 2.

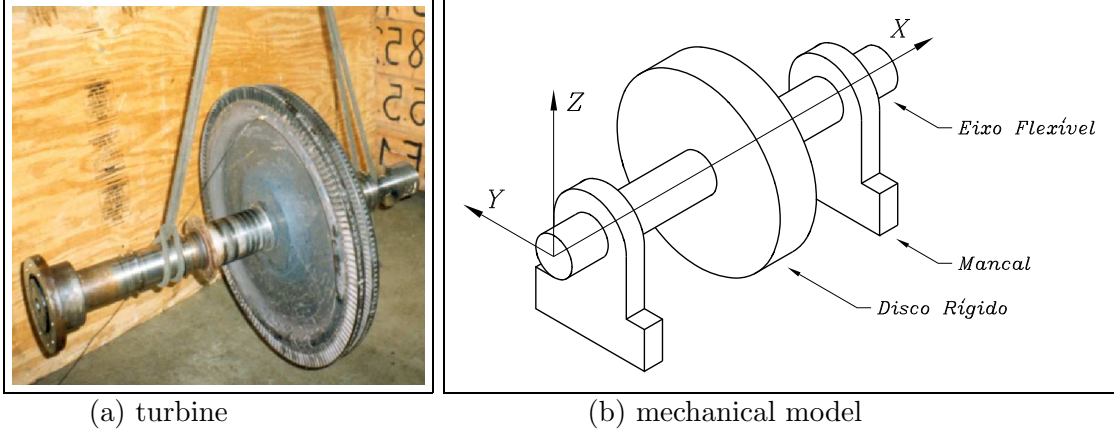


Figure 2: *Basic components of a rotating machine – rigid disc, flexible shaft, bearing; (a) steam turbine and (b) mechanical model composed of flexible shaft and rigid disc.*

### 1.3 Mathematical Model of Rotating Machine Elements – Kinematics

#### 1.3.1 Inertial and Moving Referential Frames and Transformation Matrices

After three consecutive rotations it is possible to define three moving reference frames and three transformation matrices, which allows to transform the representation of the vectors (velocity, acceleration, force, moment etc.) from one frame to another without troubles. The three consecutive rotations are illustrated in figures 3, 4 and 5.

- Transformation matrix  $\mathbf{T}_\Gamma$  (from the inertial frame  $I$  to the moving frame  $B_1$ ):

$$\begin{Bmatrix} \vec{i}_1 \\ \vec{j}_1 \\ \vec{k}_1 \end{Bmatrix} = \mathbf{T}_\Gamma \begin{Bmatrix} \vec{i} \\ \vec{j} \\ \vec{k} \end{Bmatrix} \quad \text{where} \quad \mathbf{T}_\Gamma = \begin{bmatrix} \cos \Gamma & \sin \Gamma & 0 \\ -\sin \Gamma & \cos \Gamma & 0 \\ 0 & 0 & 1 \end{bmatrix}$$

- Transformation matrix  $\mathbf{T}_\beta$  (from the moving frame  $B_1$  to the moving frame  $B_2$ ):

$$\begin{Bmatrix} \vec{i}_2 \\ \vec{j}_2 \\ \vec{k}_2 \end{Bmatrix} = \mathbf{T}_\beta \begin{Bmatrix} \vec{i}_1 \\ \vec{j}_1 \\ \vec{k}_1 \end{Bmatrix} \quad \text{where} \quad \mathbf{T}_\beta = \begin{bmatrix} \cos \beta & 0 & -\sin \beta \\ 0 & 1 & 0 \\ \sin \beta & 0 & \cos \beta \end{bmatrix}$$

- Transformation matrix  $\mathbf{T}_\phi$  (from the moving frame  $B_2$  to the moving frame  $B_3$ ):

$$\begin{Bmatrix} \vec{i}_3 \\ \vec{j}_3 \\ \vec{k}_3 \end{Bmatrix} = \mathbf{T}_\phi \begin{Bmatrix} \vec{i}_2 \\ \vec{j}_2 \\ \vec{k}_2 \end{Bmatrix} \quad \text{where} \quad \mathbf{T}_\phi = \begin{bmatrix} 1 & 0 & 0 \\ 0 & \cos \phi & \sin \phi \\ 0 & -\sin \phi & \cos \phi \end{bmatrix}$$

where  $I$  is the inertial reference frame,  $B_1$  is the moving reference frame  $(\vec{i}_1, \vec{j}_1, \vec{k}_1)$  obtained after the first rotation around  $Z$ .  $B_2$  is the second moving reference frame  $(\vec{i}_2, \vec{j}_2, \vec{k}_2)$  obtained after the second rotation around  $Y_1$ .  $B_3$  is the third moving reference frame  $(\vec{i}_3, \vec{j}_3, \vec{k}_3)$  obtained after the third rotation around  $X_2$ .

### 1.3.2 Absolute Angular Velocity

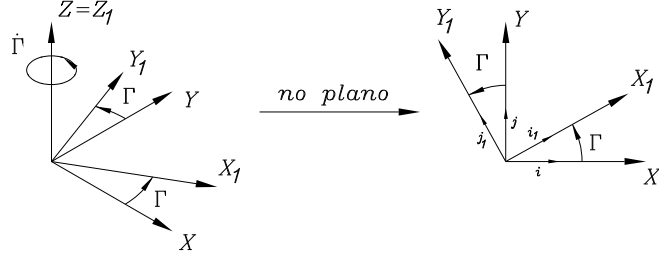


Figure 3: Rotation  $\Gamma$  around  $Z$  axis of the inertial frame  $I$ .

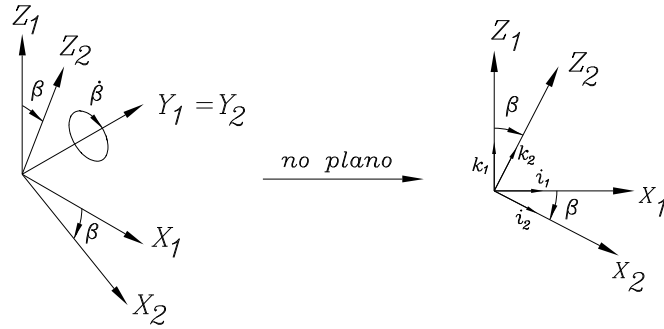


Figure 4: Rotation  $\beta$  around  $Y_1$  axis of the moving frame  $B_1$ .

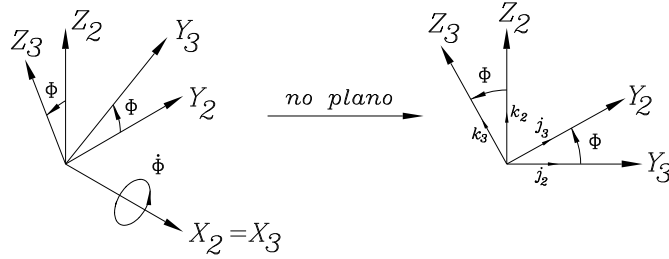


Figure 5: Rotation  $\phi$  around  $X_2$  of the moving reference frame  $B_2$ .

- Relative angular velocities of the reference frames:

$${}_I\dot{\Gamma} = \begin{Bmatrix} 0 \\ 0 \\ \dot{\Gamma} \end{Bmatrix} \quad {}_{B_1}\dot{\beta} = \begin{Bmatrix} 0 \\ \dot{\beta} \\ 0 \end{Bmatrix} \quad {}_{B_2}\dot{\phi} = \begin{Bmatrix} \dot{\phi} \\ 0 \\ 0 \end{Bmatrix}$$

Describing the absolute angular velocity ( $\omega$ ) with help of the moving reference frame  $B_3$ , which is attached to the rotor cross section, and represented by  $\vec{i}_3, \vec{j}_3, \vec{k}_3$ , one has:

$${}_{B_3}\omega = {}_{B_3}\dot{\Gamma} + {}_{B_3}\dot{\beta} + {}_{B_3}\dot{\phi} \quad (1)$$

where

$${}_{B_3}\dot{\Gamma} = \mathbf{T}_\phi \cdot \mathbf{T}_\beta \cdot \mathbf{T}_\Gamma \cdot {}_I\dot{\Gamma}$$

$${}_{B_3}\dot{\beta} = \mathbf{T}_\phi \cdot \mathbf{T}_\beta \cdot {}_{B_1}\dot{\beta}$$

$${}_{B_3}\dot{\phi} = \mathbf{T}_\phi \cdot {}_{B_2}\dot{\phi}$$

With help of the transformation matrices, one writes:

$${}_{B_3}\dot{\Gamma} = \begin{bmatrix} \cos \beta \cos \Gamma & \cos \beta \sin \Gamma & -\sin \beta \\ \sin \phi \sin \beta \cos \Gamma & \sin \phi \sin \beta \sin \Gamma + \cos \phi \cos \Gamma & \sin \phi \cos \beta \\ \cos \phi \sin \beta \cos \Gamma & \cos \phi \sin \beta \sin \Gamma - \sin \phi \cos \Gamma & \cos \phi \cos \beta \end{bmatrix} \begin{Bmatrix} 0 \\ 0 \\ \dot{\Gamma} \end{Bmatrix}$$

$${}_{B_3}\dot{\Gamma} = \dot{\Gamma} \begin{Bmatrix} -\sin \beta \\ \sin \phi \cos \beta \\ \cos \phi \cos \beta \end{Bmatrix} \quad (2)$$

$${}_{B_3}\dot{\beta} = \begin{bmatrix} \cos \beta & 0 & -\sin \beta \\ \sin \phi \sin \beta & \cos \phi & \sin \phi \cos \beta \\ \cos \phi \sin \beta & -\sin \phi & \cos \phi \cos \beta \end{bmatrix} \begin{Bmatrix} 0 \\ \dot{\beta} \\ 0 \end{Bmatrix} \Rightarrow {}_{B_3}\dot{\beta} = \dot{\beta} \begin{Bmatrix} 0 \\ \cos \phi \\ -\sin \phi \end{Bmatrix} \quad (3)$$

$${}_{B_3}\dot{\phi} = \begin{bmatrix} 1 & 0 & 0 \\ 0 & \cos \phi & \sin \phi \\ 0 & -\sin \phi & \cos \phi \end{bmatrix} \begin{Bmatrix} \dot{\phi} \\ 0 \\ 0 \end{Bmatrix} \Rightarrow {}_{B_3}\dot{\phi} = \begin{Bmatrix} \dot{\phi} \\ 0 \\ 0 \end{Bmatrix} \quad (4)$$

Rewriting equation (1) as a function of equations (2), (3) e (4), one has:

$${}_{B_3}\omega = \dot{\Gamma} \begin{Bmatrix} -\sin \beta \\ \sin \phi \cos \beta \\ \cos \phi \cos \beta \end{Bmatrix} + \dot{\beta} \begin{Bmatrix} 0 \\ \cos \phi \\ -\sin \phi \end{Bmatrix} + \begin{Bmatrix} \dot{\phi} \\ 0 \\ 0 \end{Bmatrix}$$

Using matrix notation:

$$\begin{Bmatrix} \omega_a \\ \omega_b \\ \omega_c \end{Bmatrix} = \begin{bmatrix} 1 & 0 & -\sin \beta \\ 0 & \cos \phi & \sin \phi \cos \beta \\ 0 & -\sin \phi & \cos \phi \cos \beta \end{bmatrix} \begin{Bmatrix} \dot{\phi} \\ \dot{\beta} \\ \dot{\Gamma} \end{Bmatrix}$$

Setting a constant rotational speed and neglecting torsional vibrations, the spin angle  $\phi$  can be written as  $\Omega t$  where  $\Omega$  is the constant angular velocity of the rotor.

## 1.4 Mathematical Model of the Rotating Machine Elements – Equations of Motion

### 1.4.1 Rigid Discs – Gears, Impellers, etc.

- Kinetic energy of a rigid disc can be written as

$$E_{kin} = \underbrace{\frac{1}{2} \begin{Bmatrix} \dot{V} \\ \dot{W} \end{Bmatrix}^T \begin{bmatrix} m_D & 0 \\ 0 & m_D \end{bmatrix} \begin{Bmatrix} \dot{V} \\ \dot{W} \end{Bmatrix}}_{(I)} + \underbrace{\frac{1}{2} \begin{Bmatrix} w_a \\ w_b \\ w_c \end{Bmatrix}^T \begin{bmatrix} I_P & 0 & 0 \\ 0 & I_D & 0 \\ 0 & 0 & I_D \end{bmatrix} \begin{Bmatrix} w_a \\ w_b \\ w_c \end{Bmatrix}}_{(II)} \quad (5)$$

where the first term of the equation (5), term (*I*), is related to the linear motion of a rotating disc and the second part, term (*II*), to its angular motion.

Using equation (??) and the second term (*II*) of (5) can be written as:

$$(II) \quad \frac{1}{2} \begin{Bmatrix} w_a \\ w_b \\ w_c \end{Bmatrix}^T \begin{bmatrix} I_P & 0 & 0 \\ 0 & I_D & 0 \\ 0 & 0 & I_D \end{bmatrix} \begin{Bmatrix} w_a \\ w_b \\ w_c \end{Bmatrix} = \frac{1}{2} \begin{Bmatrix} -\dot{\Gamma} \sin \beta + \dot{\phi} \\ \dot{\Gamma} \cos \beta \sin \phi + \dot{\beta} \cos \phi \\ \dot{\Gamma} \cos \beta \cos \phi - \dot{\beta} \sin \phi \end{Bmatrix}^T \begin{bmatrix} I_P & 0 & 0 \\ 0 & I_D & 0 \\ 0 & 0 & I_D \end{bmatrix} \begin{Bmatrix} -\dot{\Gamma} \sin \beta + \dot{\phi} \\ \dot{\Gamma} \cos \beta \sin \phi + \dot{\beta} \cos \phi \\ \dot{\Gamma} \cos \beta \cos \phi - \dot{\beta} \sin \phi \end{Bmatrix} \quad (6)$$

Solving eq.(6) one can get the kinetic energy related to the angular motions of the rigid disc:

$$(II) \quad \frac{1}{2} \left\{ I_P \left( \dot{\Gamma}^2 \sin^2 \beta - 2\dot{\Gamma} \dot{\phi} \sin \beta + \dot{\phi}^2 \right) + I_D \left( \dot{\Gamma}^2 \cos^2 \beta \sin^2 \phi + 2\dot{\Gamma} \dot{\beta} \cos \phi \sin \phi \cos \beta + \dot{\beta}^2 \cos^2 \phi \right) + I_D \left( \dot{\Gamma}^2 \cos^2 \beta \cos^2 \phi - 2\dot{\Gamma} \dot{\beta} \cos \phi \sin \phi \cos \beta + \dot{\beta}^2 \sin^2 \phi \right) \right\} \quad (7)$$

For small amplitudes of  $\beta$  one can consider  $\sin \beta = \beta$  and  $\cos \beta = 1$  and the second order terms can be neglected. In this matter eq.(7) becomes

$$(II) \quad \frac{1}{2} \left\{ I_P \left( -2\dot{\Gamma} \dot{\phi} \beta + \dot{\phi}^2 \right) + I_D \left( \dot{\Gamma}^2 \sin^2 \phi + \dot{\Gamma}^2 \cos^2 \phi + \dot{\beta}^2 \cos^2 \phi + \dot{\beta}^2 \sin^2 \phi \right) \right\} \quad (8)$$

The kinetic energy, equation (5), is rewritten then as:

$$E_{kin} = \frac{1}{2} \begin{Bmatrix} \dot{V} \\ \dot{W} \end{Bmatrix}^T \begin{bmatrix} m_D & 0 \\ 0 & m_D \end{bmatrix} \begin{Bmatrix} \dot{V} \\ \dot{W} \end{Bmatrix} + \frac{1}{2} \begin{Bmatrix} \dot{\beta} \\ \dot{\Gamma} \end{Bmatrix}^T \begin{bmatrix} I_D & 0 \\ 0 & I_D \end{bmatrix} \begin{Bmatrix} \dot{\beta} \\ \dot{\Gamma} \end{Bmatrix} - \dot{\phi} \dot{\Gamma} \beta I_P + \frac{1}{2} I_P \dot{\phi}^2 \quad (9)$$

$$E_{kin} = \frac{1}{2} \left( \dot{V}^2 m_D + \dot{W}^2 m_D \right) + \frac{1}{2} \left( \dot{\beta}^2 I_D + \dot{\Gamma}^2 I_D \right) - \dot{\phi} \dot{\Gamma} \beta I_P + \frac{1}{2} I_P \dot{\phi}^2 \quad (10)$$

• Lagrange's equation:

$$\frac{\partial}{\partial t} \left( \frac{\partial E_{kin}}{\partial \dot{q}_i} \right) - \left( \frac{\partial E_{kin}}{\partial q_i} \right) + \left( \frac{\partial E_{pot}}{\partial q_i} \right) = \mathcal{F}_i \quad (i = 1, \dots, n) \quad (11)$$

where  $q_i$  are the generalized coordinates,  $i = 1, 2, 3, \dots, n$  is the number of degree of freedom. For the rigid disc,  $n = 4$  :

$$q_1 = V \quad ; \quad q_2 = W \quad ; \quad q_3 = \beta \quad ; \quad q_4 = \Gamma$$

Assuming that the disc is rigid, no potential energy due to disc deformation is stored,  $E_{pot} = 0$ . Combining equations (10) and (11) one achieves the equations of motion to mathematically describe the rigid disc movements:



- 1<sup>st</sup> equation ( $q_1 = V$ ):

$$\frac{d}{dt} (\dot{V} m_D) = F_V \Rightarrow \ddot{V} m_D = F_V$$

- 2<sup>nd</sup> equation ( $q_2 = W$ ):

$$\frac{d}{dt} (\dot{W} m_D) = F_W \Rightarrow \ddot{W} m_D = F_W$$

- 3<sup>rd</sup> equation ( $q_3 = \beta$ ):

$$\frac{d}{dt} (\dot{\beta} \cdot I_D) + \dot{\phi} \dot{\Gamma} I_P = F_\beta \Rightarrow \ddot{\beta} I_D + \dot{\phi} \dot{\Gamma} I_P = F_\beta$$

- 4<sup>th</sup> equation ( $q_4 = \Gamma$ ):

$$\frac{d}{dt} (\dot{\Gamma} \cdot I_D - \dot{\phi} \beta I_P) = F_\Gamma \Rightarrow \ddot{\Gamma} I_D - \dot{\phi} \dot{\beta} I_P = F_\Gamma$$

Rewriting the four equations in matrix form, one has:

$$\begin{bmatrix} m_D & 0 & 0 & 0 \\ 0 & m_D & 0 & 0 \\ 0 & 0 & I_D & 0 \\ 0 & 0 & 0 & I_D \end{bmatrix} \begin{Bmatrix} \ddot{V} \\ \ddot{W} \\ \ddot{\beta} \\ \ddot{\Gamma} \end{Bmatrix} - \Omega \begin{bmatrix} 0 & 0 & 0 & 0 \\ 0 & 0 & 0 & 0 \\ 0 & 0 & 0 & -I_P \\ 0 & 0 & I_P & 0 \end{bmatrix} \begin{Bmatrix} \dot{V} \\ \dot{W} \\ \dot{\beta} \\ \dot{\Gamma} \end{Bmatrix} = \begin{Bmatrix} F_V \\ F_W \\ F_\beta \\ F_\Gamma \end{Bmatrix} \quad (12)$$

Eq.(12) can be rewritten as:

$$\mathbf{M}^d \cdot \ddot{\mathbf{q}}^d - \Omega \cdot \mathbf{G}^d \cdot \dot{\mathbf{q}}^d = \mathbf{Q}^d \quad (13)$$

where

$M^d \rightarrow$  mass matrix of the disc considering the linear and angular motions;

$G^d \rightarrow$  gyroscopic matrix of the disc;

$\ddot{q}^d \rightarrow$  acceleration vector;

$\dot{q}^d \rightarrow$  velocity vector;

$Q^d \rightarrow$  is a vector with forces and moments acting on the disc, including unbalance for example.

#### 1.4.2 Flexible Shaft Element

Recalling Beam Theory from section ??, the angular deformation of a beam can be written as

$$\beta = -\frac{\partial W}{\partial s} \quad ; \quad \Gamma = \frac{\partial V}{\partial s} \quad (14)$$

The minimal coordinates for representing the flexible shaft movements are:  $q_1, q_2, q_3, q_4, q_5, q_6, q_7$  and  $q_8$ . All them are time depending and describe the linear and angular motion of the shaft element extremities presented in figure 6.

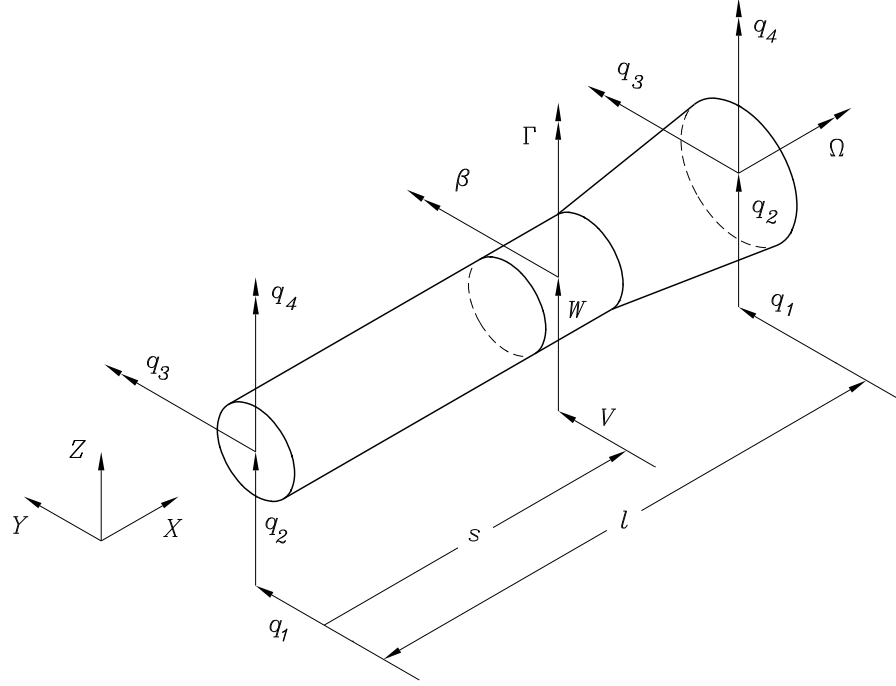


Figure 6: *Coordinates of the shaft elements: 4 linear deformations and 4 angular deformations.*

$$\left. \begin{matrix} q_1 \\ q_2 \\ q_3 \\ q_4 \end{matrix} \right\} \rightarrow \begin{matrix} \boxed{\text{linear and angular motion at } s=0} \\ q_1 = \text{linear motion in } Y \\ q_2 = \text{linear motion in } Z \\ q_3 = \text{angular motion around } Y \\ q_4 = \text{angular motion around } Z \end{matrix} \quad \left. \begin{matrix} q_5 \\ q_6 \\ q_7 \\ q_8 \end{matrix} \right\} \rightarrow \begin{matrix} \boxed{\text{linear and angular motion at } s=l} \\ q_5 = \text{linear motion in } Y \\ q_6 = \text{linear motion in } Z \\ q_7 = \text{angular motion around } Y \\ q_8 = \text{angular motion around } Z \end{matrix}$$

Aiming at describing the movements of a point inside of the shaft element one can introduce to form functions of a continuous beam (shaft element). Considering firstly the plane XY, where translation in Y direction and rotation around Z axis can occur, one obtain four different cases and four different form functions for representing the beam deformations, as can be seen in figure 7.

One can write four form functions, where the main characteristic of such functions is that they are a polynomial functions of  $3^{rd}$  order:

- Form function for describing the linear deformations:

$$\psi(s) = A + Bs + Cs^2 + Ds^3$$

- Form function for describing the angular deformations:

$$\theta = \frac{\partial \psi(s)}{\partial s} = B + 2Cs + 3Ds^2$$

Plano XY

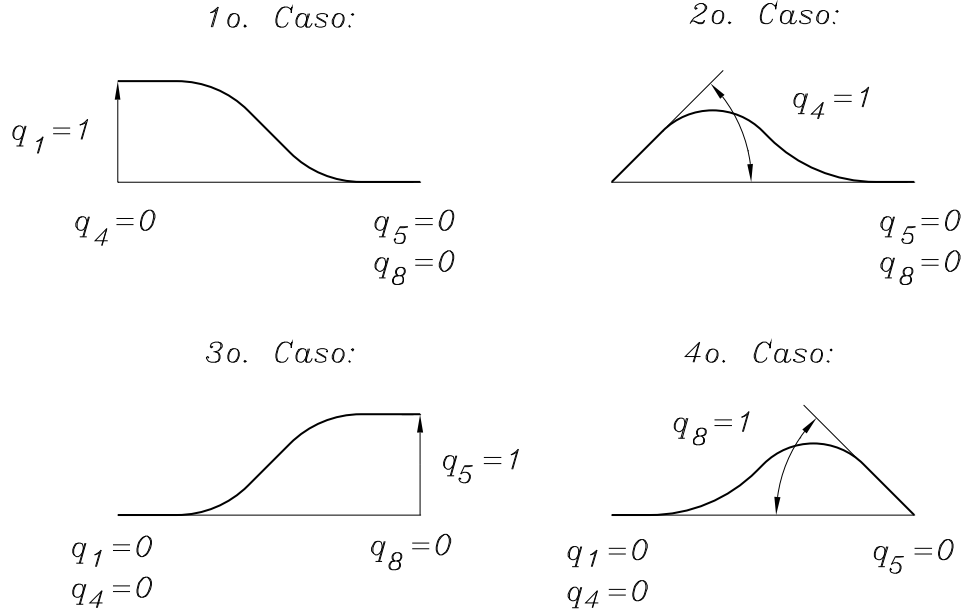


Figure 7: Form functions for representing the flexible shaft deformations in the plane XY.

• 1<sup>st</sup> Case – Boundary conditions for the shaft element (plane XY) are:

$$q_1 = 1 \quad ; \quad q_4 = 0 \quad ; \quad q_5 = 0 \quad ; \quad q_8 = 0$$

Finding the constants A, B, C and D:

$$s = 0 \rightarrow \psi(0) = q_1 = 1 \Rightarrow \psi(0) = A + B0 + C0^2 + D0^3 = 1 \rightarrow A = 1$$

$$s = 0 \rightarrow \theta(0) = q_4 = 0 \Rightarrow \theta(0) = B + 2C0 + 3D0^2 = 0 \rightarrow B = 0$$

$$s = l \rightarrow \psi(l) = q_5 = 0 \Rightarrow \psi(l) = A + Bl + Cl^2 + Dl^3 = 0 \rightarrow Cl^2 + Dl^3 = -1 \quad (*)$$

$$s = l \rightarrow \theta(l) = q_8 = 0 \Rightarrow \theta(l) = B + 2Cl + 3Dl^2 = 0 \rightarrow 2Cl + 3Dl^2 = 0 \quad (**)$$

From (\*) and (\*\*) one gets

$$\begin{aligned} Cl^2 + Dl^3 = -1 \\ 2Cl + 3Dl^2 = 0 \end{aligned} \Rightarrow \begin{bmatrix} l^2 & l^3 \\ 2l & 3l^2 \end{bmatrix} \begin{Bmatrix} C \\ D \end{Bmatrix} = \begin{Bmatrix} -1 \\ 0 \end{Bmatrix}$$

$$\begin{Bmatrix} C \\ D \end{Bmatrix} = \frac{1}{3l^4 - 2l^4} \begin{bmatrix} 3l^2 & -l^3 \\ -2l & l^2 \end{bmatrix} \begin{Bmatrix} -1 \\ 0 \end{Bmatrix} = \frac{1}{l^4} \begin{Bmatrix} -3l^2 \\ 2l \end{Bmatrix} = \begin{Bmatrix} \frac{-3}{l^2} \\ \frac{2}{l^3} \end{Bmatrix}$$

$$A = 1 \quad B = 0 \quad C = \frac{-3}{l^2} \quad D = \frac{2}{l^3}$$

$$\psi_1(s) = 1 - \frac{3}{l^2}s^2 + \frac{2}{l^3}s^3 \quad \text{and} \quad \theta_1(s) = -\frac{6}{l^2}s + \frac{6}{l^3}s^2$$

• **2<sup>nd</sup> Case** – Boundary conditions for the shaft element (plane  $XY$ ) are:

$$q_1 = 0 \quad ; \quad q_4 = 1 \quad ; \quad q_5 = 0 \quad ; \quad q_8 = 0$$

Finding the constants  $A, B, C$  and  $D$ :

$$\begin{aligned} s = 0 &\rightarrow \psi(0) = q_1 = 0 &\Rightarrow &\psi(0) = A = 0 \rightarrow A = 0 \\ s = 0 &\rightarrow \theta(0) = q_4 = 1 &\Rightarrow &\theta(0) = B = 1 \rightarrow B = 1 \\ s = l &\rightarrow \psi(l) = q_5 = 0 &\Rightarrow &Cl^2 + Dl^3 = -l \\ s = l &\rightarrow \theta(l) = q_8 = 0 &\Rightarrow &2Cl + 3Dl^2 = -1 \end{aligned}$$

Solving the linear system as it was done for the 1<sup>st</sup> case, one gets:

$$A = 0 \quad B = 1 \quad C = \frac{-2}{l} \quad D = \frac{1}{l^2}$$

$$\psi_2(s) = s - \frac{2}{l}s^2 + \frac{1}{l^2}s^3 \quad \text{and} \quad \theta_2(s) = 1 - \frac{4}{l}s + \frac{3}{l^2}s^2$$

• **3<sup>rd</sup> Case** – Boundary conditions for the shaft element (plane  $XY$ ) are:

$$q_1 = 0 \quad ; \quad q_4 = 0 \quad ; \quad q_5 = 1 \quad ; \quad q_8 = 0$$

Finding the constants  $A, B, C$  and  $D$ :

$$\begin{aligned} s = 0 &\rightarrow \psi(0) = q_1 = 0 &\Rightarrow &\psi(0) = A = 0 \rightarrow A = 0 \\ s = 0 &\rightarrow \theta(0) = q_4 = 0 &\Rightarrow &\theta(0) = B = 0 \rightarrow B = 0 \\ s = l &\rightarrow \psi(l) = q_5 = 1 &\Rightarrow &Cl^2 + Dl^3 = 1 \\ s = l &\rightarrow \theta(l) = q_8 = 0 &\Rightarrow &2Cl + 3Dl^2 = 0 \end{aligned}$$

$$A = 0 \quad B = 0 \quad C = \frac{3}{l^2} \quad D = \frac{-2}{l^3}$$

$$\psi_3(s) = 3\frac{s^2}{l^2} - 2\frac{s^3}{l^3} \quad \text{and} \quad \theta_3(s) = \frac{6}{l^2}s - \frac{6}{l^3}s^2$$

• 4<sup>th</sup> Case – Boundary conditions for the shaft element (plane XY) are:

$$q_1 = 0 \quad ; \quad q_4 = 0 \quad ; \quad q_5 = 0 \quad ; \quad q_8 = 1$$

Finding the constants  $A$ ,  $B$ ,  $C$  and  $D$ :

$$s = 0 \rightarrow \psi(0) = q_1 = 0 \quad \Rightarrow \quad \psi(0) = A = 0 \rightarrow A = 0$$

$$s = 0 \rightarrow \theta(0) = q_4 = 0 \quad \Rightarrow \quad \theta(0) = B = 0 \rightarrow B = 0$$

$$s = l \rightarrow \psi(l) = q_5 = 0 \quad \Rightarrow \quad Cl^2 + Dl^3 = 0$$

$$s = l \rightarrow \theta(l) = q_8 = 1 \quad \Rightarrow \quad 2Cl + 3Dl^2 = 1$$

$$A = 0 \quad B = 0 \quad C = \frac{-1}{l} \quad D = \frac{1}{l^2}$$

$$\psi_4(s) = \frac{-s^2}{l} + \frac{s^3}{l^2} \quad \text{and} \quad \theta_4(s) = -\frac{2}{l}s + \frac{3}{l^2}s^2$$

The linear deformation inside of the shaft element can be described as a linear combination of the four form functions and the movements of the shaft element extremities (nodes or degree of freedom of the discrete mathematical model):

$$V(s, t) = \psi_1(s) \cdot q_1(t) + \psi_2(s) \cdot q_4(t) + \psi_3(s) \cdot q_5(t) + \psi_4(s) \cdot q_8(t) \quad (15)$$

The angular deformation inside of the shaft element can be described as:

$$\Gamma(s, t) = \frac{\partial V(s, t)}{\partial s} = \theta_1(s) \cdot q_1(t) + \theta_2(s) \cdot q_4(t) + \theta_3(s) \cdot q_5(t) + \theta_4(s) \cdot q_8(t) \quad (16)$$

Making the same analysis for the plane XZ, the linear deformation inside of the shaft element can be described as:

$$W(s, t) = \psi_1(s) \cdot q_2(t) - \psi_2(s) \cdot q_3(t) + \psi_3(s) \cdot q_6(t) - \psi_4(s) \cdot q_7(t) \quad (17)$$

Making the same analysis for the plane XZ, the angular deformation inside of the shaft element can be described as:

$$\beta(s, t) = -\frac{\partial W(s, t)}{\partial s} = -\theta_1(s) \cdot q_2(t) + \theta_2(s) \cdot q_3(t) - \theta_3(s) \cdot q_6(t) + \theta_4(s) \cdot q_7(t) \quad (18)$$

Rewriting in matrix form the linear and angular deformations of the flexible shaft in both planes, XY as well as XZ, one achieves:

$$\begin{Bmatrix} V(s, t) \\ W(s, t) \end{Bmatrix} = \mathbf{\Psi}(s) \mathbf{q}^e(t) \quad (19)$$

$$\begin{Bmatrix} \beta(s, t) \\ \Gamma(s, t) \end{Bmatrix} = \mathbf{\Theta}(s) \mathbf{q}^e(t) \quad (20)$$

where

$$\mathbf{\Psi}(s) = \begin{bmatrix} \psi_1(s) & 0 & 0 & \psi_2(s) & \psi_3(s) & 0 & 0 & \psi_4(s) \\ 0 & \psi_1(s) & -\psi_2(s) & 0 & 0 & \psi_3(s) & -\psi_4(s) & 0 \end{bmatrix}$$

$$\mathbf{\Theta}(s) = \begin{bmatrix} \Theta_\beta(s) \\ \Theta_\Gamma(s) \end{bmatrix} = \begin{bmatrix} 0 & -\theta_1(s) & \theta_2(s) & 0 & 0 & -\theta_3(s) & \theta_4(s) & 0 \\ \theta_1(s) & 0 & 0 & \theta_2(s) & \theta_3(s) & 0 & 0 & \theta_4(s) \end{bmatrix}$$

and

$$\mathbf{q}^e(t) = [ q_1(t) \quad q_2(t) \quad q_3(t) \quad q_4(t) \quad q_5(t) \quad q_6(t) \quad q_7(t) \quad q_8(t) ]^T$$

- Potential energy related to the bending motion of an infinitesimal disc:

$$dE_{pot}^e = \frac{1}{2} \begin{Bmatrix} V'' \\ W'' \end{Bmatrix}^T \begin{bmatrix} EI & 0 \\ 0 & EI \end{bmatrix} \begin{Bmatrix} V'' \\ W'' \end{Bmatrix} ds \quad (21)$$

where  $E$  is the elasticity modulus of the material,  $I$  area moment of inertia,  $V'' = \frac{\partial^2}{\partial s^2} V(s, t)$  and  $W'' = \frac{\partial^2}{\partial s^2} W(s, t)$

- Kinetic energy related to the linear and angular motions of an infinitesimal disc:

$$dE_{kin}^e = \frac{1}{2} \begin{Bmatrix} \dot{V} \\ \dot{W} \end{Bmatrix}^T \begin{bmatrix} \mu & 0 \\ 0 & \mu \end{bmatrix} \begin{Bmatrix} \dot{V} \\ \dot{W} \end{Bmatrix} ds + \frac{1}{2} \dot{\phi}^2 I_p ds + \frac{1}{2} \begin{Bmatrix} \dot{\beta} \\ \dot{\Gamma} \end{Bmatrix}^T \begin{bmatrix} I_d & 0 \\ 0 & I_d \end{bmatrix} \begin{Bmatrix} \dot{\beta} \\ \dot{\Gamma} \end{Bmatrix} ds - \dot{\phi} \dot{\Gamma} \beta I_p ds \quad (22)$$

where  $\mu$  is distributed mass per length,  $\dot{V} = \frac{\partial V(s, t)}{\partial t}$  and  $\dot{W} = \frac{\partial W(s, t)}{\partial t}$ .

Using equations (19) and (20) one achieves:

$$dE_{pot}^e = \frac{1}{2} EI \cdot \mathbf{q}^{eT} \cdot \mathbf{\Psi}''^T \cdot \mathbf{\Psi}'' \cdot \mathbf{q}^e ds \quad (23)$$

$$dE_{kin}^e = \frac{1}{2} \mu \cdot \dot{\mathbf{q}}^{eT} \cdot \mathbf{\Psi}^T \cdot \mathbf{\Psi} \cdot \dot{\mathbf{q}}^e ds + \frac{1}{2} \dot{\phi}^2 I_p ds + \frac{1}{2} I_d \cdot \dot{\mathbf{q}}^{eT} \cdot \mathbf{\Theta}^T \cdot \mathbf{\Theta} \cdot \dot{\mathbf{q}}^e ds - \dot{\phi} I_p \cdot \dot{\mathbf{q}}^{eT} \cdot \mathbf{\Theta}_\Gamma^T \cdot \mathbf{\Theta}_\beta \cdot \dot{\mathbf{q}}^e ds \quad (24)$$

Aiming at obtaining the total energy related to the movements of the flexible shaft one integrates eq.(23) and (24) with respect to the shaft length  $l$ , resulting in the following matrices:

$$\left. \begin{aligned} \mathbf{M}_T^e &= \int_0^l \mu \cdot \boldsymbol{\Psi}^T \cdot \boldsymbol{\Psi} ds \\ \mathbf{M}_R^e &= \int_0^l I_d \cdot \boldsymbol{\Theta}^T \cdot \boldsymbol{\Theta} ds \\ \mathbf{N}^e &= \int_0^l I_p \cdot \boldsymbol{\Theta}_\Gamma^T \cdot \boldsymbol{\Theta}_\beta ds \\ \mathbf{K}_B^e &= \int_0^l EI \cdot \boldsymbol{\Psi}''^T \cdot \boldsymbol{\Psi}'' ds \end{aligned} \right\} \quad (25)$$

The total potential energy related to the bending deformation of the shaft is rewritten as:

$$E_{pot}^e = \frac{1}{2} \mathbf{q}^{eT} \mathbf{K}_B^e \mathbf{q}^e \quad (26)$$

The total kinetic energy related to the linear and angular movements of the shaft is rewritten as:

$$E_{kin}^e = \frac{1}{2} \dot{\mathbf{q}}^{eT} (\mathbf{M}_T^e - \mathbf{M}_R^e) \dot{\mathbf{q}}^e + \frac{1}{2} I_p \dot{\phi}^2 - \dot{\phi} \dot{\mathbf{q}}^{eT} \mathbf{N}^e \mathbf{q}^e \quad (27)$$

Using Lagrange's equation 11, one can get the equation of motion of the flexible shaft element, while considering the angular velocity  $\dot{\phi} = \Omega$  constant, and as a function of its extremities movements:

$$(\mathbf{M}_T^e + \mathbf{M}_R^e) \cdot \ddot{\mathbf{q}}^e - \Omega \cdot \mathbf{G}^e \cdot \dot{\mathbf{q}}^e + \mathbf{K}_B^e \cdot \mathbf{q}^e = \mathbf{Q}^e \quad (28)$$

where  $\ddot{\mathbf{q}}^e$  is the acceleration vector composed of the extremities of the shaft element,  $\dot{\mathbf{q}}^e$  is the velocity vector composed of the extremities of the shaft element,  $\mathbf{q}^e$  is the displacement vector composed of the extremities of the shaft element and  $\mathbf{Q}^e$  excitation vector with forces and moments acting on the extremities of the shaft element.

The matrices given in equation (28) are obtained from the integration of equation (25), and  $\mathbf{G}^e = (\mathbf{N}^e - \mathbf{N}^{eT})$ . For the case of a shaft element with constant cross section, one achieves the matrices following:

- Mass matrix of the shaft element (considering the linear motion)

$$\mathbf{M}_T^e = \frac{\mu l}{420} \begin{bmatrix} 156 & & & & & & & & \\ & 156 & & & & & & & \\ & 0 & -22l & 4l^2 & & & & & \\ & 22l & 0 & 0 & 4l^2 & & & & \\ & 54 & 0 & 0 & 13l & 156 & & & \\ & 0 & 54 & -13l & 0 & 0 & 156 & & \\ & 0 & 13l & -3l^2 & 0 & 0 & 22l & 4l^2 & \\ & -13l & 0 & 0 & -3l^2 & -22l & 0 & 0 & 4l^2 \end{bmatrix} \quad \mathbf{M}_T^e = \mathbf{M}_T^{eT}$$

- Mass matrix of the shaft element (considering the angular motion)

$$\mathbf{M}_R^e = \frac{\mu r^2}{120l} \begin{bmatrix} 36 & & & & & & & & \\ & 36 & & & & & & & \\ & 0 & -3l & 4l^2 & & & & & \\ & 3l & 0 & 0 & 4l^2 & & & & \\ & -36 & 0 & 0 & -3l & 36 & & & \\ & 0 & -36 & 3l & 0 & 0 & 36 & & \\ & 0 & -3l & -l^2 & 0 & 0 & 3l & 4l^2 & \\ & 3l & 0 & 0 & -l^2 & -3l & 0 & 0 & 4l^2 \end{bmatrix} \quad \mathbf{M}_R^e = \mathbf{M}_R^{eT}$$

- Gyroscopic matrix of the shaft element

$$\mathbf{G}^e = \frac{2\mu r^2}{120l} \begin{bmatrix} 0 & & & & & & & & \\ & 36 & 0 & & & & & & \\ & -3l & 0 & 0 & & & & & \\ & 0 & -3l & 4l^2 & 0 & & & & \\ & 0 & 36 & -3l & 0 & 0 & & & \\ & -36 & 0 & 0 & -3l & 36 & 0 & & \\ & -3l & 0 & 0 & l^2 & 3l & 0 & 0 & \\ & 0 & -3l & -l^2 & 0 & 0 & 3l & 4l^2 & 0 \end{bmatrix} \quad \mathbf{G}^e = -\mathbf{G}^{eT}$$

- Stiffness matrix considering the bending motion of the shaft element

$$\mathbf{K}_B^e = \frac{EI}{l^3} \begin{bmatrix} 12 & & & & & & & & \\ & 12 & & & & & & & \\ & 0 & -6l & 4l^2 & & & & & \\ & 6l & 0 & 0 & 4l^2 & & & & \\ & -12 & 0 & 0 & -6l & 12 & & & \\ & 0 & -12 & 6l & 0 & 0 & 12 & & \\ & 0 & -6l & 2l^2 & 0 & 0 & 6l & 4l^2 & \\ & 6l & 0 & 0 & 2l^2 & -6l & 0 & 0 & 4l^2 \end{bmatrix} \quad \mathbf{K}_B^e = \mathbf{K}_B^{eT}$$

### 1.4.3 Bearings

• Mechanical Model – In rotor dynamics modelling the bearings are normally represented by springer and damper as can be seen in figure 8(a). Such mechanical elements are mathematically quantified by means of spring and damping coefficients, as can be seen in figure 8(b).

• Mathematical Model – The equation of motion for a linear bearing is represented by the follow equation:



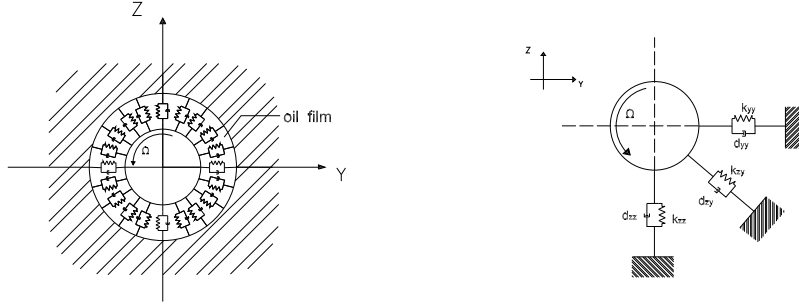


Figure 8: *Mechanical model of bearings – Representation of bearing by means of springers and dampers.*

$$-\mathbf{C}^b \cdot \dot{\mathbf{q}}^b - \mathbf{K}^b \cdot \mathbf{q}^b = \mathbf{Q}^b \quad (29)$$

where

$\mathbf{q}^b = \begin{Bmatrix} V \\ W \end{Bmatrix}$  is the linear displacement of the center of shaft, where the bearing is mounted,

$\mathbf{K}^b = \begin{bmatrix} K_{VV}^b & K_{VW}^b \\ K_{WV}^b & K_{WW}^b \end{bmatrix}$  is the bearing stiffness matrix,

$\mathbf{C}^b = \begin{bmatrix} C_{VV}^b & C_{VW}^b \\ C_{WV}^b & C_{WW}^b \end{bmatrix}$  is the bearing damping matrix and

$\mathbf{Q}^b \rightarrow$  is the resultant force supported by the bearing.

The elements  $K_{VV}^b$ ,  $K_{VW}^b$ ,  $K_{WV}^b$  and  $K_{WW}^b$  describe the stiffness and  $C_{VV}^b$ ,  $C_{VW}^b$ ,  $C_{WV}^b$  and  $C_{WW}^b$  the viscous damping. More about how to achieve such coefficients, will be presented in section 1.8.

#### 1.4.4 Excitation Forces – Unbalance Mass on the Rigid Disc

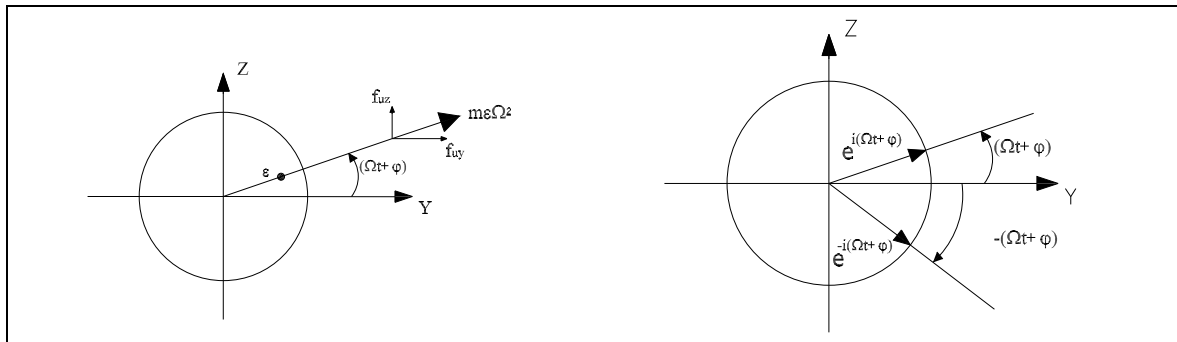


Figure 9: Concentrated unbalance mass and mathematical representation in real and complex forms.

For being completed with the notes in the classes!

#### 1.4.5 Excitation Forces – Distributed Unbalance along the Shaft Length

Considering a shaft element with eccentricity  $(\eta(s); \xi(s))$ , the unbalance force will be given by:

$$\mathbf{Q}^e = \int_0^l \mu \cdot \Omega^2 \cdot \psi^T \cdot \left( \left\{ \begin{array}{c} \eta(s) \\ \xi(s) \end{array} \right\} \cdot \cos \Omega t + \left\{ \begin{array}{c} -\xi(s) \\ \eta(s) \end{array} \right\} \sin \Omega t \right) ds = \mathbf{Q}_C^e \cdot \cos \Omega t + \mathbf{Q}_S^e \cdot \sin \Omega t \quad (30)$$

For a linear distributed unbalance along the finite shaft element one has:

$$\eta(s) = \eta_L \left(1 - \frac{s}{l}\right) + \eta_R \left(\frac{s}{l}\right) \quad \text{e} \quad \xi(s) = \xi_L \left(1 - \frac{s}{l}\right) + \xi_R \left(\frac{s}{l}\right) \quad (31)$$

where  $(\eta_L, \xi_L)$  and  $(\eta_R, \xi_R)$  represent the eccentricities of the center of mass in  $s=0$  and  $s=l$  respectively.

With help of eq.(30) and eq.(31), one can get  $Q_c^e$  and  $Q_s^e$  as:

$$\mathbf{Q}_c^e = \mu \Omega^2 \left\{ \begin{array}{c} \frac{7}{20} \eta_L l + \frac{3}{20} \eta_R l \\ \frac{7}{20} \xi_L l + \frac{3}{20} \xi_R l \\ \frac{-1}{20} \xi_L l^2 - \frac{1}{30} \xi_R l^2 \\ \frac{1}{20} \eta_L l^2 + \frac{1}{30} \eta_R l^2 \\ \frac{3}{20} \eta_L l + \frac{7}{20} \eta_R l \\ \frac{3}{20} \xi_L l + \frac{7}{20} \xi_R l \\ \frac{1}{30} \xi_L l^2 + \frac{1}{20} \xi_R l^2 \\ \frac{-1}{30} \eta_L l^2 - \frac{1}{20} \eta_R l^2 \end{array} \right\} \quad \mathbf{Q}_s^e = \mu \Omega^2 \left\{ \begin{array}{c} \frac{-7}{20} \xi_L l - \frac{3}{20} \xi_R l \\ \frac{7}{20} \eta_L l + \frac{3}{20} \eta_R l \\ \frac{-1}{20} \eta_L l^2 - \frac{1}{30} \eta_R l^2 \\ \frac{-1}{20} \xi_L l^2 - \frac{1}{30} \xi_R l^2 \\ \frac{-3}{20} \xi_L l - \frac{7}{20} \xi_R l \\ \frac{3}{20} \eta_L l + \frac{7}{20} \eta_R l \\ \frac{1}{30} \eta_L l^2 + \frac{1}{20} \eta_R l^2 \\ \frac{1}{30} \xi_L l^2 + \frac{1}{20} \xi_R l^2 \end{array} \right\}$$

## 1.5 Global Model and Equation of Motion

The equation of motion of the global system will be achieved by combining the equation of motion of discs, flexible shaft elements and bearings. One introduces here the global displacement vector ( $q^s$ ) with contain the local vectors  $q^e$ ,  $q^d$  e  $q^b$ , where each  $q_i^s$  represents the linear and angular motion of the nodes of the rotor discrete model. Considering 2 linear motions  $V$  e  $W$  and 2 angular motions  $\beta$  e  $\Gamma$ , each node has 4 degrees of freedom.

Each rigid disc is placed in a particular node and influences directly this node with 4 degrees of freedom. That is the same for the bearing element, which is directly attached to a node. The shaft element has a length  $l$ , connecting 2 different nodes. It means the shaft element will influence 2 nodes( $s=0$ ) and ( $s=l$ ), where each extremity represents one node of the mechanical model. Thus, the shaft element has 8 degrees of freedom.

Considering the example presented in figure (10) the equation of motion can be structured as shown in figure 11, where the sub-matrices  $M_1$   $M_2$   $M_3$  and  $M_4$  correspond to the shaft elements (A, B, C e D) of fig.(10) including the bearing elements (stiffness and damping) and disc (inertia and gyroscopic effects) located in the nodes 2, 3 and 4. The gyroscopic and damping effects are represented in the global matrix  $D^s$ .

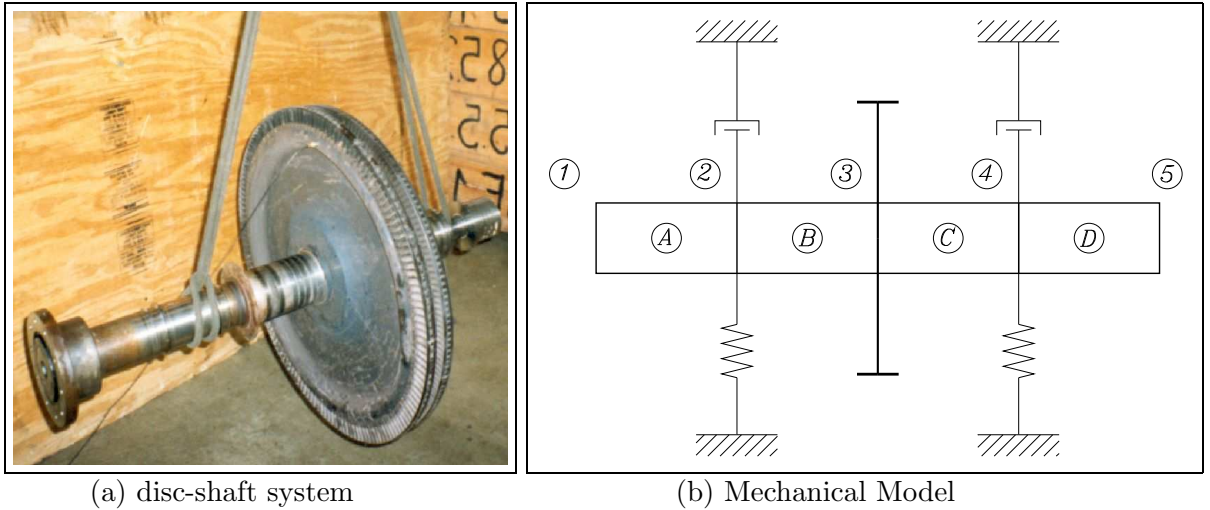


Figure 10: (a) Rotating machine outside of the housing; (b) Mechanical model with 4 finite shaft elements.

The global equation of motion can be written as:

$$\mathbf{M}^s \cdot \ddot{\mathbf{q}}^s + \mathbf{D}^s \cdot \dot{\mathbf{q}}^s + \mathbf{K}^s \cdot \mathbf{q}^s = \mathbf{Q}^s \quad (32)$$

where  $\mathbf{D}^s = -(\Omega \mathbf{G}^s - \mathbf{C}^s)$ . The global matrices  $\mathbf{M}^s$ ,  $\mathbf{D}^s$ ,  $\mathbf{G}^s$  e  $\mathbf{K}^s$  are mounted from the machine elements (shaft, disc, bearing) shown in figure 10, 11 and 12.

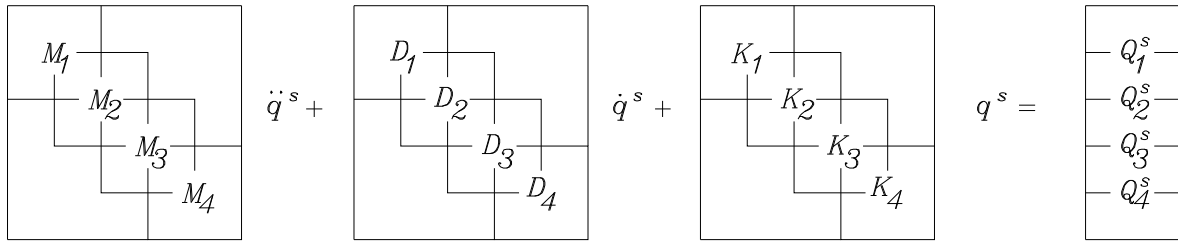


Figure 11: Structure of the global matrices – Equation of motion of the disc-shaft-bearing system with 5 nodes and 20 degrees of freedom.

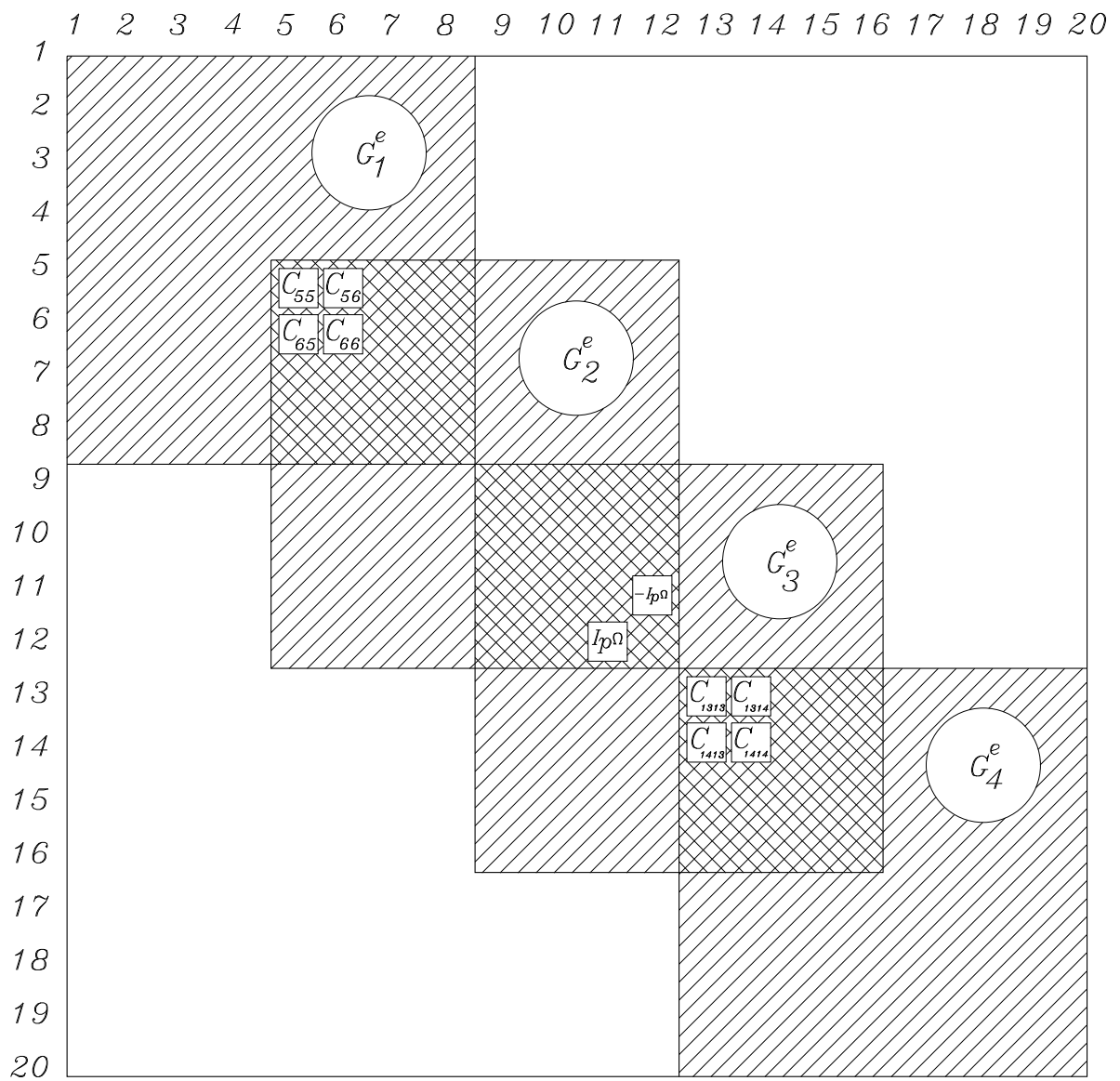


Figure 12: Structure of the matrix  $\mathbf{D}^s$  for a flexible rotor with 5 nodes and 20 degrees of freedom.

## 1.6 Example of Rotor-Bearing System Modelling

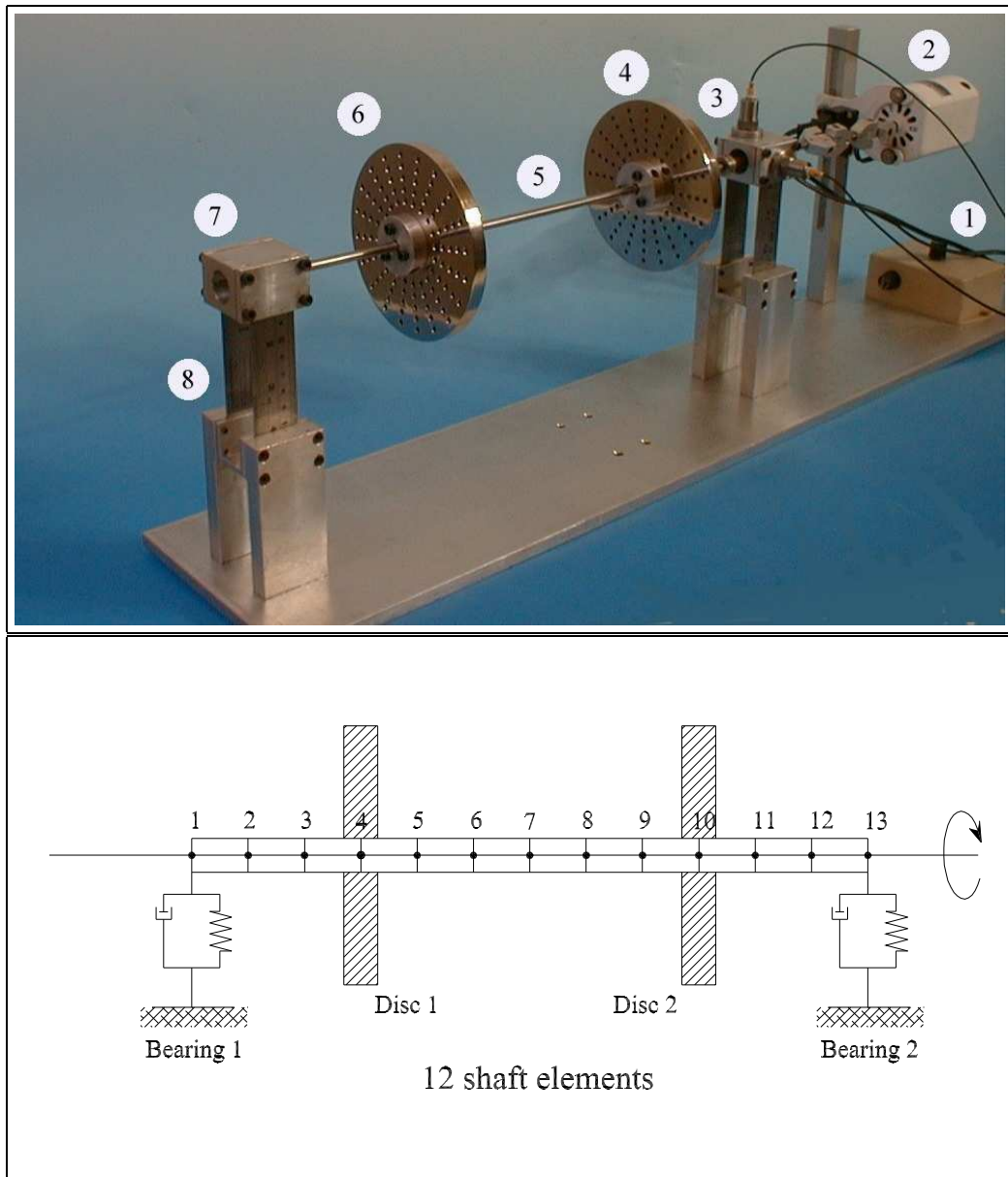


Figure 13: *Mechanical System and Mechanical Model with 13 nodes – Flexible Rotor with 2 Discs and 2 Bearings: (1) motor speed controller; (2) motor; (3) rolling bearing housing attached to a flexible support and two acceleration sensors; (4) rigid disc (5) flexible shaft (6) rigid disc (7) rolling bearing housing attached to a flexible support (8) flexible beams for generating different stiffness coefficients in the horizontal and vertical directions.*

In figure 13 it is possible to see a flexible rotating machine (laboratory prototype) built by a flexible shaft, two rigid discs and two rolling bearing housings attached to two flexible supports. The little test rig was designed aiming at visualizing the natural frequencies and modes shapes by using the human eyes. The first three natural frequencies are under 40 Hz, and the rotor-bearing system is very flexible.

### 1.6.1 Rotor-Bearing Modelling using a MatLab Program

```

%%%%%%%%%%%%%%%%%%%%%%%%%%%%%%%%%%%%%%%%%%%%%%%%%%%%%%%%%%%%%%%%%%%%%%%%
% MACHINERY DYNAMICS LECTURES (41614) %
% MEK - DEPARTMENT OF MECHANICAL ENGINEERING %
% DTU - TECHNICAL UNIVERSITY OF DENMARK %
% %
% Copenhagen, February 10th, 2001 %
% %
% Ilmar Ferreira Santos %
% %
% ROTATING MACHINES -- NATURAL FREQUENCIES AND MODES %
% %
% EXPERIMENTAL RESULTS %
% 13.0 (horizontal) %
% 14.9 (vertical) %
% 33.6 (horizontal) %
% 43.0 (horizontal) %
% 46.0 (vertical) %
% %
%%%%%%%%%%%%%%%%%%%%%%%%%%%%%%%%%%%%%%%%%%%%%%%%%%%%%%%%%%%%%%%%%%%%%%%%

clear all;
close all;

%%%%%%%%%%%%%%%%%%%%%%%%%%%%%%%%%%%%%%%%%%%%%%%%%%%%%%%%%%%%%%%%%%%%%%%%
% DEFINITION OF THE STRUCTURE OF THE MODEL %
%%%%%%%%%%%%%%%%%%%%%%%%%%%%%%%%%%%%%%%%%%%%%%%%%%%%%%%%%%%%%%%%%%%%%%%%
NE=12; % number of shaft elements
GL = (NE+1)*4; % number of degree of freedom
ND=2; % number of discs
NM=2; % number of bearings
CD1=4; % node - disc 1
CD2=10; % node - disc 2}
CMM1=1; % node - bearing 1
CMM2=13; % node - bearing 2

%%%%%%%%%%%%%%%%%%%%%%%%%%%%%%%%%%%%%%%%%%%%%%%%%%%%%%%%%%%%%%%%%%%%%%%%
% CONSTANTS %
%%%%%%%%%%%%%%%%%%%%%%%%%%%%%%%%%%%%%%%%%%%%%%%%%%%%%%%%%%%%%%%%%%%%%%%%
E = 2.0E11; % {elasticity modulus [N/m^2}
RAco = 7800; % {steel density [kg/m^3]}
RAL = 2770; % {aluminum density [kg/m^3]}

%%%%%%%%%%%%%%%%%%%%%%%%%%%%%%%%%%%%%%%%%%%%%%%%%%%%%%%%%%%%%%%%%%%%%%%%
% OPERATIONAL CONDITIONS %
%%%%%%%%%%%%%%%%%%%%%%%%%%%%%%%%%%%%%%%%%%%%%%%%%%%%%%%%%%%%%%%%%%%%%%%%
Omega= 0*2*pi; % angular velocity [rad/s]
Omegarpm = Omega*60/2/pi;

%%%%%%%%%%%%%%%%%%%%%%%%%%%%%%%%%%%%%%%%%%%%%%%%%%%%%%%%%%%%%%%%%%%%%%%%
% GEOMETRY OF THE ROTATING MACHINE %
%%%%%%%%%%%%%%%%%%%%%%%%%%%%%%%%%%%%%%%%%%%%%%%%%%%%%%%%%%%%%%%%%%%%%%%%

%%%%%%%%%%%%%%%%%%%%%%%%%%%%%%%%%%%%%%%%%%%%%%%%%%%%%%%%%%%%%%%%%%%%%%%%
%(A) DISCS %
%%%%%%%%%%%%%%%%%%%%%%%%%%%%%%%%%%%%%%%%%%%%%%%%%%%%%%%%%%%%%%%%%%%%%%%%

Rd = 6/100; % disc radius [m]
espD = 1.1/100 ; % disc thickness [m]
MasD = pi*Rd^2*espD*RAL; % disc mass [kg]

```

```

Id = 1/4*MasD*Rd^2+1/12*MasD*espD^2; % transversal mass moment of inertia of the disc [Kgm^2]
Ip = 1/2*MasD*Rd*Rd; % polar mass moment of inertia of the disc [Kgm^2]

```

```

%%%%%%%%%%%%%%%%%%%%%%%%%%%%%%%%%%%%%%%%%%%%%%%%%%%%%%%%%%%%%%%%%%%%%%%%
%(B) BEARINGS %
%%%%%%%%%%%%%%%%%%%%%%%%%%%%%%%%%%%%%%%%%%%%%%%%%%%%%%%%%%%%%%%%%%%%%%%%

```

```

MasM = 0.40698; % bearing mass [kg](housing + ball bearings)
h=1/1000; % beam thickness [m]
b=28.5/1000; % beam width [m]
Area=b*h; % beam cross section area [m^2]
I=b*h^3/12; % beam moment of inertia of area [m^4]
lr=7.5/100; % beam length [m]
Kty0=2*12*E*I/(lr^3); % equivalent beam flexural stiffness [N/m]
Ktz0=2*E*Area/lr; % equivalent bar stiffness [N/m]

```

```

% Bearing 1 - Damping
Dty1 = 0.0 ;
Dtz1 = 0.0 ;
Dry1 = 0.0 ;
Drz1 = 0.0 ;

```

```

% Bearing 2 - Damping
Dty2 = 0.0 ;
Dtz2 = 0.0 ;
Dry2 = 0.0 ;
Drz2 = 0.0 ;

```

```

% Bearing 1 - Stiffness
Kty1 = Kty0 ;
Ktz1 = Ktz0 ;
Kry1 = 0.0 ;
Krz1 = 0.0 ;

```

```

% Bearing 2 - Stiffness
Kty2 = Kty0 ;
Ktz2 = Ktz0 ;
Kry2 = 0.0 ;
Krz2 = 0.0 ;

```

```

%%%%%%%%%%%%%%%%%%%%%%%%%%%%%%%%%%%%%%%%%%%%%%%%%%%%%%%%%%%%%%%%%%%%%%%%
%(C) SHAFT %
%%%%%%%%%%%%%%%%%%%%%%%%%%%%%%%%%%%%%%%%%%%%%%%%%%%%%%%%%%%%%%%%%%%%%%%%

```

```

l1 = 435/1000; % length of shaft elements [m]
Rext = (6/2)/1000; % shaft external radius [m]
Rint = (0/2)/1000; % shaft internal radius [m]

```

```

% length of the shaft elements [m]
l(1) = 0.140/3;
l(2) = 0.140/3;
l(3) = 0.140/3;
l(4) = 0.205/6;
l(5) = 0.205/6;
l(6) = 0.205/6;
l(7) = 0.205/6;
l(8) = 0.205/6;
l(9) = 0.205/6;
l(10) = 0.090/3;
l(11) = 0.090/3;
l(12) = 0.090/3;

```

```

% external radius of shaft elements [m]
for i=1:NE,
    rx(i)=Rext;
end

```



```

% internal radius of shaft elements [m]
for i=1:NE,
    ri(i)=Rint;
end

% density of shaft elements [kg/m]
for i=1:NE,
    ro(i) = RAco;
end

% transversal areal of the shaft elements [m^2]}
for i=1:NE,
    St(i) = pi*(rx(i)^2-ri(i)^2);
end

% area moment of inertia of the shaft elements [m^4]}
for i=1:NE,
    II(i)=pi*((rx(i)+ri(i))/2)^3*(rx(i)-ri(i));
end

%%%%%%%%%%%%%%%%%%%%%%%%%%%%%%%%%%%%%%%%%%%%%%%%%%%%%%%%%%%%%%%%%%%%%%%%
%      MOUNTING THE GLOBAL MATRICES      %
%%%%%%%%%%%%%%%%%%%%%%%%%%%%%%%%%%%%%%%%%%%%%%%%%%%%%%%%%%%%%%%%%%%%%%%%

disp('MOUNTING THE GLOBAL MATRICES - WAIT!')
disp(' ')

% Defining the global matrices with zero elements
M=zeros(GL);
G=zeros(GL);
K=zeros(GL);

%%%%%%%%%%%%%%%%%%%%%%%%%%%%%%%%%%%%%%%%%%%%%%%%%%%%%%%%%%%%%%%%%%%%%%%%
% GLOBAL MASS MATRIX %
%%%%%%%%%%%%%%%%%%%%%%%%%%%%%%%%%%%%%%%%%%%%%%%%%%%%%%%%%%%%%%%%%%%%%%%%

disp('MOUNTING THE GLOBAL MASS MATRIX - WAIT!')
disp(' ')

% Mass matrices of shaft elements due to linear and angular movements

a=1; b=8;

for n=1:NE,

    MteAux= [156      0      0      22*(n)      54      0      0      -13*(n)
             0      156     -22*(n)      0      0      54      13*(n)      0
             0     -22*(n)      4*(n)^2      0      0     -13*(n)     -3*(n)^2      0
            22*(n)      0      0      4*(n)^2      13*(n)      0      0     -3*(n)^2
             54      0      0      13*(n)      156      0      0     -22*(n)
             0      54     -13*(n)      0      0      156      22*(n)      0
             0     13*(n)     -3*(n)^2      0      0      22*(n)      4*(n)^2      0
            -13*(n)      0      0     -3*(n)^2     -22*(n)      0      0      4*(n)^2];

    Mte = ((ro(n)*St(n)*l(n))/420)*MteAux;

    MreAux= [36      0      0      3*(n)     -36      0      0      3*(n)
             0      36     -3*(n)      0      0     -36     -3*(n)      0
             0     -3*(n)      4*(n)^2      0      0      3*(n)     -1*(n)^2      0
    
```

```

3*1(n)  0      0      4*1(n)^2  -3*1(n)  0      0      -1(n)^2
-36     0      0      -3*1(n)  36     0      0      -3*1(n)
0       -36    3*1(n)  0      0      36    3*1(n)  0
0       -3*1(n) -1(n)^2  0      0      3*1(n)  4*1(n)^2  0
3*1(n)  0      0      -1(n)^2  -3*1(n)  0      0      4*1(n)^2];

Mre = ((ro(n)*II(n))/(30*1(n)))*MreAux;

MauxT=Mte+Mre;

for f=a:b,
    for g=a:b,
        M(f,g)=M(f,g)+MauxT(f-(n-1)*4,g-(n-1)*4);
    end
end

a=a+4; b=b+4;

end

% Adding the mass matrices of the disc elements

M((CD1-1)*4+1,(CD1-1)*4+1)=M((CD1-1)*4+1,(CD1-1)*4+1)+MasD;
M((CD1-1)*4+2,(CD1-1)*4+2)=M((CD1-1)*4+2,(CD1-1)*4+2)+MasD;
M((CD1-1)*4+3,(CD1-1)*4+3)=M((CD1-1)*4+3,(CD1-1)*4+3)+Id;
M((CD1-1)*4+4,(CD1-1)*4+4)=M((CD1-1)*4+4,(CD1-1)*4+4)+Id;
M((CD2-1)*4+1,(CD2-1)*4+1)=M((CD2-1)*4+1,(CD2-1)*4+1)+MasD;
M((CD2-1)*4+2,(CD2-1)*4+2)=M((CD2-1)*4+2,(CD2-1)*4+2)+MasD;
M((CD2-1)*4+3,(CD2-1)*4+3)=M((CD2-1)*4+3,(CD2-1)*4+3)+Id;
M((CD2-1)*4+4,(CD2-1)*4+4)=M((CD2-1)*4+4,(CD2-1)*4+4)+Id;

% Adding the mass matrices of the bearing elements

M((CMM1-1)*4+1,(CMM1-1)*4+1)=M((CMM1-1)*4+1,(CMM1-1)*4+1)+MasM;
M((CMM1-1)*4+2,(CMM1-1)*4+2)=M((CMM1-1)*4+2,(CMM1-1)*4+2)+MasM;
M((CMM2-1)*4+1,(CMM2-1)*4+1)=M((CMM2-1)*4+1,(CMM2-1)*4+1)+MasM;
M((CMM2-1)*4+2,(CMM2-1)*4+2)=M((CMM2-1)*4+2,(CMM2-1)*4+2)+MasM;

%%%%%%%%%%%%%%%%%%%%%%%%%%%%%%%%%%%%%%%%%%%%%%%%%%%%%%%%%%%%%%%%%%%%%%%%
% GLOBAL GYROSCOPIC MATRIX %
%%%%%%%%%%%%%%%%%%%%%%%%%%%%%%%%%%%%%%%%%%%%%%%%%%%%%%%%%%%%%%%%%%%%%%%%

disp('MOUNTING THE GLOBAL GYROSCOPIC MATRIX - WAIT!')
disp(' ')

% Gyroscopic matrix of shaft elements

a=1; b=8;

for n=1:NE,

    GeAux=[0      -36      3*1(n)  0      0      36      3*1(n)  0
            36     0      0      3*1(n)  -36     0      0      3*1(n)
            -3*1(n)  0      0      -4*1(n)^2  3*1(n)  0      0      1(n)^2
            0      -3*1(n)  4*1(n)^2  0      0      3*1(n)  -1(n)^2  0
            0      36     -3*1(n)  0      0      -36    -3*1(n)  0
            -36     0      0      -3*1(n)  36     0      0      -3*1(n)
            -3*1(n)  0      0      1(n)^2  3*1(n)  0      0      -4*1(n)^2
            0      -3*1(n)  -1(n)^2  0      0      3*1(n)  4*1(n)^2  0      ];

```

```

Ge=Omega*(ro(n)*II(n))/(15*1(n))*GeAux;

for f=a:b,
    for g=a:b,
        G(f,g)=G(f,g)+Ge(f-(n-1)*4,g-(n-1)*4);
    end
end

a=a+4; b=b+4;

end

% Adding the gyroscopic matrices of the disc elements

G((CD1-1)*4+3,(CD1-1)*4+4)=G((CD1-1)*4+3,(CD1-1)*4+4)-Omega*Ip;
G((CD1-1)*4+4,(CD1-1)*4+3)=G((CD1-1)*4+4,(CD1-1)*4+3)+Omega*Ip;
G((CD2-1)*4+3,(CD2-1)*4+4)=G((CD2-1)*4+3,(CD2-1)*4+4)-Omega*Ip;
G((CD2-1)*4+4,(CD2-1)*4+3)=G((CD2-1)*4+4,(CD2-1)*4+3)+Omega*Ip;

%%%%%%%%%%%%%%%%%%%%%%%%%%%%%%%%%%%%%%%%%%%%%%%%%%%%%%%%%%%%%%%%%%%%%%%%
% GLOBAL STIFFNESS MATRIX %
%%%%%%%%%%%%%%%%%%%%%%%%%%%%%%%%%%%%%%%%%%%%%%%%%%%%%%%%%%%%%%%%%%%%%%%%

disp('MOUNTING THE GLOBAL STIFFNESS MATRIX - WAIT!')
disp(' ')

% Stiffness matrix of shaft elements due to bending

a=1; b=8;

for n=1:NE,

    KbeAux= [12      0      0      6*1(n)   -12      0      0      6*1(n)
             0      12     -6*1(n)  0         0       -12     -6*1(n)  0
             0     -6*1(n)  4*1(n)^2  0         0        6*1(n)  2*1(n)^2  0
             6*1(n)  0      0         4*1(n)^2 -6*1(n)  0      0      2*1(n)^2
             -12     0      0         -6*1(n)  12      0      0      -6*1(n)
             0      -12     6*1(n)  0         0        12     6*1(n)  0
             0     -6*1(n)  2*1(n)^2  0         0        6*1(n)  4*1(n)^2  0
             6*1(n)  0      0         2*1(n)^2 -6*1(n)  0      0      4*1(n)^2];

    Kbe = ((E*II(n))/(1(n)^3))*KbeAux;

    for f=a:b,
        for g=a:b,
            K(f,g)=K(f,g)+Kbe(f-(n-1)*4,g-(n-1)*4);
        end
    end

a=a+4; b=b+4;

end

% Adding the stiffness matrices of the bearing elements

K((CMM1-1)*4+1,(CMM1-1)*4+1)=K((CMM1-1)*4+1,(CMM1-1)*4+1)+Ktz1;
K((CMM1-1)*4+2,(CMM1-1)*4+2)=K((CMM1-1)*4+2,(CMM1-1)*4+2)+Kty1;
K((CMM2-1)*4+1,(CMM2-1)*4+1)=K((CMM2-1)*4+1,(CMM2-1)*4+1)+Ktz2;
K((CMM2-1)*4+2,(CMM2-1)*4+2)=K((CMM2-1)*4+2,(CMM2-1)*4+2)+Kty2;

```

```

%%%%%%%%%%%%%%%%%%%%%%%%%%%%%%%%%%%%%%%%%%%%%%%%%%%%%%%%%%%%%%%%%%%%%%%%
% GLOBAL MATHEMATICAL MODEL %
%%%%%%%%%%%%%%%%%%%%%%%%%%%%%%%%%%%%%%%%%%%%%%%%%%%%%%%%%%%%%%%%%%%%%%%%

Mglob=[ G M
        M zeros(size(M,1))];
Kglob=[ K zeros(size(M,1))
        zeros(size(M,1)) -M ];

%%%%%%%%%%%%%%%%%%%%%%%%%%%%%%%%%%%%%%%%%%%%%%%%%%%%%%%%%%%%%%%%%%%%%%%%
% MODAL ANALYSIS %
%%%%%%%%%%%%%%%%%%%%%%%%%%%%%%%%%%%%%%%%%%%%%%%%%%%%%%%%%%%%%%%%%%%%%%%%

disp('CALCULATING NATURAL FREQUENCIES AND MODE SHAPES - WAIT!')
disp(' ')

% Calculating Eigenvectors and Eigenvalues

[U,lambda]=eig(-Kglob,Mglob);
[lam,p]=sort(diag(lambda));
U=U(:,p);

% Number of divisions in time for plotting the mode shapes
nn=99;

N=size(U,1);
maximo=num2str((N-2)/2);
ModoVirt=N;

ModoVirt=input([' Enter the number of the mode shape to be plotted, ...
               zero to esc, highest mode ',maximo,': ']);

% For visualizing the mode shapes:

ModoReal=2*ModoVirt;

%%%%%%%%%%%%%%%%%%%%%%%%%%%%%%%%%%%%%%%%%%%%%%%%%%%%%%%%%%%%%%%%%%%%%%%%
% LOOP TO PLOT THE MODES SHAPES %
%%%%%%%%%%%%%%%%%%%%%%%%%%%%%%%%%%%%%%%%%%%%%%%%%%%%%%%%%%%%%%%%%%%%%%%%

while ModoReal>0,

% Natural frequencies
wn=imag(lam(ModoReal));
ttotal=8/abs(wn);
dt=ttotal/nn;
t=0:dt:ttotal;

% Defining v and w real e imaginary for each node

y=1:4:GL;
z=2:4:GL;

for i=1:(NE+1),
vr(i)=real(U(y(i),ModoReal));
vi(i)=imag(U(y(i),ModoReal));
wr(i)=real(U(z(i),ModoReal));
wi(i)=imag(U(z(i),ModoReal));
end

```

```

% Calculation the modal displacements v and w

for i=1:(NE+1),
    v(i,:)=vr(i)*cos(wn*t)+vi(i)*sin(wn*t);
    w(i,:)=wr(i)*cos(wn*t)+wi(i)*sin(wn*t);
end

Zero=diag(zeros(length(t)))';
Um=diag(eye(length(t)))';

for i=1:(NE+1)
    pos(i,:)=Zero+(i-1)*Um;
end

clf
hold on
for cont=1:NE+1,
    plot3(pos(cont,:),w(cont,:),v(cont,:), 'k', 'LineWidth', 2.5);
end

nm=num2str(ModoVirt);
fn=num2str(abs(wn/2/pi));
dfi=num2str(Omegarpm);
title(['Angular Velocity: ',dfi,' rpm          Mode: ',nm,' Nat. Freq.: ',fn,' Hz'],'FontSize',14)
view(-25,20);
grid on;
ModeVirt=input([' Enter the number of the mode shape to be plotted, ...
                zero to esc, highest mode ',maximo,': ']);
ModeReal=2*ModeVirt;
figure(ModeVirt)

end

```

### 1.6.2 Natural Frequencies and Mode Shapes - MatLab Program Results

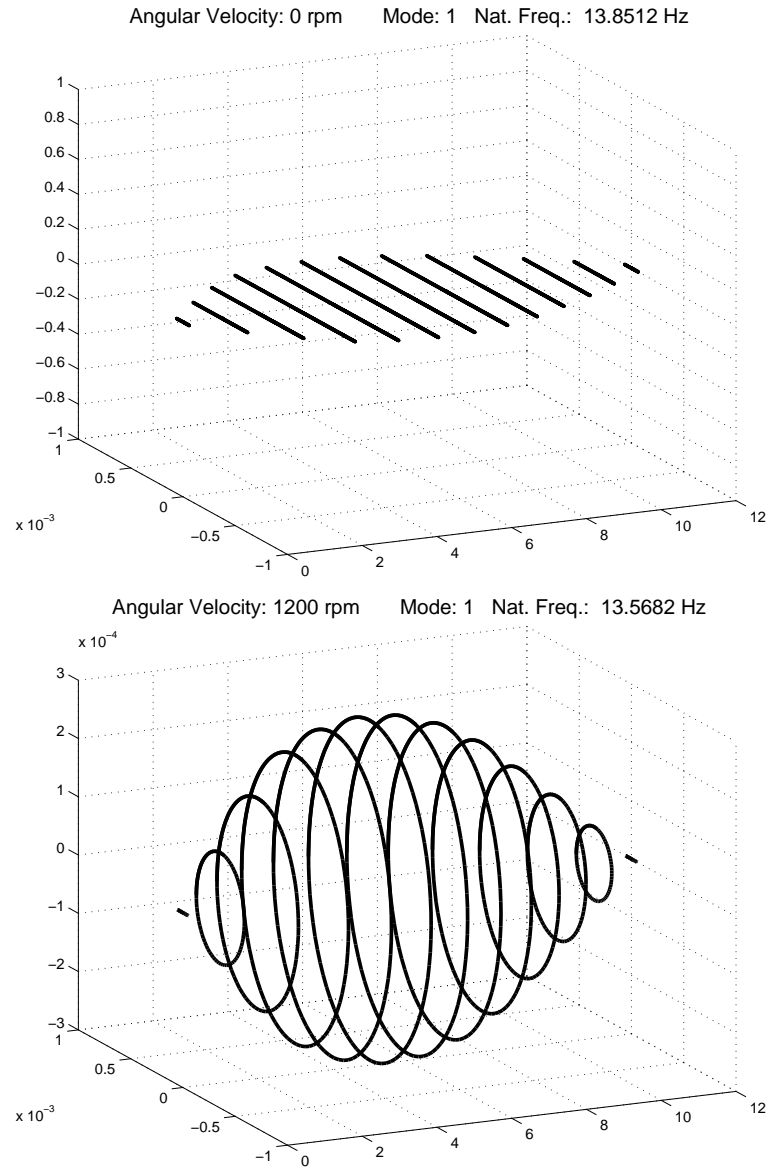


Figure 14: *First mode shape and first natural frequency calculated with the MatLab program, at zero and 1200 rpm (20Hz).*

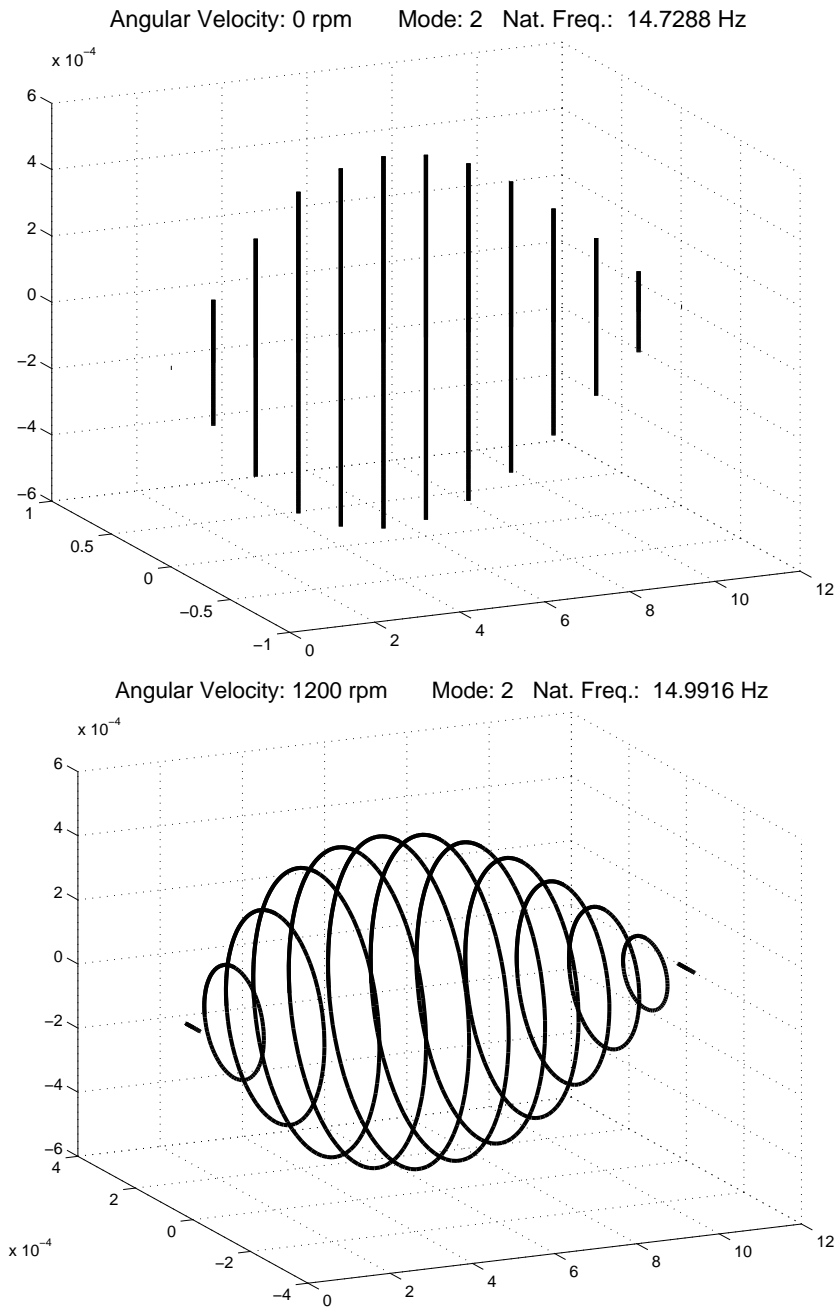


Figure 15: Second mode shape and second natural frequency calculated with the MatLab program, at zero and 1200 rpm (20Hz).

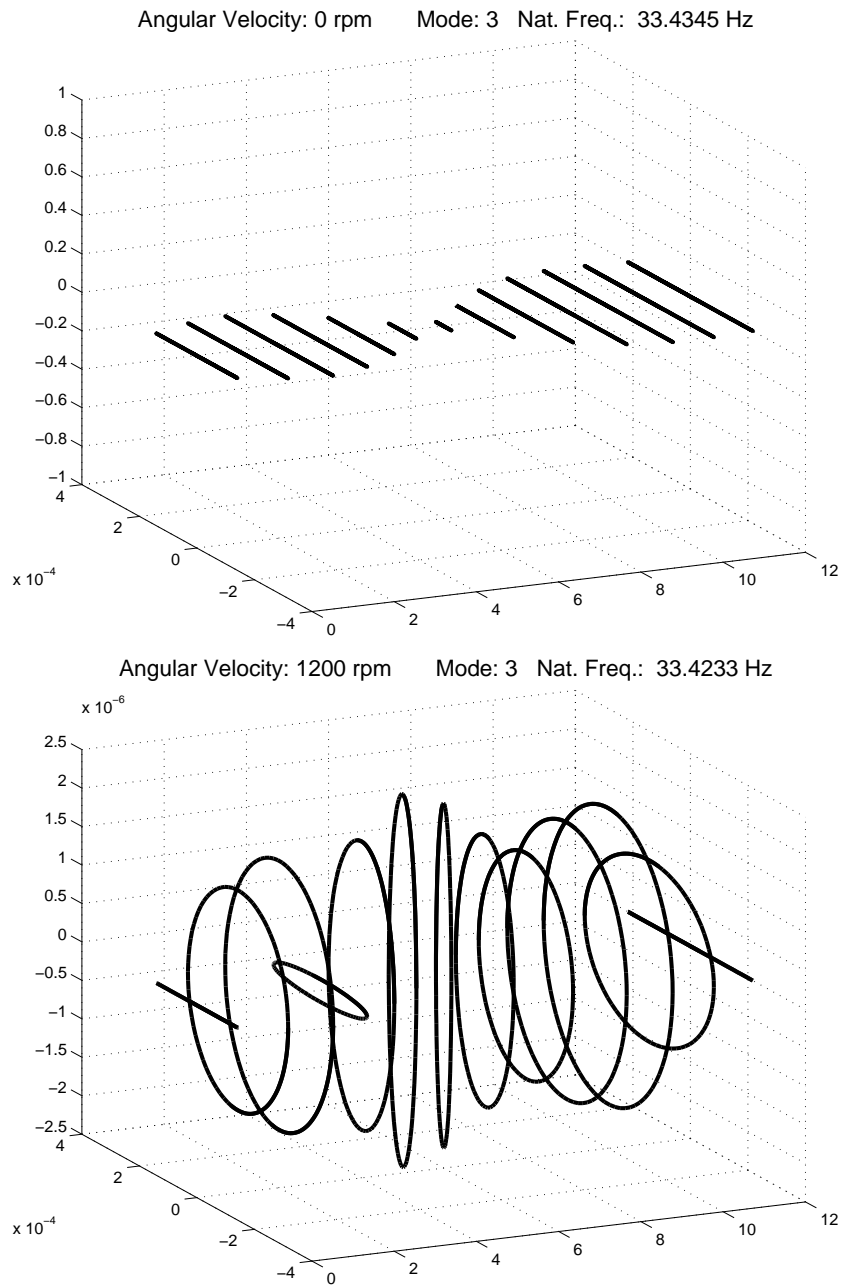


Figure 16: *Third mode shape and third natural frequency calculated with the MatLab program, at zero and 1200 rpm (20Hz).*



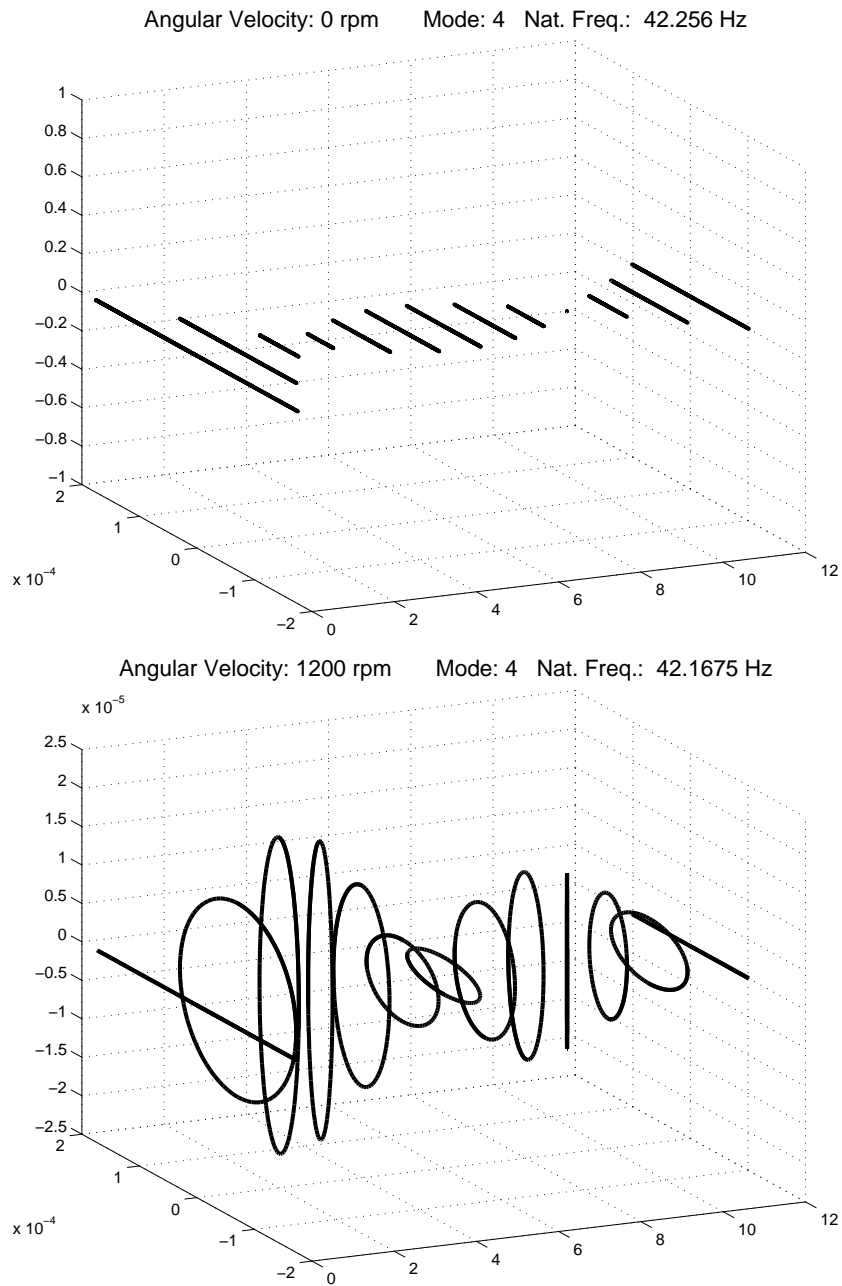


Figure 17: *Fourth mode shape and fourth natural frequency calculated with the MatLab program, at zero and 1200 rpm (20Hz).*

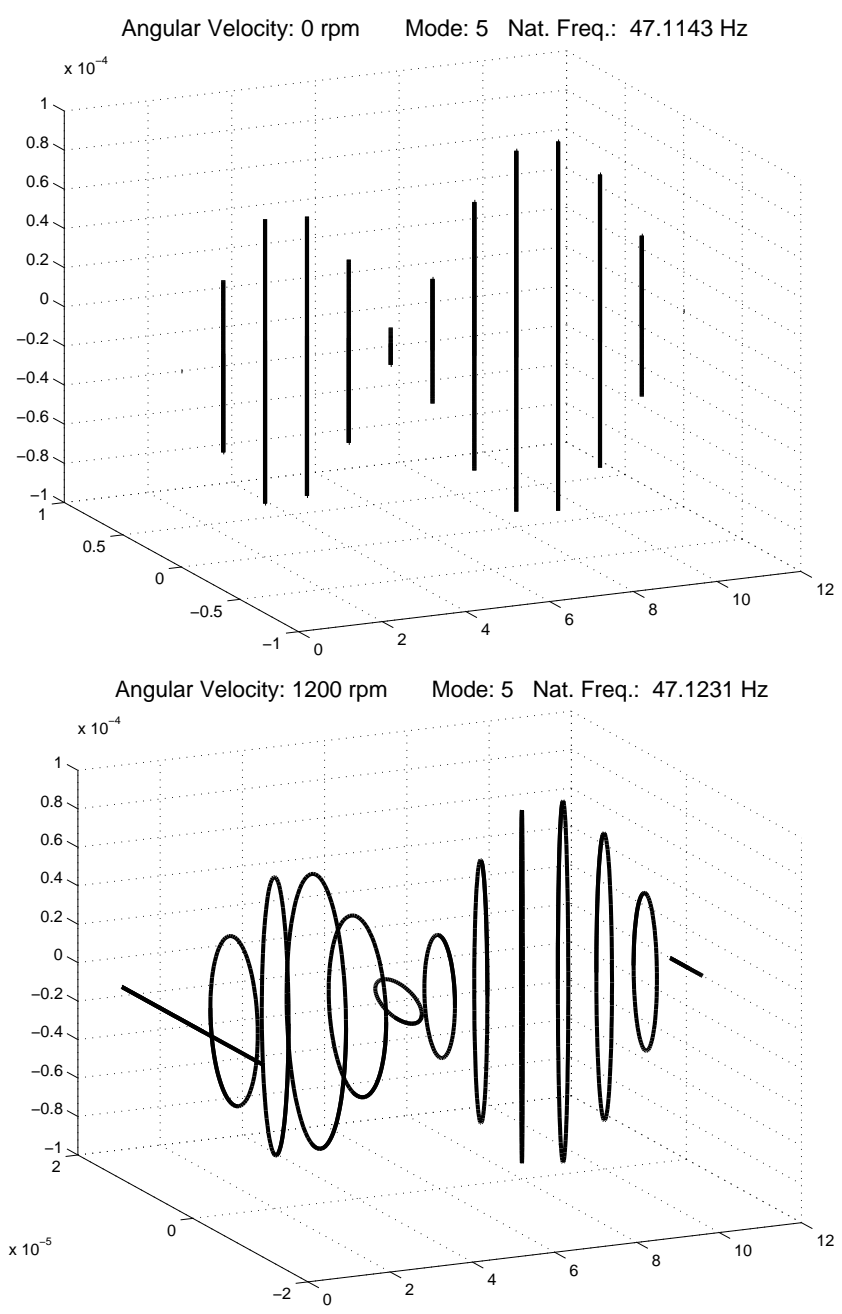


Figure 18: Fifth mode shape and fifth natural frequency calculated with the MatLab program, at zero and 1200 rpm (20Hz).

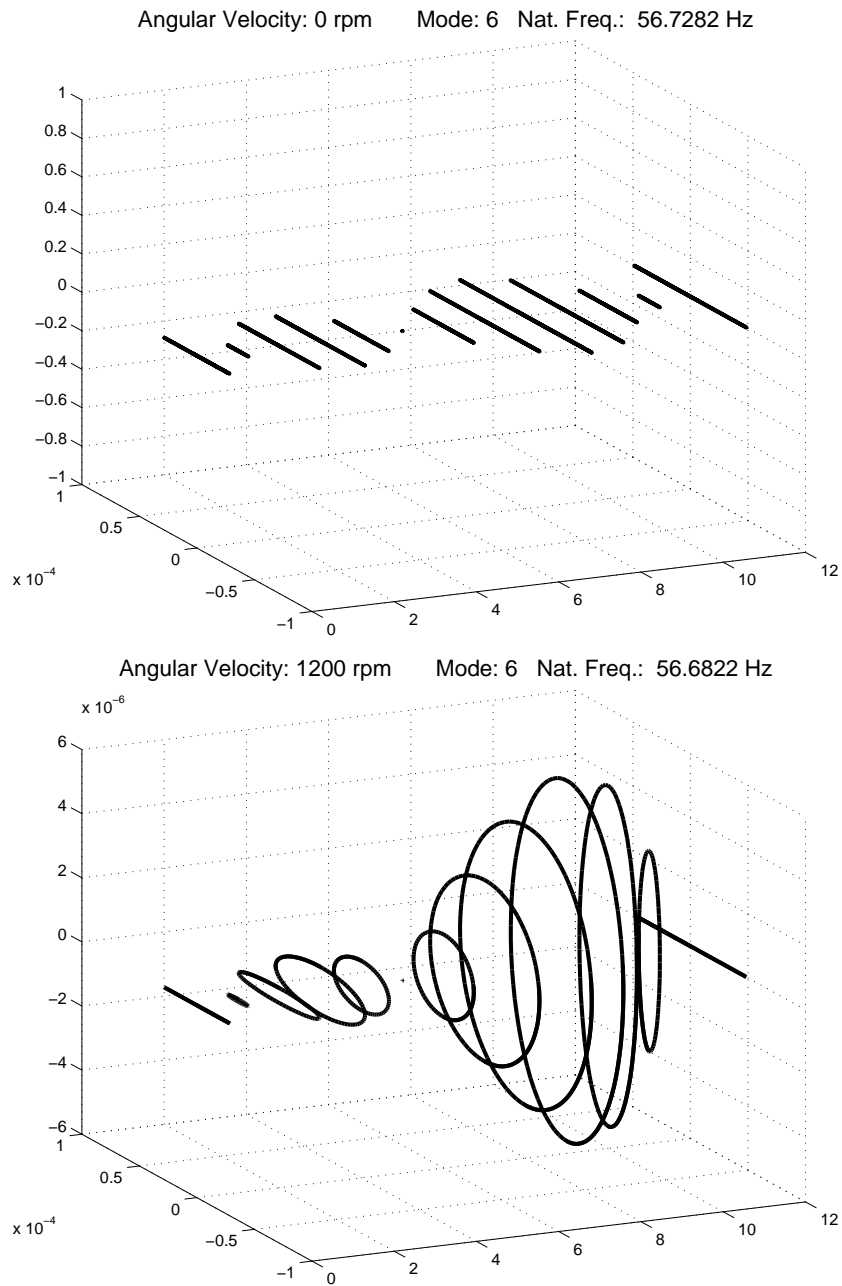


Figure 19: *Sixth mode shape and sixth natural frequency calculated with the MatLab program, at zero and 1200 rpm (20Hz).*

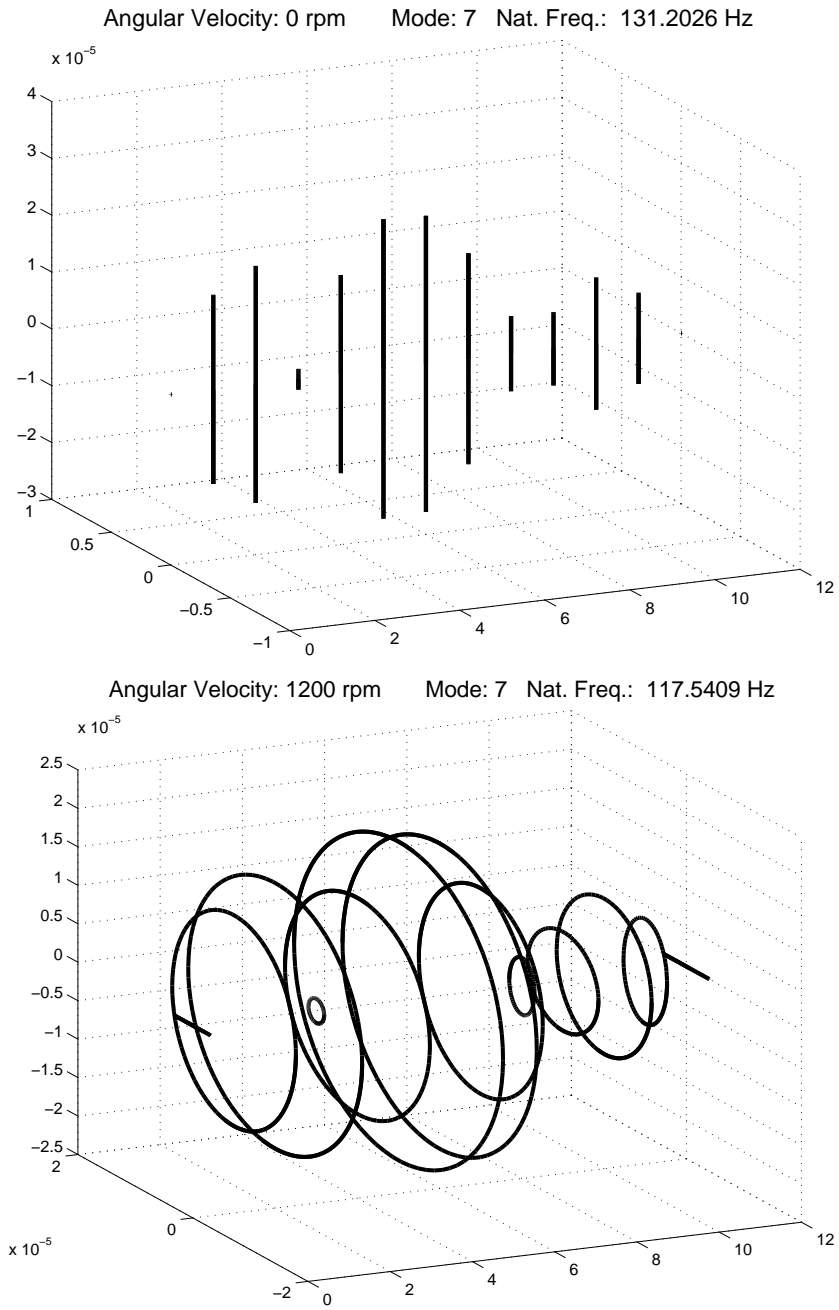


Figure 20: Seventh mode shape and sixth natural frequency calculated with the MatLab program, at zero and 1200 rpm (20Hz).

### 1.6.3 Validation of Rotor-Bearing System Modelling using Theoretical and Experimental Natural Frequencies

MODE SHAPE	PLANE	Nat. Frequency (theoretical) [Hz]	Nat. Frequency (experimental) [Hz]	Error %
1	horizontal	13.8	13.0	6.1
2	vertical	14.7	14.9	1.3
3	horizontal	33.4	33.6	0.6
4	horizontal	42.3	42.3	0.0
5	vertical	47.1	46.0	2.1
6	horizontal	56.7	55.4	2.1
7	vertical	131.	(out of range)	–

Table 1: Validation of Rotor-Bearing System Modelling using information about the theoretical and experimental natural frequencies in the range of frequencies between 0 and 60 Hz, when the rotor angular velocity is zero.

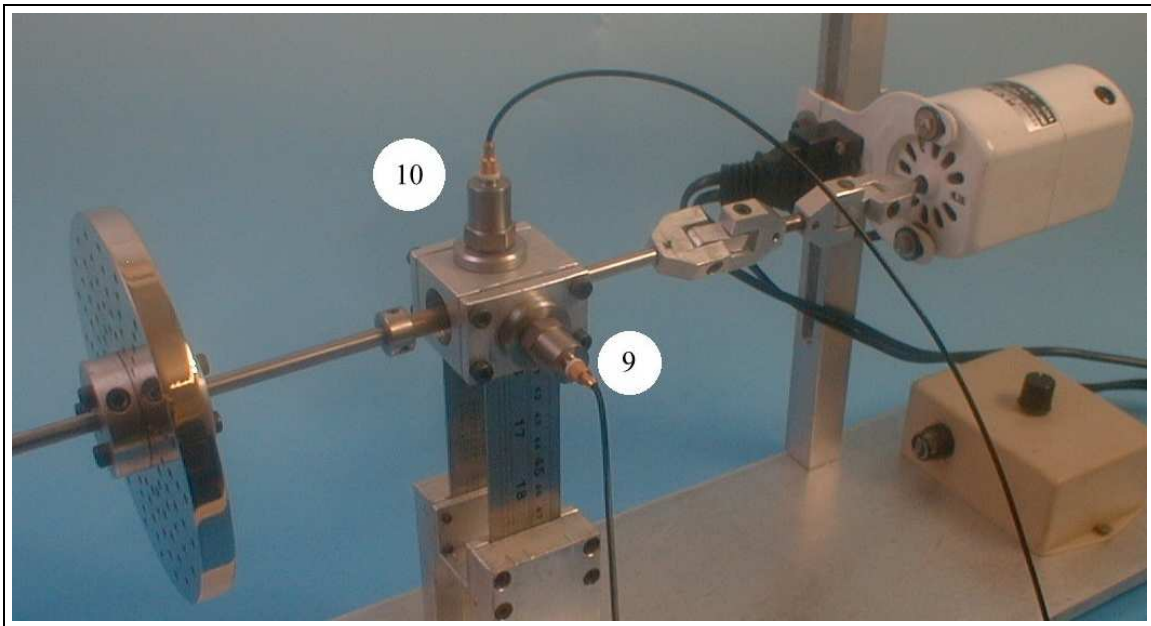


Figure 21: Acceleration sensors 9 and 10 mounted on the bearing housing, with the goal of measuring the movements of rotor-bearing system in the horizontal and vertical directions respectively.

### 1.6.4 Validation of Rotor-Bearing System Modelling – Experimental Transient Analysis

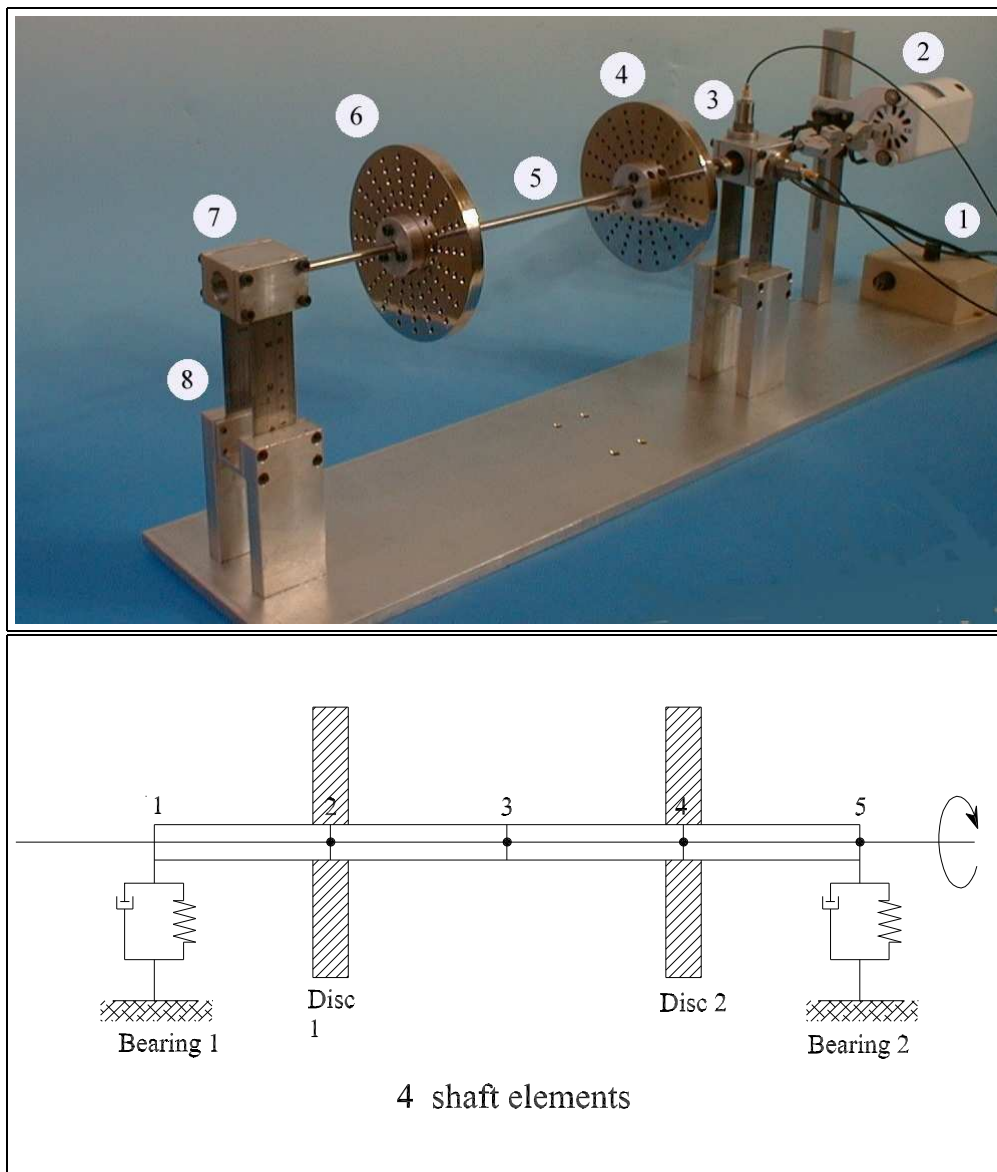


Figure 22: *Mechanical System and Mechanical Model with 5 nodes – Flexible Rotor with 2 Discs and 2 Bearings.*

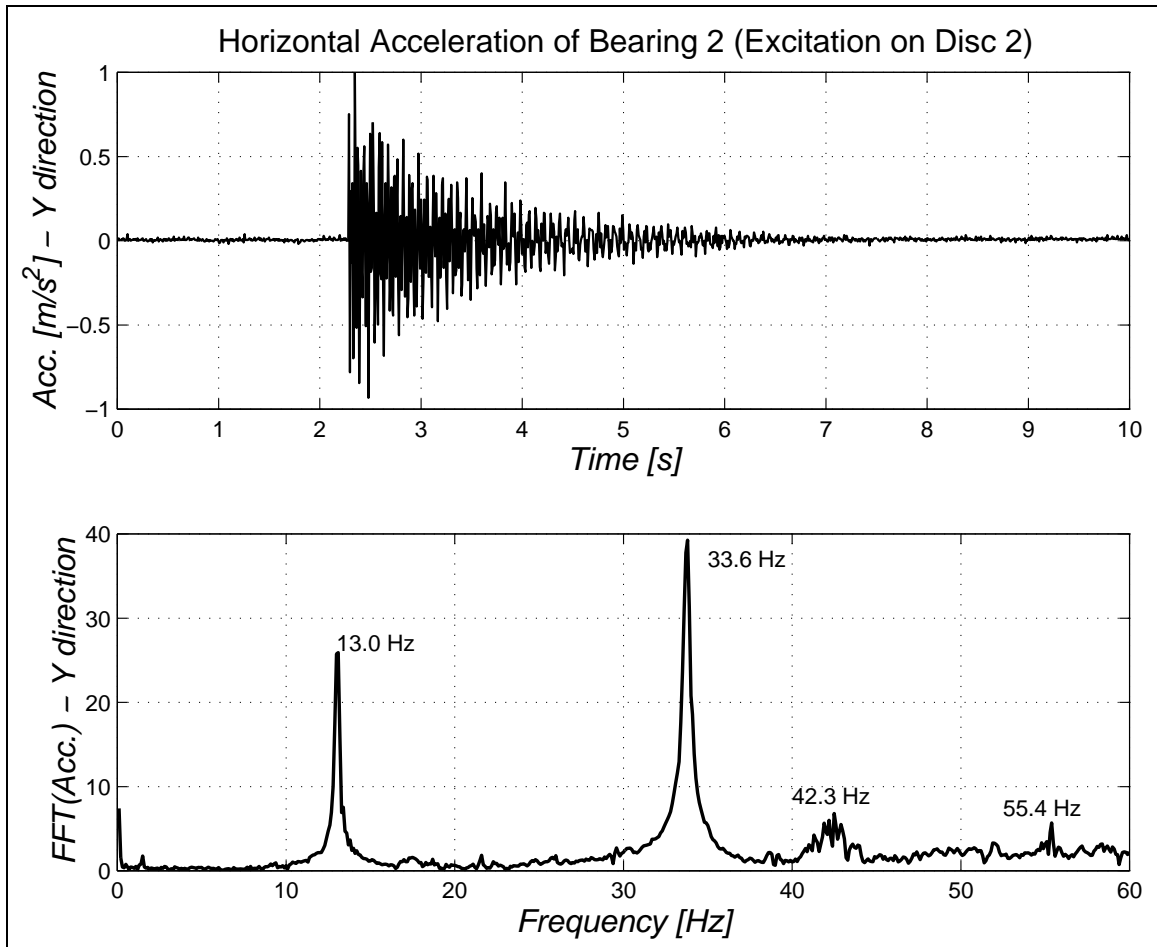


Figure 23: *Experimental Analysis – Transient lateral vibration of the rotor-bearing system, when the rotor has no angular velocity, and it is excited by a horizontal perturbation (shock) on the disc 2 (node 4) and the horizontal acceleration of the bearing 2 (node 5) is measured.*

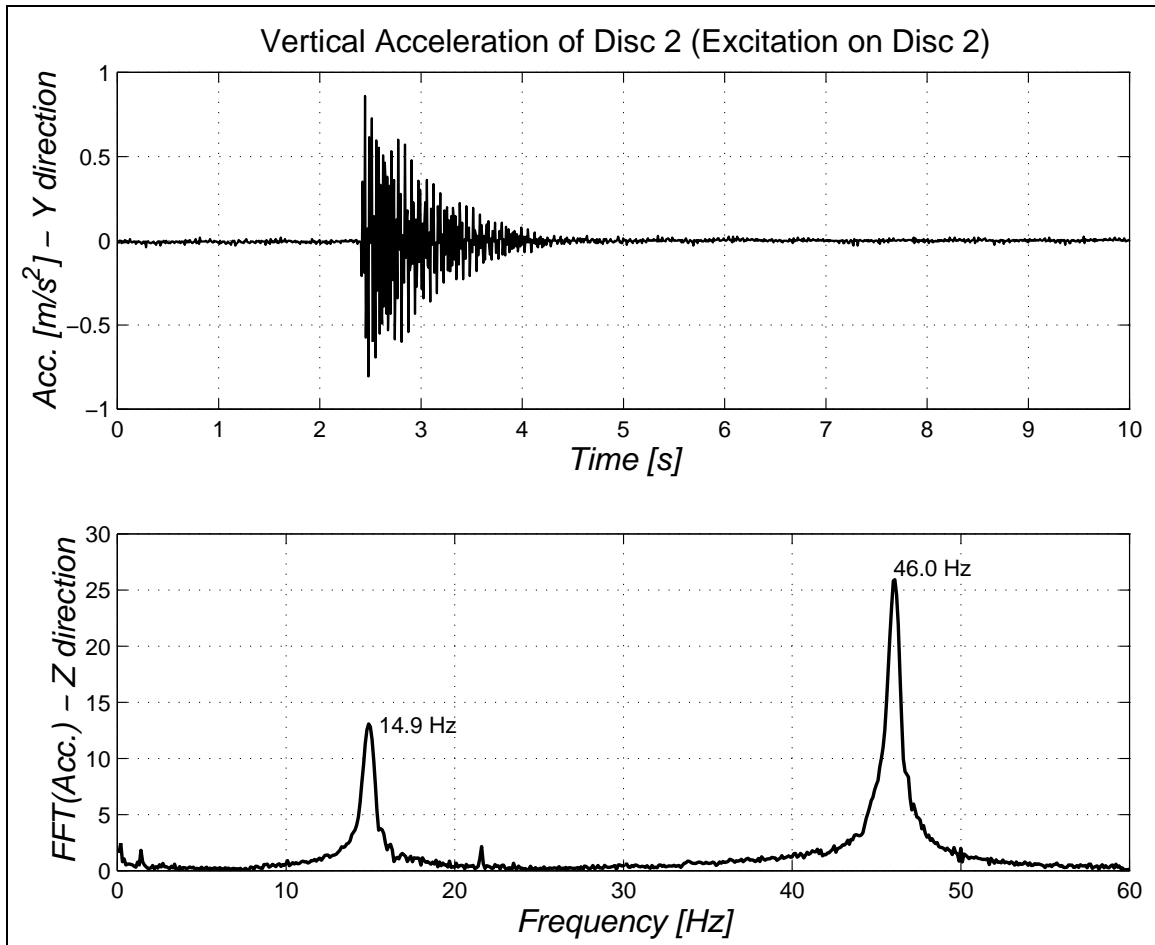


Figure 24: *Experimental Analysis – Transient lateral vibration of the rotor-bearing system, when the rotor has no angular velocity, and it is excited by a vertical perturbation (shock) on the disc 2 (node 4) and the horizontal acceleration of the disc 2 (node 4) is measured.*



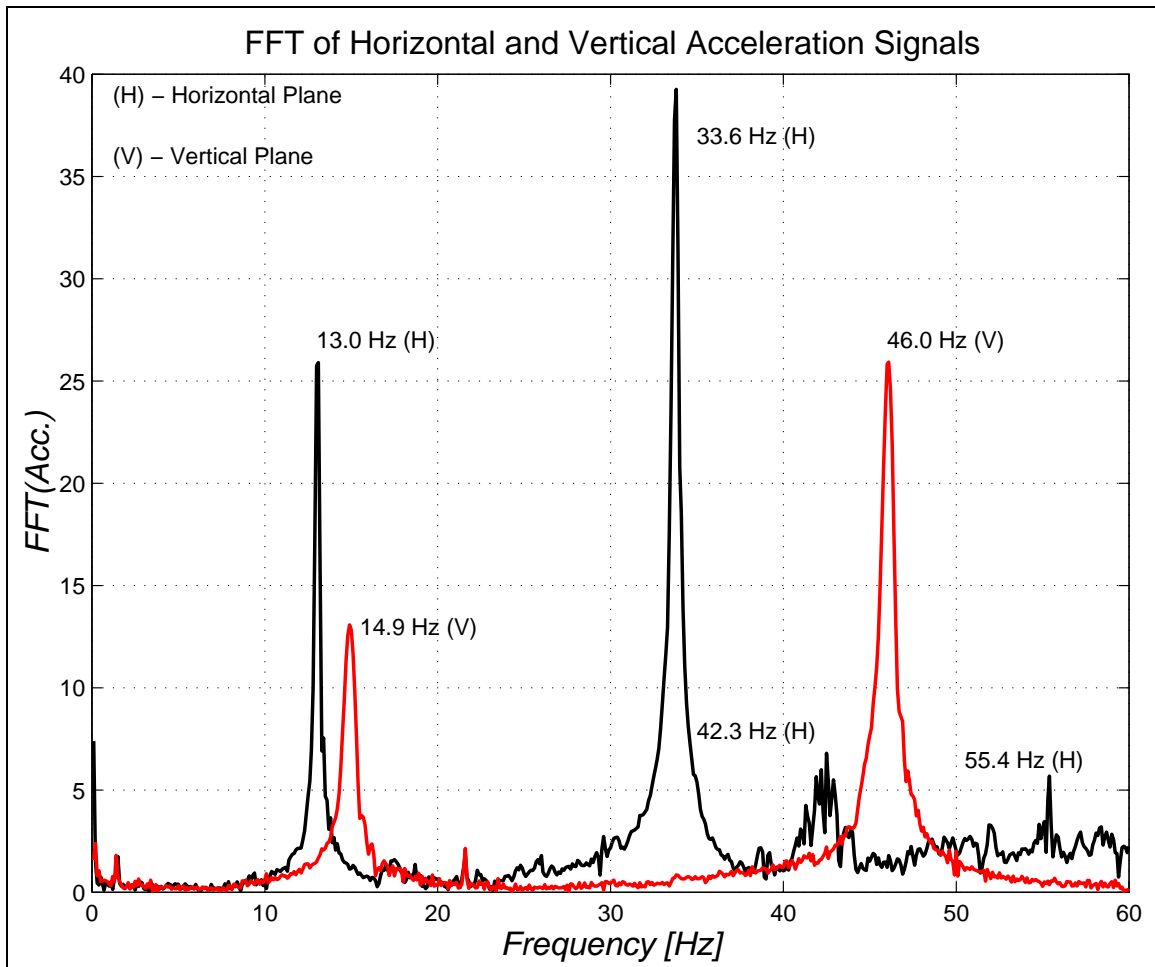


Figure 25: *Experimental Analysis - Natural frequencies of the rotor-bearing system: 13.0 Hz and 33.6 Hz in the horizontal plane, and 14.9 Hz and 46 Hz in the vertical place.*

### 1.6.5 Validation of Rotor-Bearing System Modelling – Theoretical Transient Analysis and MatLab Program

```

%%%%%%%%%%%%%%%%%%%%%%%%%%%%%%%%%%%%%%%%%%%%%%%%%%%%%%%%%%%%%%%%%%%%%%%%
% MACHINERY DYNAMICS LECTURES (41614) %
% MEK - DEPARTMENT OF MECHANICAL ENGINEERING %
% DTU - TECHNICAL UNIVERSITY OF DENMARK %
% %
% Copenhagen, February 10th, 2001 %
% %
% Ilmar Ferreira Santos %
% %
% ROTATING MACHINES -- TRANSIENT TIME DOMAIN ANALYSIS %
% %
% EXPERIMENTAL RESULTS %
% 13.0 (horizontal) %
% 14.9 (vertical) %
% 33.6 (horizontal) %
% 43.0 (horizontal) %
% 46.0 (vertical) %
% %
%%%%%%%%%%%%%%%%%%%%%%%%%%%%%%%%%%%%%%%%%%%%%%%%%%%%%%%%%%%%%%%%%%%%%%%%

clear all;
close all;

%%%%%%%%%%%%%%%%%%%%%%%%%%%%%%%%%%%%%%%%%%%%%%%%%%%%%%%%%%%%%%%%%%%%%%%%
% DEFINITION OF THE MODEL STRUCTURE %
%%%%%%%%%%%%%%%%%%%%%%%%%%%%%%%%%%%%%%%%%%%%%%%%%%%%%%%%%%%%%%%%%%%%%%%%
NE=4; % number of shaft elements
GL = (NE+1)*4; % number of degree of freedom
ND=2; % number of discs
NM=2; % number of bearings
CD1=2; % node - disc 1
CD2=4; % node - disc 2
CMM1=1; % node - bearing 1
CMM2=5; % node - bearing 2

%%%%%%%%%%%%%%%%%%%%%%%%%%%%%%%%%%%%%%%%%%%%%%%%%%%%%%%%%%%%%%%%%%%%%%%%
% CONSTANTS %
%%%%%%%%%%%%%%%%%%%%%%%%%%%%%%%%%%%%%%%%%%%%%%%%%%%%%%%%%%%%%%%%%%%%%%%%
E = 2.0E11; % elasticity modulus [N/m^2]
RAco = 7800; % steel density [kg/m^3]
RAL = 2770; % aluminum density [kg/m^3]

%%%%%%%%%%%%%%%%%%%%%%%%%%%%%%%%%%%%%%%%%%%%%%%%%%%%%%%%%%%%%%%%%%%%%%%%
% OPERATIONAL CONDITIONS %
%%%%%%%%%%%%%%%%%%%%%%%%%%%%%%%%%%%%%%%%%%%%%%%%%%%%%%%%%%%%%%%%%%%%%%%%
Omega = 20*2*pi; % angular velocity [rad/s]
Omega = 0*2*pi; % angular velocity [rad/s]

%%%%%%%%%%%%%%%%%%%%%%%%%%%%%%%%%%%%%%%%%%%%%%%%%%%%%%%%%%%%%%%%%%%%%%%%
% GEOMETRY OF THE ROTATING MACHINE %
%%%%%%%%%%%%%%%%%%%%%%%%%%%%%%%%%%%%%%%%%%%%%%%%%%%%%%%%%%%%%%%%%%%%%%%%
%(A) DISCS
Rd = 6/100; % disc radius [m]
espD = 1.1/100 ; % disc thickness [m]
MasD = pi*Rd^2*espD*RAL; % disc mass [kg]
Id = 1/4*MasD*Rd^2+1/12*MasD*espD^2; % transversal mass moment of inertia of the disc [Kgm^2]
Ip = 1/2*MasD*Rd*Rd; % polar mass moment of inertia of the disc [Kgm^2]

```

```

%(B) BEARINGS
MasM = 0.40698; % bearing mass [kg](housing + ball bearings)
h=1/1000; % beam thickness [m]
b=28.5/1000; % beam width [m]
Area=b*h; % beam cross section area [m^2]
I=b*h^3/12; % beam moment of inertia of area [m^4]
lr=7.5/100; % beam length [m]
Kty0=2*12*E*I/(lr^3); % equivalent beam flexural stiffness [N/m]
Ktz0=2*E*Area/lr; % equivalent bar stiffness [N/m]
% Bearing 1 - Damping
Dty1 = 0.0 ;
Dtz1 = 0.0 ;
Dry1 = 0.0 ;
Drz1 = 0.0 ;
% Bearing 2 - Damping
Dty2 = 0.0 ;
Dtz2 = 0.0 ;
Dry2 = 0.0 ;
Drz2 = 0.0 ; %
% Bearing 1 - Stiffness
Kty1 = Kty0 ;
Ktz1 = Ktz0 ;
Kry1 = 0.0 ;
Krz1 = 0.0 ;
% Bearing 2 - Stiffness
Kty2 = Kty0 ;
Ktz2 = Ktz0 ;
Kry2 = 0.0 ;
Krz2 = 0.0 ;

%(C) SHAFT
l1 = 435/1000; % length of shaft elements [m]
Rext = (6/2)/1000; % shaft external radius [m]
Rint = (0/2)/1000; % shaft internal radius [m]

% length of the shaft elements [m]
l(1) = 0.140;
l(2) = 0.205/2;
l(3) = 0.205/2;
l(4) = 0.090;

% external radius of shaft elements [m]
for i=1:NE,
    rx(i)=Rext;
end

% internal radius of shaft elements [m]
for i=1:NE,
    ri(i)=Rint;
end

% density of shaft elements [kg/m]
for i=1:NE,
    ro(i) = RAco;
end

% transversal areal of the shaft elements [m^2]}
for i=1:NE,
    St(i) = pi*(rx(i)^2-ri(i)^2);
end

% area moment of inertia of the shaft elements [m^4]}

```

```

for i=1:NE,
    II(i)=pi*((rx(i)+ri(i))/2)^3*(rx(i)-ri(i));
end

%%%%%%%%%%%%%%%%%%%%%%%%%%%%%%%%%%%%%%%%%%%%%%%%%%%%%%%%%%%%%%%%%%%%%%%%
%           MOUNTING THE GLOBAL MATRICES           %
%%%%%%%%%%%%%%%%%%%%%%%%%%%%%%%%%%%%%%%%%%%%%%%%%%%%%%%%%%%%%%%%%%%%%%%%

disp('MOUNTING THE GLOBAL MATRICES - WAIT!')
disp(' ')

%{Defining the global matrices with zero elements}
M=zeros(GL);
G=zeros(GL);
K=zeros(GL);

%-----
%GLOBAL MASS MATRIX
%-----

disp('MOUNTING THE GLOBAL MASS MATRIX - WAIT!')
disp(' ')

%Mass matrix of shaft elements

a=1; b=8;

for n=1:NE,

    MteAux= [156      0      0      22*(n)      54      0      0      -13*(n)
              0      156     -22*(n)      0      0      54      13*(n)      0
              0     -22*(n)   4*(n)^2      0      0     -13*(n)   -3*(n)^2      0
            22*(n)      0      0      4*(n)^2   13*(n)      0      0     -3*(n)^2
              54      0      0      13*(n)     156      0      0     -22*(n)
              0      54     -13*(n)      0      0      156     22*(n)      0
              0     13*(n)   -3*(n)^2      0      0     22*(n)   4*(n)^2      0
            -13*(n)      0      0     -3*(n)^2  -22*(n)      0      0     4*(n)^2];

    Mte = ((ro(n)*St(n)*l(n))/420)*MteAux;

    MreAux= [36      0      0      3*(n)     -36      0      0      3*(n)
              0      36     -3*(n)      0      0     -36     -3*(n)      0
              0     -3*(n)   4*(n)^2      0      0     3*(n)   -1*(n)^2      0
            3*(n)      0      0      4*(n)^2  -3*(n)      0      0     -1*(n)^2
            -36      0      0     -3*(n)     36      0      0     -3*(n)
              0     -36     3*(n)      0      0     36     3*(n)      0
              0     -3*(n)   -1*(n)^2      0      0     3*(n)   4*(n)^2      0
            3*(n)      0      0     -1*(n)^2  -3*(n)      0      0     4*(n)^2];

    Mre = ((ro(n)*II(n))/(30*(n)))*MreAux;

    MauxT=Mte+Mre;

    for f=a:b,
        for g=a:b,
            M(f,g)=M(f,g)+MauxT(f-(n-1)*4,g-(n-1)*4);
        end
    end

a=a+4; b=b+4;

```

```

end

% Adding the mass matrices of the disc elements

M((CD1-1)*4+1,(CD1-1)*4+1)=M((CD1-1)*4+1,(CD1-1)*4+1)+MasD;
M((CD1-1)*4+2,(CD1-1)*4+2)=M((CD1-1)*4+2,(CD1-1)*4+2)+MasD;
M((CD1-1)*4+3,(CD1-1)*4+3)=M((CD1-1)*4+3,(CD1-1)*4+3)+Id;
M((CD1-1)*4+4,(CD1-1)*4+4)=M((CD1-1)*4+4,(CD1-1)*4+4)+Id;
M((CD2-1)*4+1,(CD2-1)*4+1)=M((CD2-1)*4+1,(CD2-1)*4+1)+MasD;
M((CD2-1)*4+2,(CD2-1)*4+2)=M((CD2-1)*4+2,(CD2-1)*4+2)+MasD;
M((CD2-1)*4+3,(CD2-1)*4+3)=M((CD2-1)*4+3,(CD2-1)*4+3)+Id;
M((CD2-1)*4+4,(CD2-1)*4+4)=M((CD2-1)*4+4,(CD2-1)*4+4)+Id;

% Adding the mass matrices of the bearing elements

M((CMM1-1)*4+1,(CMM1-1)*4+1)=M((CMM1-1)*4+1,(CMM1-1)*4+1)+MasM;
M((CMM1-1)*4+2,(CMM1-1)*4+2)=M((CMM1-1)*4+2,(CMM1-1)*4+2)+MasM;
M((CMM2-1)*4+1,(CMM2-1)*4+1)=M((CMM2-1)*4+1,(CMM2-1)*4+1)+MasM;
M((CMM2-1)*4+2,(CMM2-1)*4+2)=M((CMM2-1)*4+2,(CMM2-1)*4+2)+MasM;

%-----
%GLOBAL GYROSCOPIC MATRIX
%-----

disp('MOUNTING THE GLOBAL GYROSCOPIC MATRIX - WAIT!')
disp(' ')

%Gyroscopic matrix of shaft elements

a=1; b=8;

for n=1:NE,

    GeAux=[0        -36        3*(n)    0        0        36        3*(n)    0
            36        0          0        3*(n)   -36        0          0        3*(n)
           -3*(n)    0          0       -4*(n)^2  3*(n)    0          0        1*(n)^2
            0       -3*(n)    4*(n)^2    0          0        3*(n)   -1*(n)^2    0
            0        36       -3*(n)    0          0       -36       -3*(n)    0
           -36        0          0       -3*(n)    36        0          0       -3*(n)
           -3*(n)    0          0        1*(n)^2  3*(n)    0          0       -4*(n)^2
            0       -3*(n)   -1*(n)^2    0          0        3*(n)   4*(n)^2    0        ];

    Ge=Omega*(ro(n)*II(n))/(15*(n))*GeAux;

    for f=a:b,
        for g=a:b,
            G(f,g)=G(f,g)+Ge(f-(n-1)*4,g-(n-1)*4);
        end
    end

a=a+4; b=b+4;

end

% Adding the gyroscopic matrices of the disc elements

G((CD1-1)*4+3,(CD1-1)*4+4)=G((CD1-1)*4+3,(CD1-1)*4+4)-Omega*Ip;
G((CD1-1)*4+4,(CD1-1)*4+3)=G((CD1-1)*4+4,(CD1-1)*4+3)+Omega*Ip;
G((CD2-1)*4+3,(CD2-1)*4+4)=G((CD2-1)*4+3,(CD2-1)*4+4)-Omega*Ip;
G((CD2-1)*4+4,(CD2-1)*4+3)=G((CD2-1)*4+4,(CD2-1)*4+3)+Omega*Ip;

%-----

```

```

%GLOBAL STIFFNESS MATRIX
%-----

disp('MOUNTING THE GLOBAL STIFFNESS MATRIX - WAIT!')
disp(' ')

% Stiffness matrix of shaft elements

a=1; b=8;

for n=1:NE,

    KbeAux= [12      0      0      6*1(n)   -12      0      0      6*1(n)
             0      12     -6*1(n)  0         0       -12     -6*1(n)  0
             0     -6*1(n)  4*1(n)^2  0         0       6*1(n)  2*1(n)^2  0
            6*1(n)  0         0      4*1(n)^2 -6*1(n)  0         0      2*1(n)^2
            -12     0         0     -6*1(n)  12        0         0     -6*1(n)
             0     -12     6*1(n)  0         0        12     6*1(n)  0
             0     -6*1(n)  2*1(n)^2  0         0       6*1(n)  4*1(n)^2  0
            6*1(n)  0         0      2*1(n)^2 -6*1(n)  0         0      4*1(n)^2];

    Kbe = ((E*II(n))/(1(n)^3))*KbeAux;

    for f=a:b,
        for g=a:b,
            K(f,g)=K(f,g)+Kbe(f-(n-1)*4,g-(n-1)*4);
        end
    end

a=a+4; b=b+4;

end

% Adding the stiffness matrices of the bearing elements

K((CMM1-1)*4+1,(CMM1-1)*4+1)=K((CMM1-1)*4+1,(CMM1-1)*4+1)+Kty1;
K((CMM1-1)*4+2,(CMM1-1)*4+2)=K((CMM1-1)*4+2,(CMM1-1)*4+2)+Ktz1;
K((CMM2-1)*4+1,(CMM2-1)*4+1)=K((CMM2-1)*4+1,(CMM2-1)*4+1)+Kty2;
K((CMM2-1)*4+2,(CMM2-1)*4+2)=K((CMM2-1)*4+2,(CMM2-1)*4+2)+Ktz2;

%%%%%%%%%%%%%%%%%%%%%%%%%%%%%%%%%%%%%%%%%%%%%%%%%%%%%%%%%%%%%%%%%%%%%%%%
% GLOBAL MATHEMATICAL MODEL %
%%%%%%%%%%%%%%%%%%%%%%%%%%%%%%%%%%%%%%%%%%%%%%%%%%%%%%%%%%%%%%%%%%%%%%%%

A=[    G          M
      M          zeros(size(M,1))];

B=[    K          zeros(size(M,1))
      zeros(size(M,1))  -M      ];

%%%%%%%%%%%%%%%%%%%%%%%%%%%%%%%%%%%%%%%%%%%%%%%%%%%%%%%%%%%%%%%%%%%%%%%%
% ANALYSIS IN TIME DOMAIN %
%%%%%%%%%%%%%%%%%%%%%%%%%%%%%%%%%%%%%%%%%%%%%%%%%%%%%%%%%%%%%%%%%%%%%%%%

%Dynamical Properties of the Rotor-Bearing System
[u,w]=eig(-B,A);          %natural frequency [rad/s]

%-----
%Inicial Condition

```

```

y_ini(1:GL)=0;           % setting initial deflections zero [m]
v_ini(1:GL)=0;           % setting initial velocities zero [m/s]
gl_of_exc=5;             % degree of freedom where the initial
                        % conditions is applied
y_ini(gl_of_exc)=0.00;   % initial deflection [m]
y_ini(gl_of_exc+1)=0.00; % initial deflection [m]
v_ini(gl_of_exc)=0.01;   % initial velocities [m/s]
v_ini(gl_of_exc+1)=0.01; % initial velocities [m/s]
freq_exc = 0.00;         % excitation frequency [Hz]
force(1:GL)=0;           % setting excitation forces zero [N]
force(gl_of_exc)=0.00;   % excitation force is applied [N]
force(gl_of_exc+1)=0.00; % excitation force is applied [N]
time_max = 5.0;          % integration time [s]
%-----

%-----
%EXACT SOLUTION
n=1200;                   % number of points for plotting
j=sqrt(-1);               % complex number
w_exc=2*pi*freq_exc;      % excitation frequency [rad/s]

z_ini      = [y_ini v_ini]';
force_exc  = [force force*0]';
INVA       = inv((j*w_exc*A + B));
vec_aux    = z_ini - INVA*force_exc;

C=inv(u)*(vec_aux);

for i=1:n,
    t(i)=(i-1)/n*time_max;
    freq(i)=(i-1)/time_max;
    y_exact(1:2*GL,1) = 0;

    for ii=1:2*GL,
        y_exact = y_exact + C(ii)*u(1:2*GL,ii)*exp(w(ii,ii)*t(i));
    end
    y_exact = y_exact + INVA*force_exc*exp(j*w_exc*t(i));

    v1_exact(i) = y_exact(1); % bearing 1 - horizontal direction
    w1_exact(i) = y_exact(2); % bearing 1 - vertical direction
    v2_exact(i) = y_exact(5); % disc 1 - horizontal direction
    w2_exact(i) = y_exact(6); % disc 1 - vertical direction

end

    FFTv1 = abs(fft(real(v1_exact))) ; % bearing 1 - horizontal direction
    FFTw1 = abs(fft(real(w1_exact))) ; % bearing 1 - vertical direction
    FFTv2 = abs(fft(real(v2_exact))) ; % disc 1 - horizontal direction
    FFTw2 = abs(fft(real(w2_exact))) ; % disc 1 - vertical direction

figure(1)
subplot(2,2,1), plot(t,real(v1_exact),'b')
title('Horizontal Response of Bearing 1','FontSize',14)
xlabel('time [s]','FontSize',14)
ylabel('v_{1}(t) [m]','FontSize',14)
grid
subplot(2,2,2), plot(freq(1:n/4),FFTv1(1:n/4),'b','LineWidth',1.5)
title('Horizontal Response of Bearing 1','FontSize',14)
xlabel('freq [Hz]','FontSize',14)
ylabel('FFT(v_{1}(t)) [m]','FontSize',14)
grid
subplot(2,2,3), plot(t,real(w1_exact),'b')

```

```

title('Vertical Response of Bearing 1','FontSize',14)
xlabel('time [s]','FontSize',14)
ylabel('w_{1}(t) [m]','FontSize',14)
grid
subplot(2,2,4), plot(freq(1:n/4),FFTw1(1:n/4),'b','LineWidth',1.5)
title('Vertical Response of Bearing 1','FontSize',14)
xlabel('freq [Hz]','FontSize',14)
ylabel('FFT(w_{1}(t)) [m]','FontSize',14)
grid

figure(2)
subplot(2,2,1), plot(t,real(v2_exact),'b')
title('Horizontal Response of Disc 1','FontSize',14)
xlabel('time [s]','FontSize',14)
ylabel('v_{2}(t) [m]','FontSize',14)
grid
subplot(2,2,2), plot(freq(1:n/4),FFTv2(1:n/4),'b','LineWidth',1.5)
title('Horizontal Response of Disc 1','FontSize',14)
xlabel('freq [Hz]','FontSize',14)
ylabel('FFT(v_{2}(t)) [m]','FontSize',14)
grid
subplot(2,2,3), plot(t,real(w2_exact),'b')
title('Vertical Response of Disc 1','FontSize',14)
xlabel('time [s]','FontSize',14)
ylabel('w_{2}(t) [m]','FontSize',14)
grid
subplot(2,2,4), plot(freq(1:n/4),FFTw2(1:n/4),'b','LineWidth',1.5)
title('Vertical Response of Disc 1','FontSize',14)
xlabel('freq [Hz]','FontSize',14)
ylabel('FFT(w_{2}(t)) [m]','FontSize',14)
grid

figure(3)
subplot(2,2,1), plot(t,real(v1_exact),'b')
title('Hor. Resp. - Bearing 1','FontSize',12)
xlabel('time [s]','FontSize',14)
ylabel('v_{1}(t) [m]','FontSize',14)
grid
subplot(2,2,2), plot(freq(1:n/4),FFTv1(1:n/4),'b','LineWidth',1.5)
title('Hor. Resp. - Bearing 1','FontSize',12)
xlabel('freq [Hz]','FontSize',12)
ylabel('FFT(v_{1}(t)) [m]','FontSize',14)
grid
subplot(2,2,3), plot(t,real(w2_exact),'b')
title('Vert. Resp. - Disc 1','FontSize',12)
xlabel('time [s]','FontSize',14)
ylabel('w_{2}(t) [m]','FontSize',14)
grid
subplot(2,2,4), plot(freq(1:n/4),FFTw2(1:n/4),'b','LineWidth',1.5)
title('Vert. Resp. - Disc 1','FontSize',12)
xlabel('freq [Hz]','FontSize',14)
ylabel('FFT(w_{2}(t)) [m]','FontSize',14)
grid

```



### 1.6.6 Validation of Rotor-Bearing System Modelling – Theoretical Transient Analysis and MatLab Program Results in Time and Frequency Domains

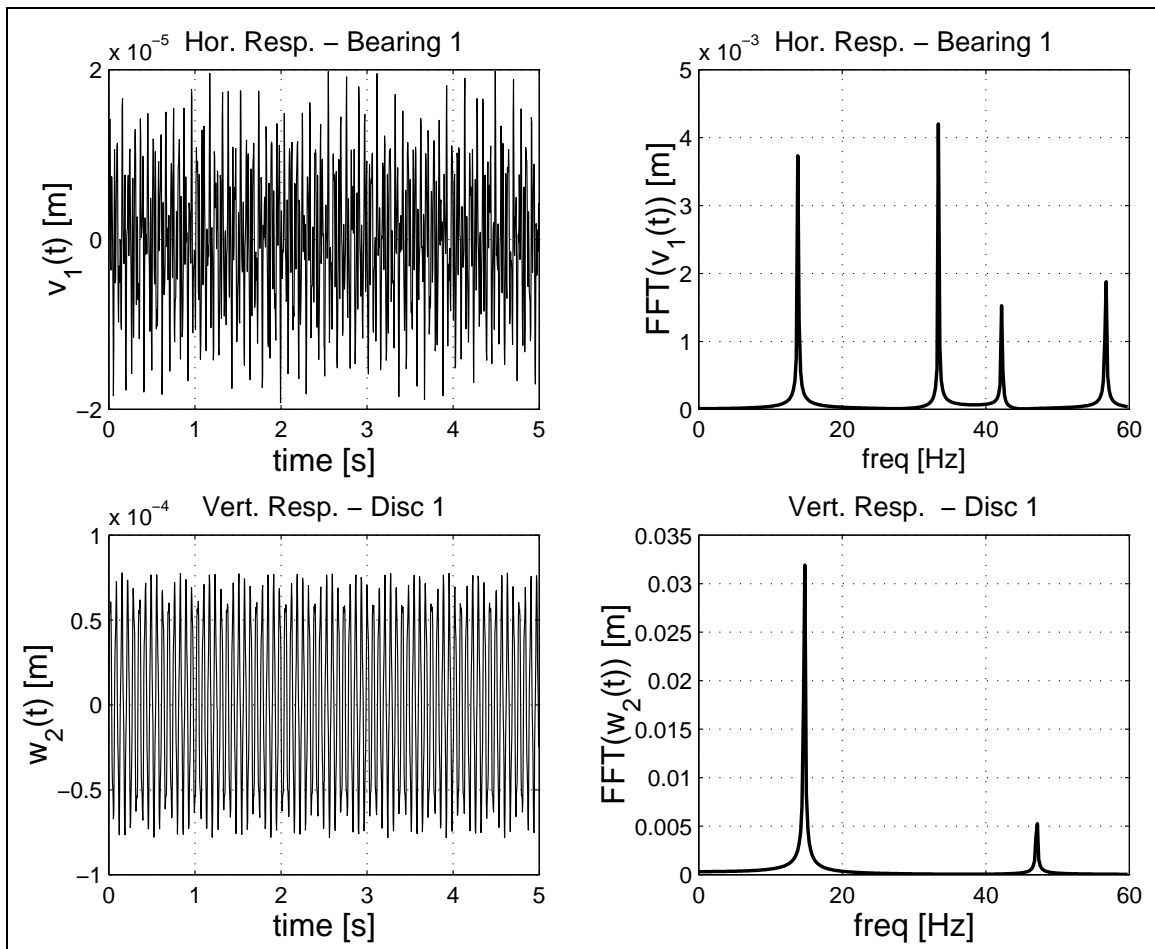


Figure 26: *Theoretical Transient Analysis - (a) Time response of the bearing 1 and disc 1 when the disc 1 is excited in the horizontal and in the vertical directions by means of a velocity perturbation; (b) FFT of the bearing 1 and disc 1 responses when the disc 1 is excited in the horizontal and in the vertical direction by means of a velocity perturbation. Theoretical natural frequencies of the rotor-bearing system: 13.8 Hz, 14.7 Hz, 33.4 Hz, 42.3 Hz, 47.1 Hz and 56.7 Hz.*

### 1.6.7 Campbell Diagram – MatLab Program and Theoretical Results

The natural frequencies of a rotor-bearing-system changes with respect to the angular velocity. With help of the Campbell's diagram one can determine the critical speeds, as can be seen in figure 27.

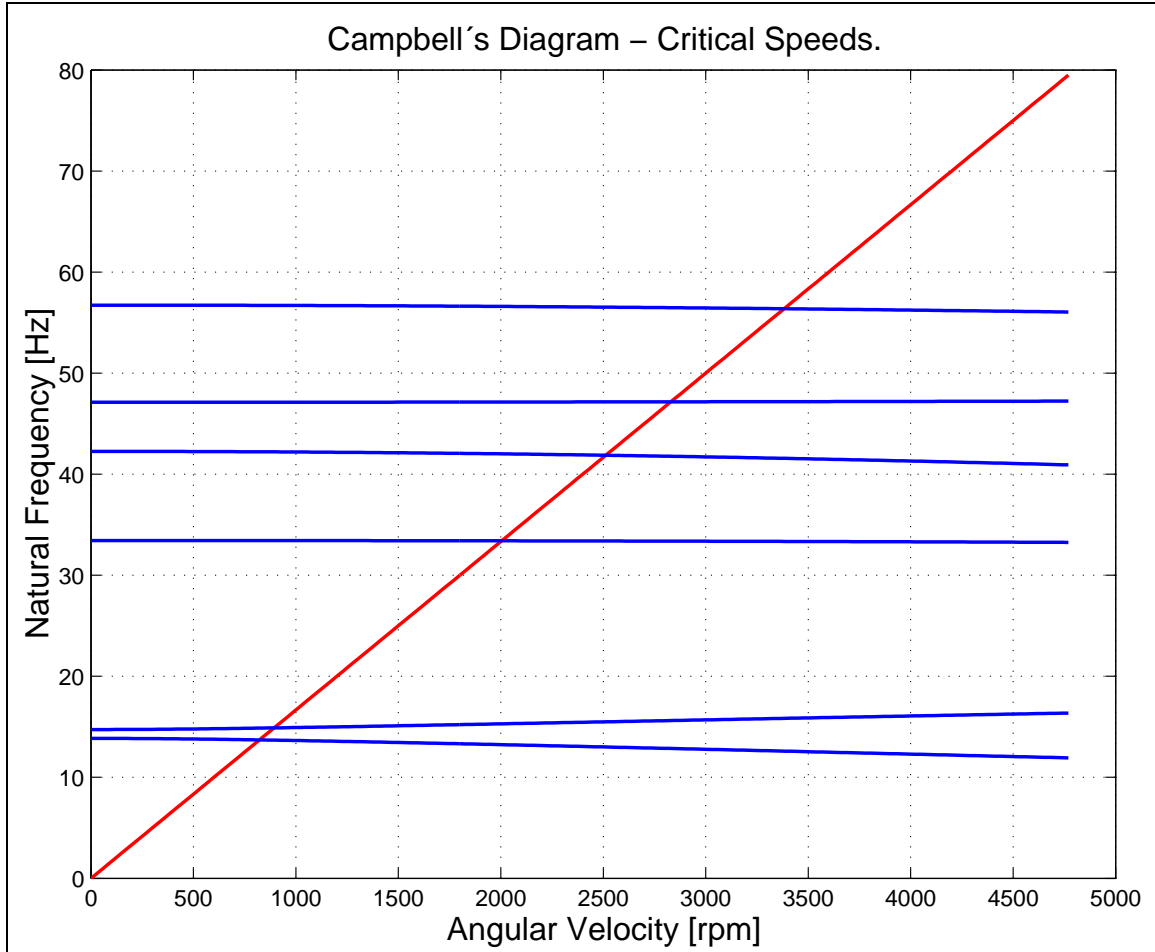


Figure 27: *Campbell's Diagram – Behavior of the six first natural frequencies of the rotor-bearing system as a function of the angular velocity.*

```

%%%%%%%%%%%%%%%%%%%%%%%%%%%%%%%%%%%%%%%%%%%%%%%%%%%%%%%%%%%%%%%%%%%%%%%%
% MACHINERY DYNAMICS LECTURES (41614) %
% MEK - DEPARTMENT OF MECHANICAL ENGINEERING %
% DTU - TECHNICAL UNIVERSITY OF DENMARK %
% %
% Copenhagen, February 10th, 2001 %
% %
% Ilmar Ferreira Santos %
% %
% ROTATING MACHINES -- CAMPBELL'S DIAGRAM %
% %
%%%%%%%%%%%%%%%%%%%%%%%%%%%%%%%%%%%%%%%%%%%%%%%%%%%%%%%%%%%%%%%%%%%%%%%%

clear all;
close all;

N_campbell = 160;

%%%%%%%%%%%%%%%%%%%%%%%%%%%%%%%%%%%%%%%%%%%%%%%%%%%%%%%%%%%%%%%%%%%%%%%%
% DEFINITION OF THE MODEL STRUCTURE %
%%%%%%%%%%%%%%%%%%%%%%%%%%%%%%%%%%%%%%%%%%%%%%%%%%%%%%%%%%%%%%%%%%%%%%%%
NE=4; % number of shaft elements
GL = (NE+1)*4; % number of degree of freedom
ND=2; % number of discs
NM=2; % number of bearings
CD1=2; % node - disc 1
CD2=4; % node - disc 2
CMM1=1; % node - bearing 1
CMM2=5; % node - bearing 2

%%%%%%%%%%%%%%%%%%%%%%%%%%%%%%%%%%%%%%%%%%%%%%%%%%%%%%%%%%%%%%%%%%%%%%%%
% CONSTANTS %
%%%%%%%%%%%%%%%%%%%%%%%%%%%%%%%%%%%%%%%%%%%%%%%%%%%%%%%%%%%%%%%%%%%%%%%%
E = 2.0E11; % elasticity modulus [N/m^2]
RAco = 7800; % steel density [kg/m^3]
RAL = 2770; % aluminum density [kg/m^3]

%%%%%%%%%%%%%%%%%%%%%%%%%%%%%%%%%%%%%%%%%%%%%%%%%%%%%%%%%%%%%%%%%%%%%%%%
% GEOMETRY OF THE ROTATING MACHINE %
%%%%%%%%%%%%%%%%%%%%%%%%%%%%%%%%%%%%%%%%%%%%%%%%%%%%%%%%%%%%%%%%%%%%%%%%
%(A) DISCS
Rd = 6/100; % disc radius [m]
espD = 1.1/100; % disc thickness [m]
MasD = pi*Rd^2*espD*RAL; % disc mass [kg]
Id = 1/4*MasD*Rd^2+1/12*MasD*espD^2; % transversal mass moment of inertia of the disc [Kgm^2]
Ip = 1/2*MasD*Rd*Rd; % polar mass moment of inertia of the disc [Kgm^2]

%(B) BEARINGS
MasM = 0.40698; % bearing mass [kg] (housing + ball bearings)
h=1/1000; % beam thickness [m]
b=28.5/1000; % beam width [m]
Area=b*h; % beam cross section area [m^2]
I=b*h^3/12; % beam moment of inertia of area [m^4]
lr=7.5/100; % beam length [m]
Kty0=2*12*E*I/(lr^3); % equivalent beam flexural stiffness [N/m]
Ktz0=2*E*Area/lr; % equivalent bar stiffness [N/m]
% Bearing 1 - Damping
Dty1 = 0.0;
Dtz1 = 0.0;
Dry1 = 0.0;
Drz1 = 0.0;

```

```

% Bearing 2 - Damping
Dty2 = 0.0 ;
Dtzt2 = 0.0 ;
Dry2 = 0.0 ;
Drz2 = 0.0 ; %
% Bearing 1 - Stiffness
Kty1 = Kty0 ;
Ktz1 = Ktz0 ;
Kry1 = 0.0 ;
Krz1 = 0.0 ;
% Bearing 2 - Stiffness
Kty2 = Kty0 ;
Ktz2 = Ktz0 ;
Kry2 = 0.0 ;
Krz2 = 0.0 ;

%(C) SHAFT
l1 = 435/1000; % length of shaft elements [m]
Rext = (6/2)/1000; % shaft external radius [m]
Rint = (0/2)/1000; % shaft internal radius [m]

% length of the shaft elements [m]
l(1) = 0.140;
l(2) = 0.205/2;
l(3) = 0.205/2;
l(4) = 0.090;

% external radius of shaft elements [m]
for i=1:NE,
    rx(i)=Rext;
end

% internal radius of shaft elements [m]
for i=1:NE,
    ri(i)=Rint;
end

% density of shaft elements [kg/m]
for i=1:NE,
    ro(i) = RAc0;
end

% transversal areal of the shaft elements [m^2]}
for i=1:NE,
    St(i) = pi*(rx(i)^2-ri(i)^2);
end

% area moment of inertia of the shaft elements [m^4]}
for i=1:NE,
    II(i)=pi*((rx(i)+ri(i))/2)^3*(rx(i)-ri(i));
end

%%%%%%%%%%%%%%%%%%%%%%%%%%%%%%%%%%%%%%%%%%%%%%%%%%%%%%%%%%%%%%%%%%%%%%%%
% OPERATIONAL CONDITIONS %
%%%%%%%%%%%%%%%%%%%%%%%%%%%%%%%%%%%%%%%%%%%%%%%%%%%%%%%%%%%%%%%%%%%%%%%%

for iii=1:N_campbell,

    Omega= (iii-1)*2*pi/2; % angular velocity [rad/s]
    Omegarpm(iii) = Omega*60/2/pi; % angular velocity [rpm]

```

```

%%%%%%%%%%%%%%%%%%%%%%%%%%%%%%%%%%%%%%%%%%%%%%%%%%%%%%%%%%%%%%%%%%%%%%%%
%      MOUNTING THE GLOBAL MATRICES      %
%%%%%%%%%%%%%%%%%%%%%%%%%%%%%%%%%%%%%%%%%%%%%%%%%%%%%%%%%%%%%%%%%%%%%%%%

disp('MOUNTING THE GLOBAL MATRICES - WAIT!')
disp(' ')

% Defining the global matrices with zero elements
M=zeros(GL);
G=zeros(GL);
K=zeros(GL);

%%%%%%%%%%%%%%%%%%%%%%%%%%%%%%%%%%%%%%%%%%%%%%%%%%%%%%%%%%%%%%%%%%%%%%%%
% GLOBAL MASS MATRIX %
%%%%%%%%%%%%%%%%%%%%%%%%%%%%%%%%%%%%%%%%%%%%%%%%%%%%%%%%%%%%%%%%%%%%%%%%

disp('MOUNTING THE GLOBAL MASS MATRIX - WAIT!') disp(' ')

% Mass matrices of shaft elements due to linear and angular movements

a=1; b=8;

for n=1:NE,

    MteAux= [156      0      0      22*(n)      54      0      0      -13*(n)
             0      156     -22*(n)      0      0      54     13*(n)      0
             0     -22*(n)    4*(n)^2      0      0     -13*(n)   -3*(n)^2      0
            22*(n)      0      0      4*(n)^2    13*(n)      0      0     -3*(n)^2
             54      0      0      13*(n)     156      0      0     -22*(n)
             0      54     -13*(n)      0      0      156     22*(n)      0
             0     13*(n)   -3*(n)^2      0      0      22*(n)    4*(n)^2      0
            -13*(n)      0      0     -3*(n)^2  -22*(n)      0      0      4*(n)^2];

    Mte = ((ro(n)*St(n)*l(n))/420)*MteAux;

    MreAux= [36      0      0      3*(n)     -36      0      0      3*(n)
             0      36     -3*(n)      0      0     -36     -3*(n)      0
             0     -3*(n)    4*(n)^2      0      0      3*(n)   -1*(n)^2      0
            3*(n)      0      0      4*(n)^2   -3*(n)      0      0     -1*(n)^2
            -36      0      0     -3*(n)      36      0      0     -3*(n)
             0     -36     3*(n)      0      0      36     3*(n)      0
             0     -3*(n)   -1*(n)^2      0      0      3*(n)    4*(n)^2      0
            3*(n)      0      0     -1*(n)^2   -3*(n)      0      0      4*(n)^2];

    Mre = ((ro(n)*II(n))/(30*(n)))*MreAux;

    MauxT=Mte+Mre;

    for f=a:b,
        for g=a:b,
            M(f,g)=M(f,g)+MauxT(f-(n-1)*4,g-(n-1)*4);
        end
    end

a=a+4; b=b+4;

end

% Adding the mass matrices of the disc elements

```

```

M((CD1-1)*4+1,(CD1-1)*4+1)=M((CD1-1)*4+1,(CD1-1)*4+1)+MasD;
M((CD1-1)*4+2,(CD1-1)*4+2)=M((CD1-1)*4+2,(CD1-1)*4+2)+MasD;
M((CD1-1)*4+3,(CD1-1)*4+3)=M((CD1-1)*4+3,(CD1-1)*4+3)+Id;
M((CD1-1)*4+4,(CD1-1)*4+4)=M((CD1-1)*4+4,(CD1-1)*4+4)+Id;
M((CD2-1)*4+1,(CD2-1)*4+1)=M((CD2-1)*4+1,(CD2-1)*4+1)+MasD;
M((CD2-1)*4+2,(CD2-1)*4+2)=M((CD2-1)*4+2,(CD2-1)*4+2)+MasD;
M((CD2-1)*4+3,(CD2-1)*4+3)=M((CD2-1)*4+3,(CD2-1)*4+3)+Id;
M((CD2-1)*4+4,(CD2-1)*4+4)=M((CD2-1)*4+4,(CD2-1)*4+4)+Id;

% Adding the mass matrices of the bearing elements

M((CMM1-1)*4+1,(CMM1-1)*4+1)=M((CMM1-1)*4+1,(CMM1-1)*4+1)+MasM;
M((CMM1-1)*4+2,(CMM1-1)*4+2)=M((CMM1-1)*4+2,(CMM1-1)*4+2)+MasM;
M((CMM2-1)*4+1,(CMM2-1)*4+1)=M((CMM2-1)*4+1,(CMM2-1)*4+1)+MasM;
M((CMM2-1)*4+2,(CMM2-1)*4+2)=M((CMM2-1)*4+2,(CMM2-1)*4+2)+MasM;

%%%%%%%%%%%%%%
% GLOBAL GYROSCOPIC MATRIX %
%%%%%%%%%%%%%%

disp('MOUNTING THE GLOBAL GYROSCOPIC MATRIX - WAIT!') disp(' ')

% Gyroscopic matrix of shaft elements

a=1; b=8;

for n=1:NE,

    GeAux=[0      -36      3*1(n)  0      0      36      3*1(n)  0
            36      0      0      3*1(n) -36      0      0      3*1(n)
           -3*1(n)  0      0      -4*1(n)^2 3*1(n)  0      0      1(n)^2
            0      -3*1(n) 4*1(n)^2 0      0      3*1(n) -1(n)^2 0
            0      36      -3*1(n) 0      0      -36      -3*1(n) 0
           -36      0      0      -3*1(n) 36      0      0      -3*1(n)
           -3*1(n) 0      0      1(n)^2 3*1(n) 0      0      -4*1(n)^2
            0      -3*1(n) -1(n)^2 0      0      3*1(n) 4*1(n)^2 0      ];

    Ge=Omega*(ro(n)*II(n))/(15*1(n))*GeAux;

    for f=a:b,
        for g=a:b,
            G(f,g)=G(f,g)+Ge(f-(n-1)*4,g-(n-1)*4);
        end
    end

a=a+4; b=b+4;

end

% Adding the gyroscopic matrices of the disc elements

G((CD1-1)*4+3,(CD1-1)*4+4)=G((CD1-1)*4+3,(CD1-1)*4+4)-Omega*Ip;
G((CD1-1)*4+4,(CD1-1)*4+3)=G((CD1-1)*4+4,(CD1-1)*4+3)+Omega*Ip;
G((CD2-1)*4+3,(CD2-1)*4+4)=G((CD2-1)*4+3,(CD2-1)*4+4)-Omega*Ip;
G((CD2-1)*4+4,(CD2-1)*4+3)=G((CD2-1)*4+4,(CD2-1)*4+3)+Omega*Ip;

%%%%%%%%%%%%%%
% GLOBAL STIFFNESS MATRIX %

```

```

%%%%%%%%%%%%%%%%%%%%%%%%%%%%%%%%%%%%%%%%%%%%%%%%%%%%%%%%%%%%%%%%%%%%%%%%
disp('MOUNTING THE GLOBAL STIFFNESS MATRIX - WAIT!') disp(' ')

% Stiffness matrix of shaft elements due to bending

a=1; b=8;

for n=1:NE,

    KbeAux= [12      0      0      6*1(n)   -12      0      0      6*1(n)
             0      12     -6*1(n)  0         0       -12     -6*1(n)  0
             0     -6*1(n)  4*1(n)^2  0         0       6*1(n)  2*1(n)^2  0
            6*1(n)  0         0      4*1(n)^2 -6*1(n)  0         0      2*1(n)^2
            -12     0         0     -6*1(n)  12         0         0      -6*1(n)
             0     -12     6*1(n)  0         0         12        6*1(n)  0
             0     -6*1(n)  2*1(n)^2  0         0       6*1(n)  4*1(n)^2  0
            6*1(n)  0         0      2*1(n)^2 -6*1(n)  0         0      4*1(n)^2];

    Kbe = ((E*II(n))/(l(n)^3))*KbeAux;

    for f=a:b,
        for g=a:b,
            K(f,g)=K(f,g)+Kbe(f-(n-1)*4,g-(n-1)*4);
        end
    end

a=a+4; b=b+4;

end

% Adding the stiffness matrices of the bearing elements

K((CMM1-1)*4+1,(CMM1-1)*4+1)=K((CMM1-1)*4+1,(CMM1-1)*4+1)+Ktz1;
K((CMM1-1)*4+2,(CMM1-1)*4+2)=K((CMM1-1)*4+2,(CMM1-1)*4+2)+Kty1;
K((CMM2-1)*4+1,(CMM2-1)*4+1)=K((CMM2-1)*4+1,(CMM2-1)*4+1)+Ktz2;
K((CMM2-1)*4+2,(CMM2-1)*4+2)=K((CMM2-1)*4+2,(CMM2-1)*4+2)+Kty2;

%%%%%%%%%%%%%%%%%%%%%%%%%%%%%%%%%%%%%%%%%%%%%%%%%%%%%%%%%%%%%%%%%%%%%%%%
% GLOBAL MATHEMATICAL MODEL %
%%%%%%%%%%%%%%%%%%%%%%%%%%%%%%%%%%%%%%%%%%%%%%%%%%%%%%%%%%%%%%%%%%%%%%%%

Mglob=[ G      M
        M      zeros(size(M,1))];
Kglob=[ K      zeros(size(M,1))
        zeros(size(M,1))  -M      ];

%%%%%%%%%%%%%%%%%%%%%%%%%%%%%%%%%%%%%%%%%%%%%%%%%%%%%%%%%%%%%%%%%%%%%%%%
% MODAL ANALYSIS %
%%%%%%%%%%%%%%%%%%%%%%%%%%%%%%%%%%%%%%%%%%%%%%%%%%%%%%%%%%%%%%%%%%%%%%%%

disp('CALCULATING NATURAL FREQUENCIES AND MODE SHAPES - WAIT!')
disp(' ')

% Calculating Eigenvectors and Eigenvalues

[U,lambda]=eig(-Kglob,Mglob);
[lam,p]=sort(abs(diag(lambda)));
U=U(:,p);

```

```

lambda_campbell(iii,:)=lam'/2/pi;

end

figure(1) plot(Omegarpm,Omegarpm/60,'r','LineWidth',1.5) grid hold
on
plot(Omegarpm,lambda_campbell(1:N_campbell,1),'b','LineWidth',1.5)
hold on
plot(Omegarpm,lambda_campbell(1:N_campbell,3),'b','LineWidth',1.5)
hold on
plot(Omegarpm,lambda_campbell(1:N_campbell,5),'b','LineWidth',1.5)
hold on
plot(Omegarpm,lambda_campbell(1:N_campbell,7),'b','LineWidth',1.5)
hold on
plot(Omegarpm,lambda_campbell(1:N_campbell,9),'b','LineWidth',1.5)
hold on
plot(Omegarpm,lambda_campbell(1:N_campbell,11),'b','LineWidth',1.5)
hold on title('Campbell's Diagram - Critical
Speeds.','FontSize',14)

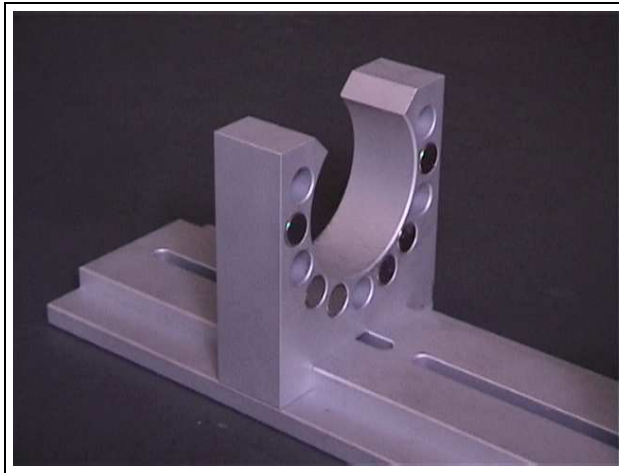
xlabel('Angular Velocity [rpm]','FontSize',14)
ylabel('NaturalFrequency [Hz]','FontSize',14)

```

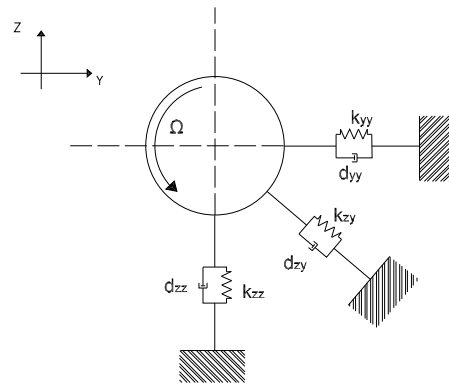


## 1.7 Basic Phenomenology of Rotor-Bearing Systems

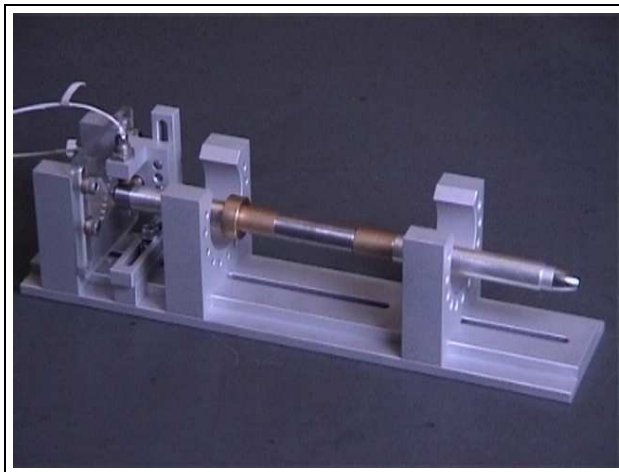
### 1.7.1 Steady-State Response due to Unbalance Excitation - Forward and Backward Orbits



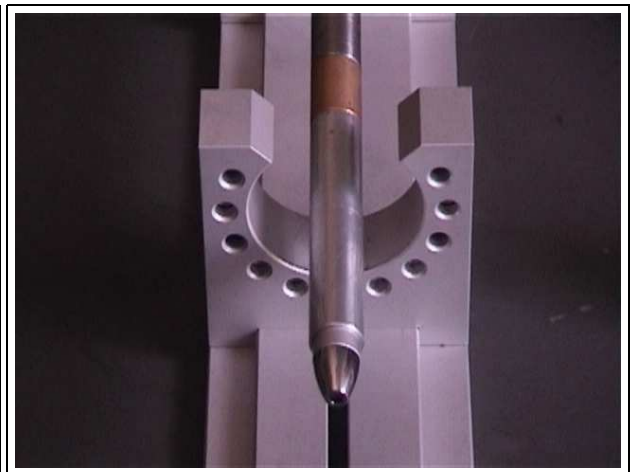
(a) passive magnetic bearing



(b) mechanical model



(c) rotor supported by magnetic forces



(d) rotor-bearing system

Figure 28: (a) *Passive magnetic bearing – resultant magnetic forces in the horizontal and vertical direction are depending on the distribution of magnets around the bearing housing;* (b) *Magnetic forces represented as springs and dampers (idealization);* (c) and (d) *Mechanical model of the passive magnetic bearing – Rotor as a rigid body supported by springs and dampers.*

Forward and Backward Orbits

For being completed with the notes in the classes!

### 1.7.2 Cross-Coupling Stiffness and Rotor-Bearing Stability Analysis

Based on the mechanical model presented in figure 28, one mathematical model of 2 degrees of freedom is created and implement using MatLab. In the program the real and imaginary parts of the system eigenvalues is plotted as a function of the cross-coupling stiffness.

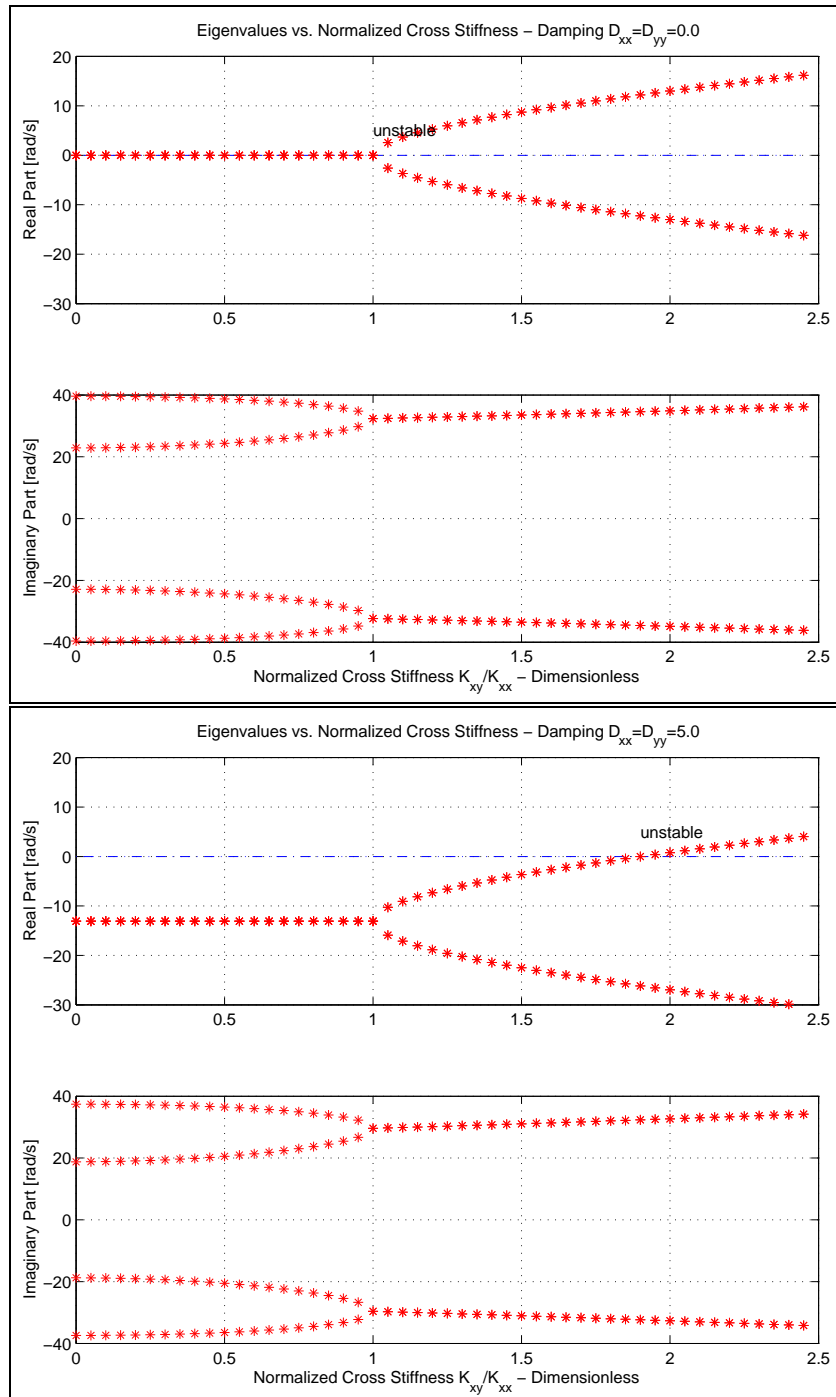


Figure 29: Stability analysis for the rotor-bearing system as a function of the cross-coupling stiffness coefficients and direct damping coefficients.

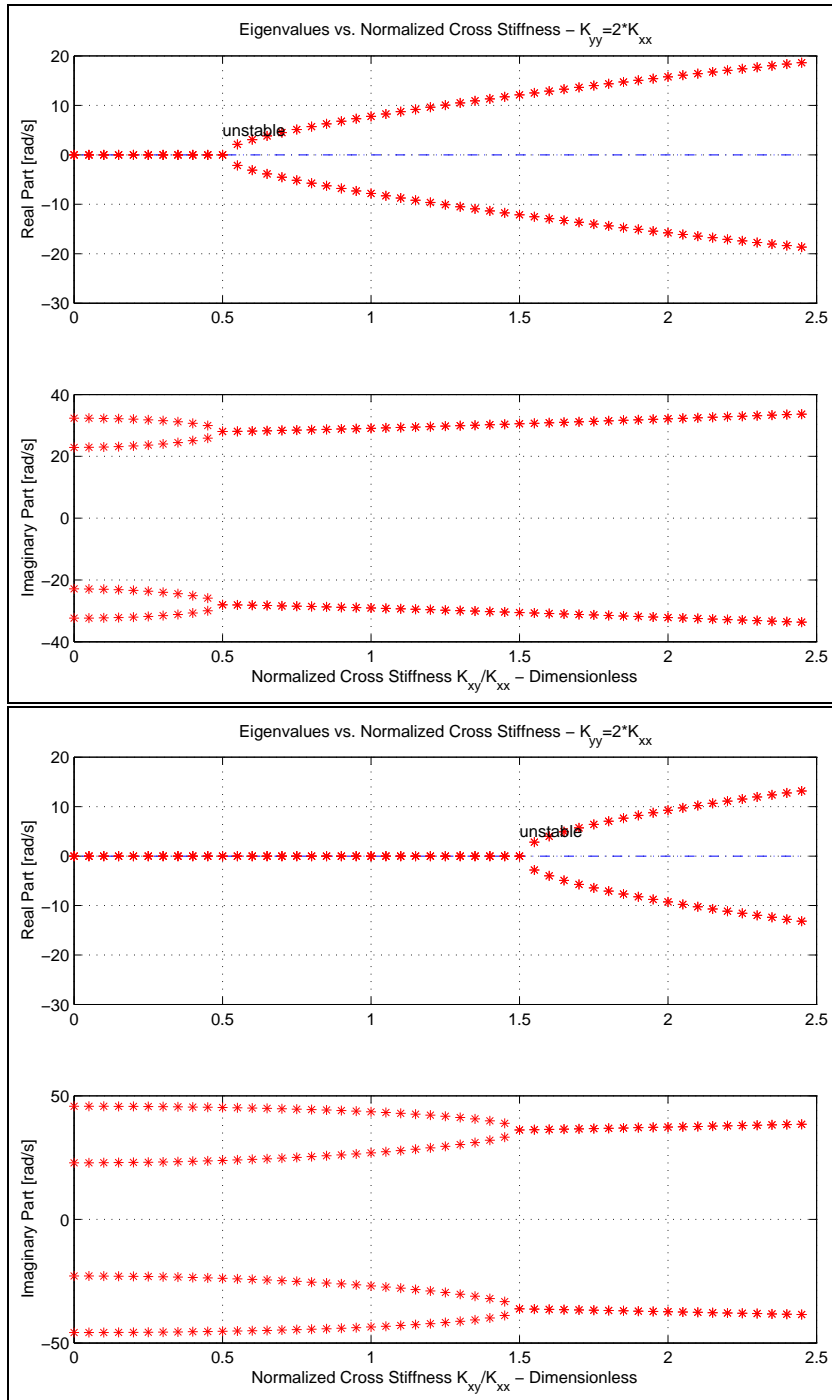


Figure 30: Stability analysis for the rotor-bearing system as a function of the cross-coupling stiffness coefficients and difference between the direct stiffness coefficients.

- MatLab program for analyzing rotor-bearing stability.

```

%%%%%%%%%%%%%%%%%%%%%%%%%%%%%%%%%%%%%%%%
% MACHINERY DYNAMICS LECTURES (72213) %
% MEK - DEPARTMENT OF MECHANICAL ENGINEERING %
% DTU - TECHNICAL UNIVERSITY OF DENMARK %
% %

```

```

%                               Copenhagen, March 3th, 2002                               %
%                               IFS                                                       %
%                               %                                                         %
% 2 D.O.F. SYSTEMS - ROOTS OF ROTOR-BEARING SYSTEM                                     %
%                               AND STABILITY ANALYSIS                                    %
%%%%%%%%%%%%%%%%%%%%%%%%%%%%%%%%%%%%%%%%%%%%%%%%%%%%%%%%%%%%%%%%%%%%%%%%%%

clear all;
close all;

N=40;

%Concentred Masses
m1= 0.191; %[Kg]
m2= 0.191; %[Kg]

%Elastic Properties of the Beam of 600 mm
E= 2e11;          %elasticity modulus [N/m^2]
b= 0.030 ;       %width [m]
h= 0.0012 ;      %thickness [m]
I= (b*h^3)/12;   %area moment of inertia [m^4]

for i=1:N;

% Coefficients of the Stiffness Matrix
LL = 0.310;      %beam length [m]
KK = 3*E*I/LL^3; %equivalent stiffness [N/m]

K11 = 1.0*KK;    %equivalent stiffness [N/m]
K12 = ((i-1)*0.05)*KK; %equivalent stiffness [N/m]
Kxy(i) = K12/K11;
K22 = 2.0*KK;    %quivalent stiffness [N/m]

%Mass Matrix
M= [m1 0;
    0 m2];
%Stiffness Matrix
K= [ K11 K12;
    K12 K22];

%Damping Matrix 0.0, 1.0, 2.0, 3.0, 5.0
D= [ 0.0 0.0 ;
    0.0 0.0 ];

%State Matrices
A= [      M      D      ;
    zeros(size(M)) M ];

B= [ zeros(size(M))      K      ;
    -M      zeros(size(M))];

%Dynamical Properties of the Mass-Spring System
[u,w]=eig(-B,A);          %natural frequency [rad/s]

%Dynamical Properties of the Mass-Spring System
w=diag(w); w_imag=imag(w);
[ws,pos]=sort(w_imag); %natural frequency [rad/s]

ww(i,1)=w(pos(1))/2/pi;
ww(i,2)=w(pos(2))/2/pi;
ww(i,3)=w(pos(3))/2/pi;
ww(i,4)=w(pos(4))/2/pi;

```

```

%ww(i,:)
end; subplot(2,1,1);
plot(Kxy,real(ww(:,1)),'r*',Kxy,real(ww(:,2)),'r*',Kxy,real(ww(:,3)),'r*',Kxy,real(ww(:,4)),'r*')
grid
title('Real and Imaginary Parts of the Eigenvalues vs. Cross
Coupling Stiffness')
ylabel('Real Part [rad/s]')

subplot(2,1,2);
plot(Kxy,imag(ww(:,1)),'r*',Kxy,imag(ww(:,2)),'r*',Kxy,imag(ww(:,3)),'r*',Kxy,imag(ww(:,4)),'r*')
grid
xlabel('Dimensionless Cross Stiffness')
ylabel('Imaginary
Part [rad/s]')

```

## 1.8 Stability Analysis of Rotor-Journal Bearing Systems

- The static equilibrium position of a rotor supported by a two-axial-groove journal bearing (figure 31) is illustrated in table 2 and figure 32, as a function of Sommerfeld number  $S$ .

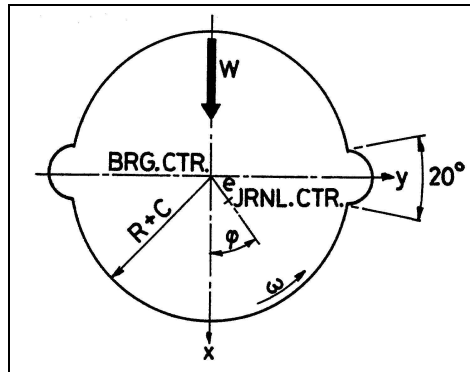


Figure 31: *Two-axial groove journal bearing,  $L/D=0.5$ .*

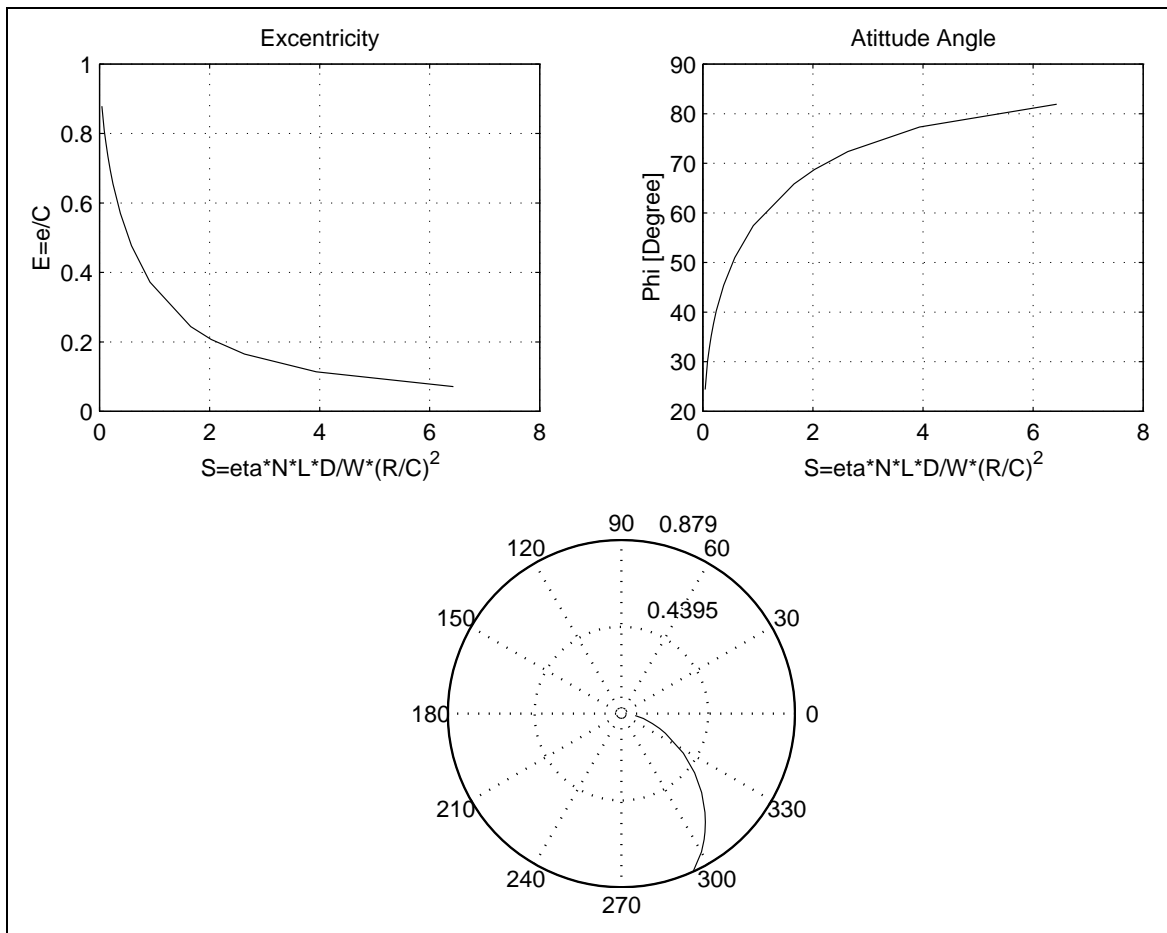


Figure 32: *Static properties of a two-axial groove journal bearing,  $L/D=0.5$ .*

$S$	$\epsilon$	$\Phi$	$K_{vv}$	$K_{vw}$	$K_{wv}$	$K_{ww}$	$C_{vv}$	$C_{vw}$	$C_{wv}$	$C_{ww}$
6.430	0.071	81.89	1.55	14.41	-6.60	1.88	28.75	1.89	1.89	13.31
3.937	0.114	77.32	1.57	9.27	-4.20	1.89	18.44	1.93	1.93	8.58
2.634	0.165	72.36	1.61	6.74	-3.01	1.91	13.36	2.00	2.00	6.28
2.030	0.207	68.75	1.65	5.67	-2.50	1.93	11.18	2.07	2.07	5.33
1.656	0.244	65.85	1.69	5.06	-2.20	1.95	9.93	2.15	2.15	4.80
0.917	0.372	57.45	2.12	4.01	-1.30	1.85	7.70	2.06	2.06	3.23
0.580	0.477	51.01	2.67	3.70	-0.78	1.75	6.96	1.94	1.94	2.40
0.378	0.570	45.43	3.33	3.64	-0.43	1.68	6.76	1.87	1.87	1.89
0.244	0.655	40.25	4.21	3.74	-0.13	1.64	6.87	1.82	1.82	1.54
0.194	0.695	37.72	4.78	3.84	0.01	1.62	7.03	1.80	1.80	1.40
0.151	0.734	35.20	5.48	3.98	0.15	1.61	7.26	1.79	1.79	1.27
0.133	0.753	33.93	5.89	4.07	0.22	1.60	7.41	1.79	1.79	1.20
0.126	0.761	33.42	6.07	4.11	0.25	1.60	7.48	1.79	1.79	1.18
0.116	0.772	32.65	6.36	4.17	0.30	1.60	7.59	1.79	1.79	1.15
0.086	0.809	30.04	7.51	4.42	0.47	1.59	8.03	1.79	1.79	1.03
0.042	0.879	24.41	11.45	5.23	0.92	1.60	9.48	1.80	1.80	0.82

Table 2: Example of a table with the dynamic properties of a two-axial-groove journal bearing as a function of the bearing parameters:  $D$  - rotor diameter [m];  $L$  - bearing width [m];  $R = D/2$  - rotor radius [m];  $C$  - bearing clearance [m];  $W$  - external load [N];  $\eta$  - oil viscosity [ $N.s/m^2$ ];  $N$  - rotor angular velocity [1/s];  $\omega = 2 * \pi * N$  - rotor angular velocity [rad/s];  $S = \eta * N * L * D/W * (R/C)^2$  - Sommerfeld number;  $\epsilon = e/C$  - eccentricity;  $\Phi$  - attitude angle;  $K_{ij} = (C/W)*k_{ij}$  ( $i, j = x, y$ ) - dimensionless stiffness coefficients;  $B_{ij} = (C*w/W)*k_{ij}$  ( $i, j = x, y$ ) - dimensionless damping coefficients. OBS: This values can only be used when  $L/D = 0.5$ .

- Stiffness and damping coefficients of a two-axial-groove journal bearing presented in figure 31 are shown in table 2 and figure 33 as a function of Sommerfeld number  $S$ .

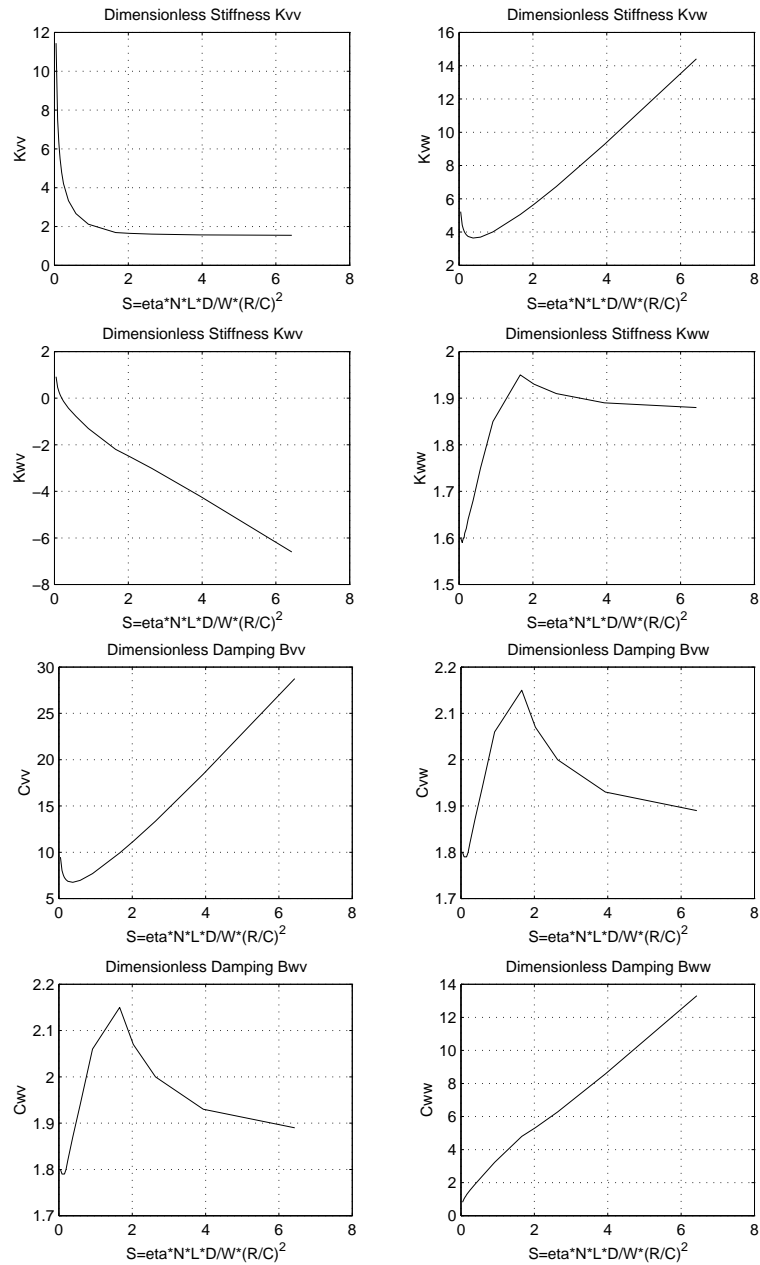


Figure 33: Dimensionless oil film stiffness and damping of a two-axial groove journal bearing,  $L/D=0.5$ .



- Rotor-journal bearing stability as a function of the rotational speed. Example based on the two-axial-groove journal bearing, presented in figure 31, and on the data shown in table 2.

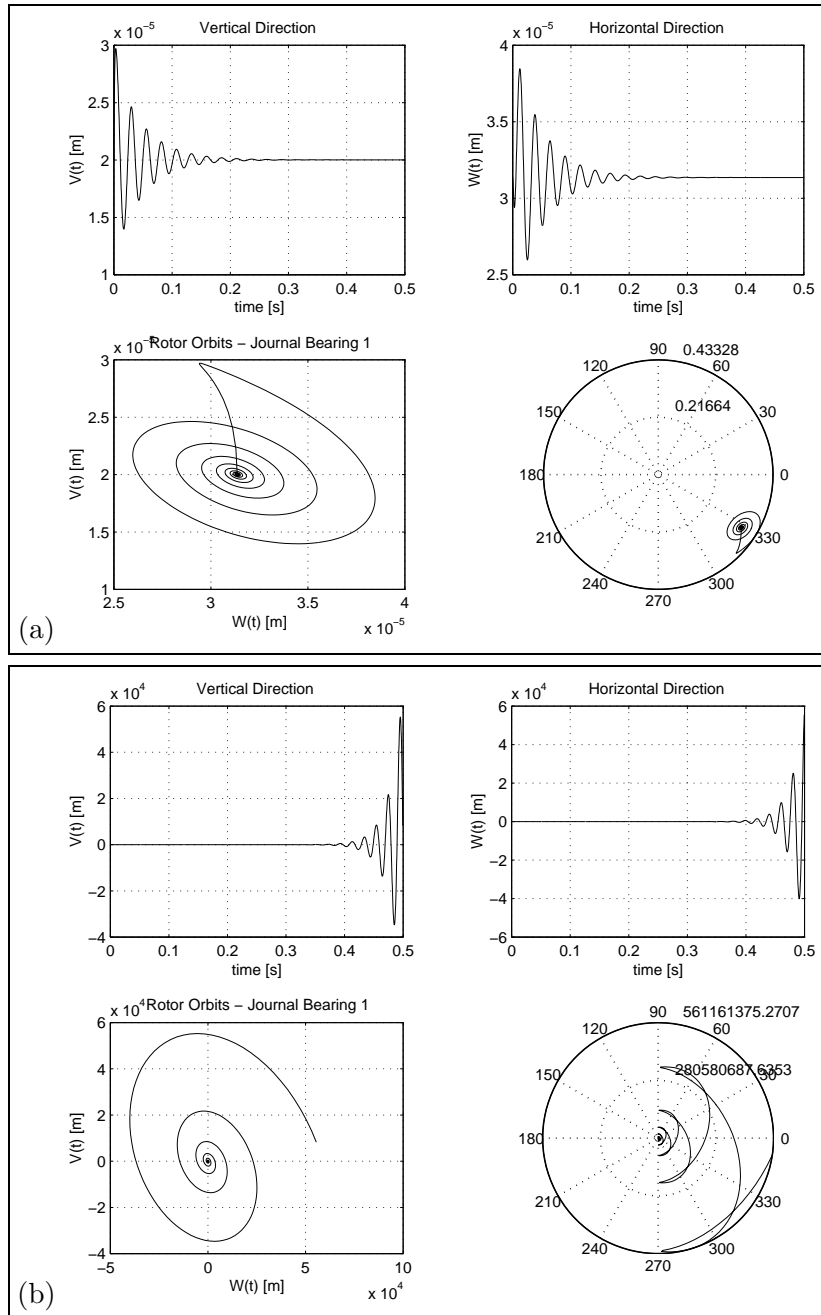


Figure 34: Stability Analysis of a two-axial groove journal bearing,  $L/D=0.5$  with two different angular velocities (a)  $N = 66.3218$  (STABLE) and (b)  $N = 119.7697$  (UNSTABLE)

- Example of MatLab program for analyzing rotor-journal bearing stability as a function of stiffness and damping coefficients. Example based on the two-axial-groove journal bearing, presented in figure 31, and on the data shown in table 2.

```

%%%%%%%%%%%%%%%%%%%%%%%%%%%%%%%%%%%%%%%%%%%%%%%%%%%%%%%%%%%%%%%%%%%%%%%%
% MACHINERY DYNAMICS LECTURES (41614) %
% MEK - DEPARTMENT MECHANICAL ENGINEERING %
% DTU - TECHNICAL UNIVERSITY OF DENMARK %
% %
% Copenhagen, October 22, 2000 %
% %
% Ilmar F. Santos %
% %
% JOURNAL BEARING DYNAMICS & STABILITY ANALYSIS %
%%%%%%%%%%%%%%%%%%%%%%%%%%%%%%%%%%%%%%%%%%%%%%%%%%%%%%%%%%%%%%%%%%%%%%%%

% Definition of Non-dimensional Bearing Parameters
% S = eta*N*L*D/W*(R/C)^2; Sommerfeld Number
% E = e/C; Eccentricity
% Phi Attitude Angle
% Kij = (C/W)*kij (i,j=x,y) dimensionless stiffness coefficients
% Bij = (C*w/W)*kij (i,j=x,y) dimensionless damping coefficients
%
% Definition of Journal Bearing Parameters
% D rotor diameter
% L bearing width
% R = D/2; rotor radius
% C bearing clearance
% W external load [N]
% eta oil viscosity [N.s/m2]
% N rotor angular velocity [1/s]
% w = 2*pi*N rotor angular velocity [rad/s]

clear all;
close all;

% Bearing Properties
% Table 1a : Two-axial-groove bearing, L/D = 0.5
%
% S E Phi Q P T Kxx Kxy Kyx Kyy Bxx Bxy Byx Byy
%
Table=[6.430 0.071 81.89 0.121 0.860 5.7 1.55 14.41 -6.60 1.88 28.75 1.89 1.89 13.31
3.937 0.114 77.32 0.192 0.846 5.9 1.57 9.27 -4.20 1.89 18.44 1.93 1.93 8.58
2.634 0.165 72.36 0.271 0.833 6.2 1.61 6.74 -3.01 1.91 13.36 2.00 2.00 6.28
2.030 0.207 68.75 0.332 0.835 6.6 1.65 5.67 -2.50 1.93 11.18 2.07 2.07 5.33
1.656 0.244 65.85 0.383 0.835 7.0 1.69 5.06 -2.20 1.95 9.93 2.15 2.15 4.80
0.917 0.372 57.45 0.540 0.850 8.5 2.12 4.01 -1.30 1.85 7.70 2.06 2.06 3.23
0.580 0.477 51.01 0.651 0.900 10.5 2.67 3.70 -0.78 1.75 6.96 1.94 1.94 2.40
0.378 0.570 45.43 0.737 0.977 13.4 3.33 3.64 -0.43 1.68 6.76 1.87 1.87 1.89
0.244 0.655 40.25 0.804 1.096 17.9 4.21 3.74 -0.13 1.64 6.87 1.82 1.82 1.54
0.194 0.695 37.72 0.833 1.156 21.3 4.78 3.84 0.01 1.62 7.03 1.80 1.80 1.40
0.151 0.734 35.20 0.858 1.240 25.8 5.48 3.98 0.15 1.61 7.26 1.79 1.79 1.27
0.133 0.753 33.93 0.870 1.289 28.7 5.89 4.07 0.22 1.60 7.41 1.79 1.79 1.20
0.126 0.761 33.42 0.875 1.310 30.0 6.07 4.11 0.25 1.60 7.48 1.79 1.79 1.18
0.116 0.772 32.65 0.881 1.343 32.2 6.36 4.17 0.30 1.60 7.59 1.79 1.79 1.15
0.086 0.809 30.04 0.902 1.473 41.4 7.51 4.42 0.47 1.59 8.03 1.79 1.79 1.03
0.042 0.879 24.41 0.936 1.881 80.9 11.45 5.23 0.92 1.60 9.48 1.80 1.80 0.82 ];

figure(1)
title('Journal Bearing -- Static Properties')

```

```

subplot(2,2,1), plot(Table(:,1),Table(:,2),'b')
title('Eccentricity')
xlabel('S=eta*N*L*D/W*(R/C)^2')
ylabel('E=e/C')
grid
subplot(2,2,2), plot(Table(:,1),Table(:,3),'b')
title('Attitude Angle')
xlabel('S=eta*N*L*D/W*(R/C)^2')
ylabel('Phi [Degree]')
grid
subplot(2,2,3.5),
polar(3*pi/2+Table(:,3)*pi/180,Table(:,2))
title('Eccentricity E=e/C & Attitude Angle Phi')
grid

figure(2)
title('Journal Bearing -- Dynamic Properties')
subplot(2,2,1), plot(Table(:,1),Table(:,7),'b')
title('Dimensionless Stiffness Kxx')
xlabel('S=eta*N*L*D/W*(R/C)^2')
ylabel('Kxx')
grid
subplot(2,2,2), plot(Table(:,1),Table(:,8),'b')
title('Dimensionless Stiffness Kxy')
xlabel('S=eta*N*L*D/W*(R/C)^2')
ylabel('Kxy')
grid
subplot(2,2,3), plot(Table(:,1),Table(:,9),'b')
title('Dimensionless Stiffness Kyx')
xlabel('S=eta*N*L*D/W*(R/C)^2')
ylabel('Kyx')
grid
subplot(2,2,4), plot(Table(:,1),Table(:,10),'b')
title('Dimensionless Stiffness Kyy')
xlabel('S=eta*N*L*D/W*(R/C)^2')
ylabel('Kyy')
grid

figure(3)
title('Journal Bearing -- Dynamic Properties')
subplot(2,2,1), plot(Table(:,1),Table(:,11),'b')
title('Dimensionless Damping Bxx')
xlabel('S=eta*N*L*D/W*(R/C)^2')
ylabel('Bxx')
grid
subplot(2,2,2), plot(Table(:,1),Table(:,12),'b')
title('Dimensionless Damping Bxy')
xlabel('S=eta*N*L*D/W*(R/C)^2')
ylabel('Bxy')
grid
subplot(2,2,3), plot(Table(:,1),Table(:,13),'b')
title('Dimensionless Damping Byx')
xlabel('S=eta*N*L*D/W*(R/C)^2')
ylabel('Byx')
grid
subplot(2,2,4), plot(Table(:,1),Table(:,14),'b')
title('Dimensionless Damping Byy')
xlabel('S=eta*N*L*D/W*(R/C)^2')
ylabel('Byy')
grid

% bearing geometry

```

```

D    = 0.100 ;    % [m]
L    = 0.050 ;    % [m]
R    = D/2;      % [m]
r    = 0.0499 ;  % [m]
C    = 100e-6 ;  % [m]
C    = R-r;      % [m]
% oil properties
eta  = 0.0271;   % [N.s/m2]
% acceleration of gravity
g    = 9.8;      % [m/s^2]
% rotor mass and weight
mass = 500;      % [kg]
W    = mass*g/2; % [N]
% N = rotational velocity [1/s]
% N = Table(1,1)*(W)/(eta*L*D)/(R/C)^2
N    = 3.0376;   line = 16;
N    = 6.2199;   line = 15;
N    = 8.3897;   line = 14;
N    = 9.1129;   line = 13;
N    = 9.6192;   line = 12;
N    = 10.9210;  line = 11;
N    = 14.0310;  line = 10;
N    = 17.6472;  line = 9;
N    = 27.3387;  line = 8;
N    = 41.9483;  line = 7;
N    = 66.3218;  line = 6;    % STABLE   !!!
% N = 119.7697; line = 5;    % UNSTABLE !!!
% N = 146.8192; line = 4;
% N = 190.5033; line = 3;
% N = 284.7424; line = 2;
% N = 465.0480; line = 1;

w    = 2*pi*N;   % [rad/s]
S    = eta*N*L*D/W*(R/C)^2 % Sommerfeld Number

% Coefficients of the Stiffness Matrix
kxx = Table(line,7)*W/C ; % [N/m]
kxy = Table(line,8)*W/C ; % [N/m]
kyx = Table(line,9)*W/C ; % [N/m]
kyy = Table(line,10)*W/C ; % [N/m]

% Coefficients of the Damping Matrix
bxx= Table(line,11)*W/(w*C) ; % [N/(m/s)]
bxy= Table(line,12)*W/(w*C) ; % [N/(m/s)]
byx= Table(line,13)*W/(w*C) ; % [N/(m/s)]
byy= Table(line,14)*W/(w*C) ; % [N/(m/s)]

x_st = Table(line,2)*cos(Table(line,3)*pi/180)*C; % equilibrium position [m]
y_st = Table(line,2)*sin(Table(line,3)*pi/180)*C; % equilibrium position [m]

%Mass Matrix
M= [mass 0; 0 mass];

%Damping Matrix
B=[bxx bxy; byx byy];

%Stiffness Matrix
K= [kxx kxy; kyx kyy];

%State Matrix
A1= [      M      B      ;
     zeros(size(M)) M ] ;

```

```

A2= [ zeros(size(M))      K      ;
      -M      zeros(size(M))];

%Dynamical Properties of the Mass-Spring System
[u,s]=eig(-A2,A1);      % eigenvectors [ ] & eigenvalues [rad/s]
s      % eigenvalues [rad/s]

pause;

%-----
%Inicial Condition
x_ini = 0.000;      % initial displacement [m]
y_ini = 0.000;      % initial displacement [m]
vx_ini = 0.01;      % initial perturbation velocity [m/s]
vy_ini = 0.000;      % initial perturbation velocity [m/s]
time_max = 0.5;      % integration time [s]

%-----
%-----
%EXACT SOLUTION
n=2000;      % number of points for plotting
j=sqrt(-1);      % complex number

z_ini = [vx_ini vy_ini x_ini y_ini]';

s1=s(1,1);
s2=s(2,2);
s3=s(3,3);
s4=s(4,4);

u1=u(1:4,1);
u2=u(1:4,2);
u3=u(1:4,3);
u4=u(1:4,4);

C_ini=inv(u)*(z_ini);

c1=C_ini(1);
c2=C_ini(2);
c3=C_ini(3);
c4=C_ini(4);

for i=1:n,
    t(i)=(i-1)/n*time_max;
    z_exact = c1*u1*exp(s1*t(i)) + ...
              c2*u2*exp(s2*t(i)) + ...
              c3*u3*exp(s3*t(i)) + ...
              c4*u4*exp(s4*t(i));

    % cartesian coordinates
    x_exact(i) = x_st + real(z_exact(3));
    y_exact(i) = y_st + real(z_exact(4));

    % polar coordinates
    polar_rho(i) = sqrt(x_exact(i)*x_exact(i)+y_exact(i)*y_exact(i));
    polar_angle(i) = acos(x_exact(i)/polar_rho(i));

end

figure(4)

```

```

title('Journal Bearing Stability - Time Domain Analysis')
subplot(2,2,1), plot(t,x_exact,'b')
title('Vertical Direction ')
xlabel('time [s]')
ylabel('x(t) [m]')
grid

subplot(2,2,2), plot(t,y_exact,'b')
title('Horizontal Direction ')
xlabel('time [s]')
ylabel('y(t) [m]')
grid

subplot(2,2,3), plot(y_exact,x_exact,'b')
title('Rotor Orbits - Journal Bearing 1')
xlabel('y(t) [m]')
ylabel('x(t) [m]')
grid

subplot(2,2,4),
polar(3*pi/2+polar_angle,polar_rho/C)
title('Rotor Orbits - Dimensionless')
grid

```

## 1.9 Further Bibliography related to Journal Bearing Properties – Research and Development

### 1.9.1 On the Adjusting of the Dynamic Coefficients of Tilting-Pad Journal Bearings

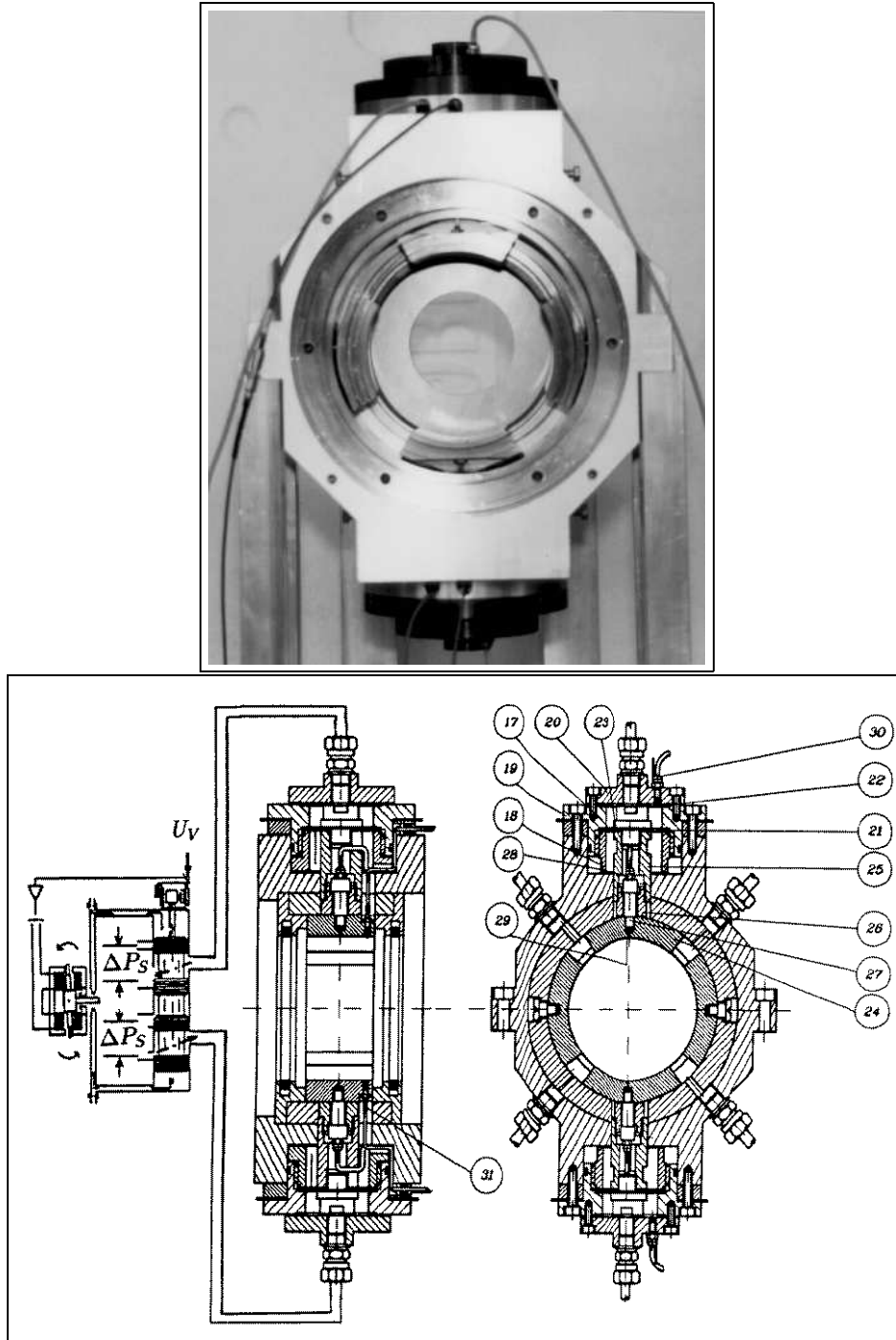


Figure 35: Adjust of the Dynamic Coefficients of Tilting-Pad Journal Bearings by means of Hydraulic Chamber Systems.

### 1.9.2 Tilting-Pad Journal Bearings with Electronic Radial Oil Injection

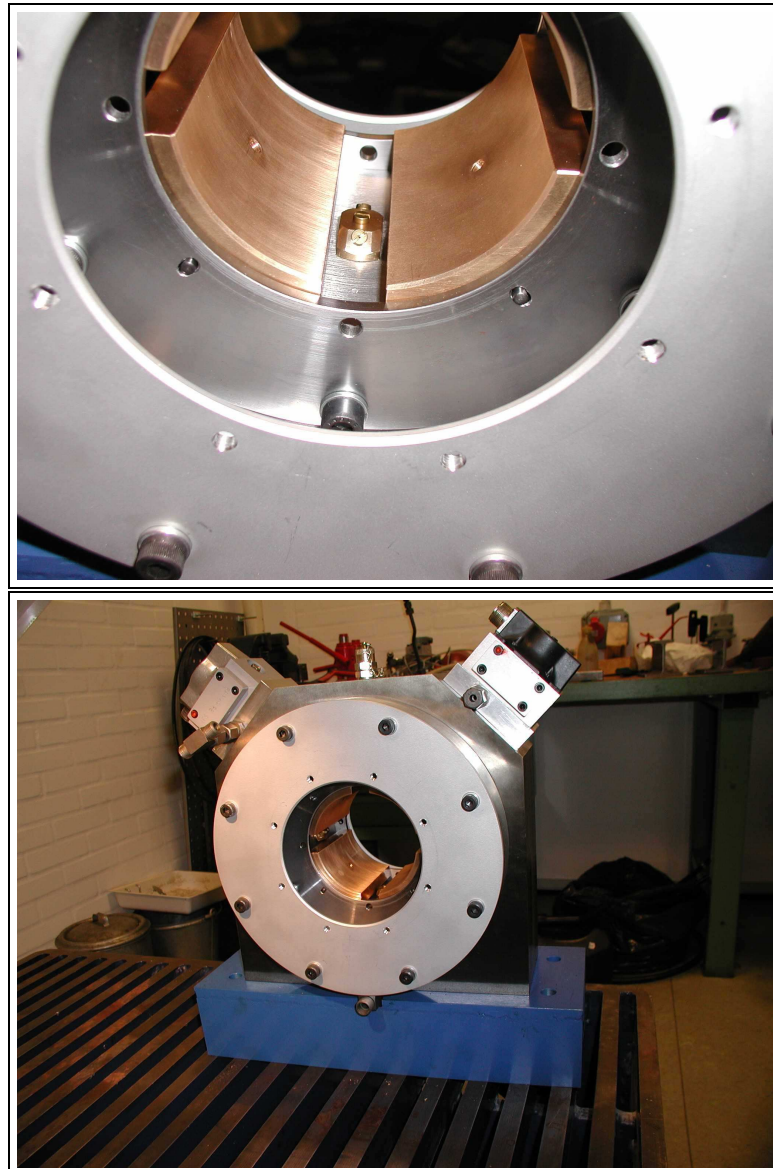


Figure 36: *New Test Rig built at MEK-DTU with financial support of Myhrwolds Foundation – Interior of the active lubricated tilting-pad bearing illustrating the orifice machined on the pad surface (active lubrication) and the conventional lubrication between pads (hydrodynamic lubrication).*



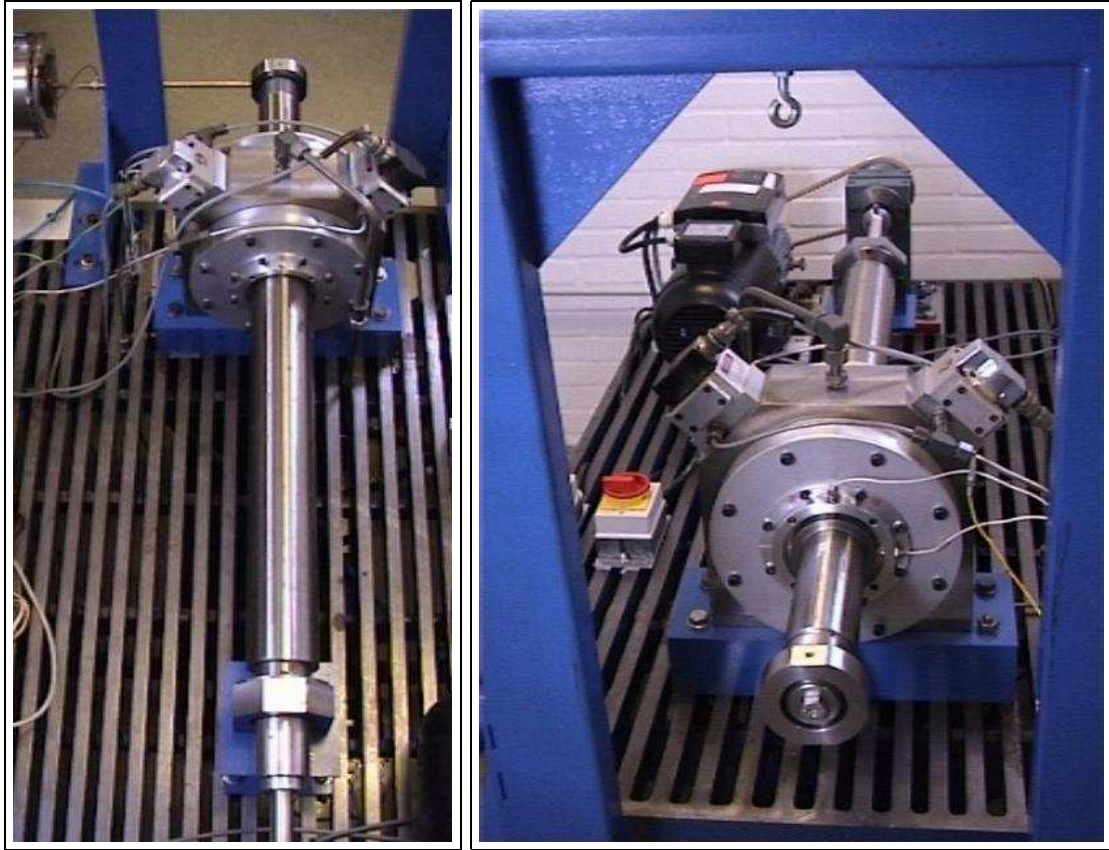


Figure 37: *New Test Rig built at MEK-DTU with financial support of Myhrwolds Foundation – Electromagnetic shaker attached to the shaft extremity, active lubricated bearing with servo valves mounted on the bearing housing, motor connected to the shaft by belt.*

### 1.10 Exercises using MatLab Program

For the overhang rotor illustrated in figure 38:

- (1) Elaborate a simple mechanical model.
- (2) Create a simple mathematical model using only one shaft and one disc finite elements.
- (3) Set some values for the overhang rotor:

- DISC

$Rd = 0.100$  – disc radius [m]

$espD = 0.010$  – disc thickness [m]

$Ral = 7800$  – steel density [ $kg/m^3$ ]

$MasD = pi * Rd^2 * espD * Ral$  – disc mass [kg]

$Id = 1/4 * MasD * Rd^2 + 1/12 * MasD * espD^2$  – transversal mass moment of inertia [ $Kgm^2$ ]

$Ip = 1/2 * MasD * Rd * Rd$  – polar mass moment of inertia [ $Kgm^2$ ]

- SHAFT

$L = 0.500$  – length of shaft elements [m]

$rx = 0.003$  – shaft external radius [m]

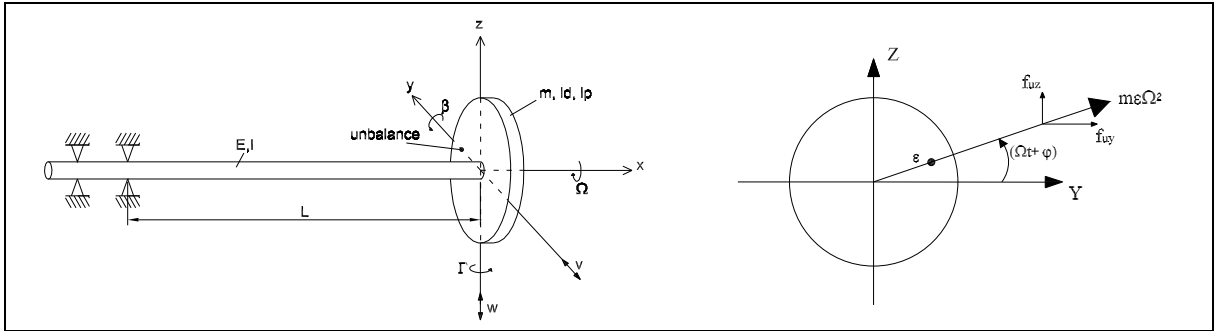


Figure 38: *Overhang Rotor with Unbalance Mass.*

- (4) Find the natural frequencies of the overhang rotor.
- (5) Plot the forward component  $\{x_{for}\}$  of the displacement coordinates  $V$  and  $W$  as function of rotational speed  $\Omega$ . Choose a range a rotational speed, which covers the natural frequencies of the overhang rotor.
- (6) Plot the backward component  $\{x_{back}\}$  of the displacement coordinates  $V$  and  $W$  as function of rotational speed  $\Omega$ . Choose a range a rotational speed, which covers the natural frequencies of the overhang rotor.
- (7) What can you conclude about the orbits which will be described by the rotor in the difference range of rotational speed?
- (8) Change the stiffness matrix of the overhung rotor, adding two different stiffness in the diagonal of the stiffness matrix, in  $V$  and  $W$  coordinates,  $k_{vv} = 0.0 [N/m]$  and  $k_{ww} = 10^5 [N/m]$ .
- (9) Find the natural frequencies of the overhang rotor for the case (4).
- (10) Plot the forward component  $\{x_{for}\}$  of the displacement coordinates  $V$  and  $W$  as function of rotational speed  $\Omega$ . Choose a range a rotational speed, which covers the natural frequencies of the overhang rotor.
- (11) Plot the backward component  $\{x_{back}\}$  of the displacement coordinates  $V$  and  $W$  as function of rotational speed  $\Omega$ . Choose a range a rotational speed, which covers the natural frequencies of the overhang rotor.
- (12) What can you conclude about the orbits which will be described by the rotor in the difference range of rotational speed, when you have different stiffness in the horizontal and vertical planes?

close all clear all

%Physical Dimensions

Rd=0.100;	%Disc radius	[m]
espD=0.010;	%Disc thickness	[m]
Ral=7800;	%Steel density	[kg/m <sup>3</sup> ]
l=0.0600;	%Length of shaft	
	%elements	[m]
rx=0.003;	%Shaft external	
	%radius	[m]

```

frqmax=60*2*pi;           %Maximum
                           %angular velocity [rad/s]
E=2e11;                   %Elasticity modulus [N/m^2]
m=0.005;                  %Unbalance mass [kg]
epsilon=0.001;           %Radial placement of
                           %unbalance mass [m]

%Constants
MasD=pi*Rd^2*espD*Ral;    %Disc mass [kg]
Id=1/4*MasD*Rd^2+1/2*MasD*espD^2;%Transversal mass
                           %moment of inertia [Kgm^2]
Ip=1/2*MasD*Rd^2;        %Polar mass moment
                           %of inertia [kgm^2]
I=pi/4*rx^4;             %Area moment of
                           %inertia [m^4]
timemax=10;              %Maximum time [s]
n=1000;                  %Number of points [1]
fi=0;                   %Phasedelay [radians]

%Matrices for the mathematical model

%Mass matrix
M=[MasD    0    0    0;
   0    MasD    0    0;
   0    0    Id    0;
   0    0    0    Id];

%Gyroscopic matrix
G= [ 0    0    0    0;
     0    0    0    0;
     0    0    0    Ip;
     0    0   -Ip    0 ];

%Stiffness matrix
K_shaft=E*I/l^3* [ 12    0    0    6*1;
                  0    12   -6*1    0;
                  0   -6*1    4*1^2    0;
                  6*1    0    0    4*1^2];

K_fluid = E*I/l^3* [ 0    0    0    0;
                   0    10   0    0;
                   0    0    0    0;
                   0    0    0    0];

K = K_shaft + K_fluid;

% Damping matrix
% Proportional Damping D=alpha*M + beta*K;
alpha=0.221*0.03;
beta =0.00182*0.03;

```

```

D_damping=alpha*M + beta*K;

N_campbell = 50;

for iii=1:N_campbell,

    Omega= 10*(iii-1)*2*pi/2;    % angular velocity [rad/s]
    Omegarpm(iii) = Omega*60/2/pi; % angular velocity [rpm]

%Mathematical model
A=[ M                Omega*G + D_damping    ;
   zeros(size(M))    M                    ];

B=[ zeros(size(M))    K                ;
   -M                zeros(size(M))];

[U,lambda]=eig(-B,A);

[lam,p]=sort(abs(diag(lambda)));

lambda_campbell(iii,:)=lam'/2/pi;

end

figure(1) plot(Omegarpm,Omegarpm/60,'r','LineWidth',1.5) grid hold
on
plot(Omegarpm,lambda_campbell(1:N_campbell,1),'b','LineWidth',1.5)
hold on
plot(Omegarpm,lambda_campbell(1:N_campbell,3),'b','LineWidth',1.5)
hold on
plot(Omegarpm,lambda_campbell(1:N_campbell,5),'b','LineWidth',1.5)
hold on
plot(Omegarpm,lambda_campbell(1:N_campbell,7),'b','LineWidth',1.5)
hold on
title('Campbell`s Diagram - 4 First Natural
Frequencies.','FontSize',14)
xlabel('Angular Velocity [rpm]','FontSize',14)
ylabel('Natural Frequency [Hz]','FontSize',14)

figure(9) subplot(1,3,1),
plot(Omegarpm,Omegarpm/60,'r','LineWidth',1.5)
grid
hold on
plot(Omegarpm,lambda_campbell(1:N_campbell,1),'b','LineWidth',1.5)
hold on
plot(Omegarpm,lambda_campbell(1:N_campbell,3),'b','LineWidth',1.5)
hold on
plot(Omegarpm,lambda_campbell(1:N_campbell,5),'b','LineWidth',1.5)
hold on

```

```

plot(Omegarpm,lambda_campbell(1:N_campbell,7),'b','LineWidth',1.5)
hold on
title('Campbell`s Diagram','FontSize',10)
xlabel('Angular Velocity [rpm]','FontSize',10)
ylabel('Natural Frequency [Hz]','FontSize',10)
axis([0,15000,0,300])

```

```

subplot(1,3,2), plot(X(1,1:i),omega/2/pi,'b','LineWidth',1.5)
ylabel('Angular Velocity [Hz]','FontSize',10)
xlabel('Displ. V [m]','FontSize',10)
title('Unbalance Reponse - V','FontSize',10)
axis([0,1e-4,0,300])
grid

```

```

subplot(1,3,3), plot(X(2,1:i),omega/2/pi,'b','LineWidth',1.5)
ylabel('Angular Velocity [Hz]','FontSize',10)
xlabel('Displ. W [m]','FontSize',10)
title('Unbalance Reponse - W','FontSize',10)
axis([0,1e-4,0,300])
grid

```

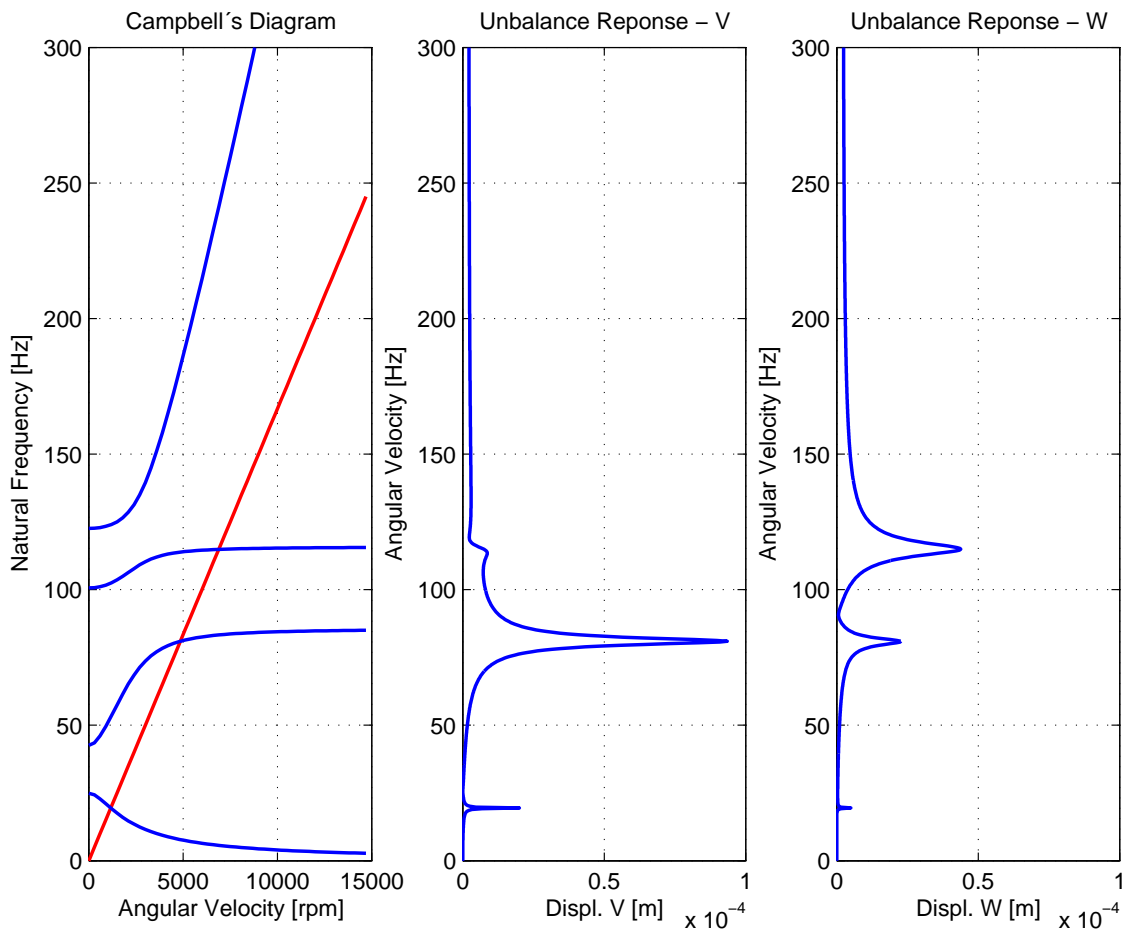


Figure 39: *Overhang Rotor – Campbell Diagram and Frequency Response Function.*

### 1.11 Project 3 – Rotor-Journal Bearing Stability - Lateral Dynamics

The aim of the third project is to become familiar with the prediction of critical speeds in rotating machines. Using the drawings of the shaft of the rotating machine, as in the real life in the design phase, elaborate a mechanical and a mathematical models to analyze lateral vibrations. The mathematical model will be based on Finite Element Method. After simulating the dynamic behavior of the shaft in a free-free condition, you have the possibility of checking the model accuracy by means of comparison with experimental natural frequencies of the shaft in the free-free condition attached here. Mounting the shaft in a journal bearing new natural frequencies and modes shapes will be calculated. This will allow a prediction of critical speeds, reserve of damping and stability range.

(Technical report until 14/05/2004)

1. MODELLING – Create a mechanical model for the rotor-bearing system illustrated in the technical drawings and discuss your assumptions (see attached pages).
2. MODELLING – Create a mathematical model (set of differential equations) for representing the dynamical behavior of the rotor-bearing system using Finite Element Methods. Use the information delivered in the technical drawings (attached pages).
3. MODELLING – Choose the model parameters (mass, stiffness, etc.) with help of theoretical or experimental procedures, and define the coefficients of your set of differential equations. Use the information delivered in the technical drawings (attached pages).
4. SIMULATION – Implement your mathematical model using the MatLab program presented in section 1.6.1.
5. ANALYSIS – With help of your mathematical model and your MatLab code calculate the natural frequencies of the flexible shaft (without discs) in the range of frequencies from 0 until 2000 Hz considering a free-free condition. In figure 40(a) one can see the flexible shaft without discs prepared for the experimental tests.
6. ANALYSIS – With help of your mathematical model and your MatLab code calculate the natural frequencies of the flexible shaft (with 1 disc) in the range of frequencies from 0 until 2000 Hz considering a free-free condition. In figure 40(b) one can see the flexible shaft with one disc prepared for the experimental tests.
7. ANALYSIS – With help of your mathematical model and your MatLab code calculate the natural frequencies of the flexible shaft (with 2 disc) in the range of frequencies from 0 until 2000 Hz considering a free-free condition. In figure 40(c) one can see the flexible shaft with one disc prepared for the experimental tests.
8. VERIFICATION & EXPERIMENTAL VALIDATION – With the natural frequencies of the flexible shaft (without discs) in a free-free condition presented in figure 41(a), try to validate your mathematical model.
9. VERIFICATION & EXPERIMENTAL VALIDATION – With the natural frequencies of the flexible shaft with 1 disc in a free-free condition presented in figure 41(b), try to validate your mathematical model.
10. VERIFICATION & EXPERIMENTAL VALIDATION – With the natural frequencies of the flexible shaft with 1 disc in a free-free condition presented in figure 41(c), try to validate your mathematical model.

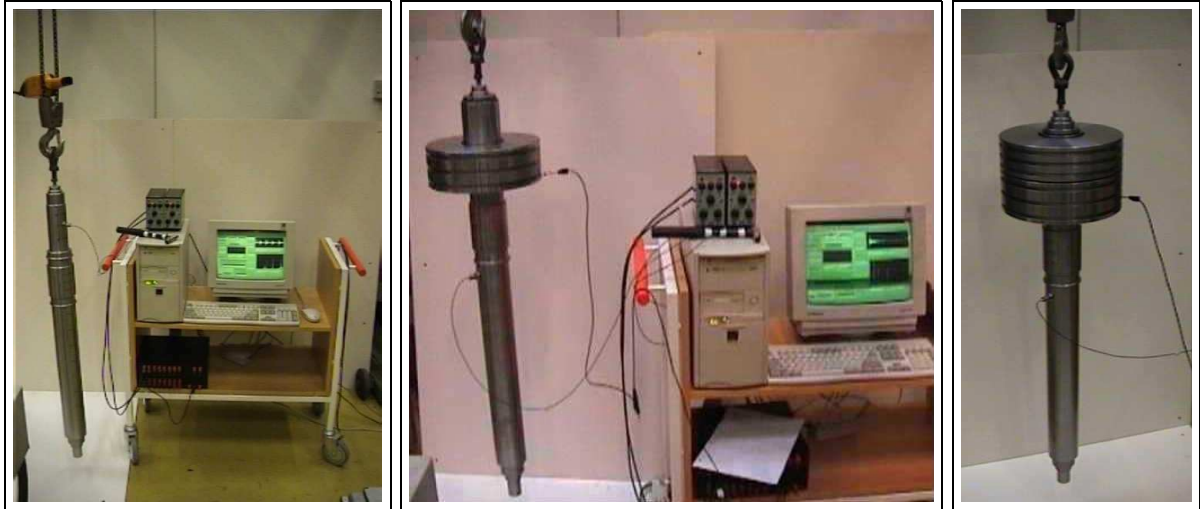


Figure 40: (a) Flexible shaft in a free-free condition – (b) Flexible shaft and one disc in a free-free condition – (c) Flexible shaft and two discs in a free-free condition.

11. VERIFICATION & EXPERIMENTAL VALIDATION – Compare theoretical and experimental results and discuss possible causes of discrepancies between theoretical and experimental results.
12. APPLICATION – PREDICTION OF ROTOR-BEARING STABILITY – The flexible shaft with 2 discs will be mounted on two different bearings. At one extremity a ball bearing will be used. Its stiffness, for the purposes of this analysis, can be considered infinite. At a given distance  $L$  from the extremity, a two-axial-groove journal bearing (figure 42) is mounted. The static equilibrium position, stiffness and damping coefficients of the rotor-bearing system can be obtained with help of the Sommerfeld number  $S = \eta * N * L * D / W * (R/C)^2$  and the table 3, if all parameters  $\eta$ ,  $N$ ,  $L$ ,  $D$ ,  $W$ ,  $R$  and  $C$  are known.
 

The bearings will be lubricated using the *ISO VG 32* oil. Its viscosity can be described by the expression  $\eta = 0.0277 * e^{[0.034 * (40 - T)]}$ ,  $\eta$  in  $[N \cdot s / m^2]$  and  $T$  in  $[C]$ . In this initial analysis the dependency of the oil temperature on the rotor angular velocity will be neglected. Based on experience with other machines with the same size one can assume that the mean temperature  $T$  will be  $67 [C]$ . In other words the stability analysis have to be led assuming an isothermal lubrication. The maximum angular velocity  $N$  has to be defined, and this is the most important part of the model application. The rotor diameter  $D [m]$  can be obtained from the technical drawings. The relationship  $L/D = 0.5$ ,  $R = D/2$  and the bearing clearance  $C = 120 [\mu m]$  are pre-defined parameters. Calculate the external load due to the weight acting on the bearing  $W [N]$ . The Sommerfeld number will be a function of the angular speed of the machine  $N$ .
13. APPLICATION – Plot the Campbell's diagram for the rotor-bearing system and define the 4 first critical speeds of the rotating machine. Use the MatLab program presented in section 1.6.7.
14. APPLICATION – Choose an angular velocity and plot the first 4 undamped natural modes shapes of the rotor-bearing system. OBS: Neglect the damping coefficients in this case and use the MatLab program presented in section 1.6.1.
15. APPLICATION – What is the maximum angular speed  $N$  that the rotating machine can operate without instability problem?

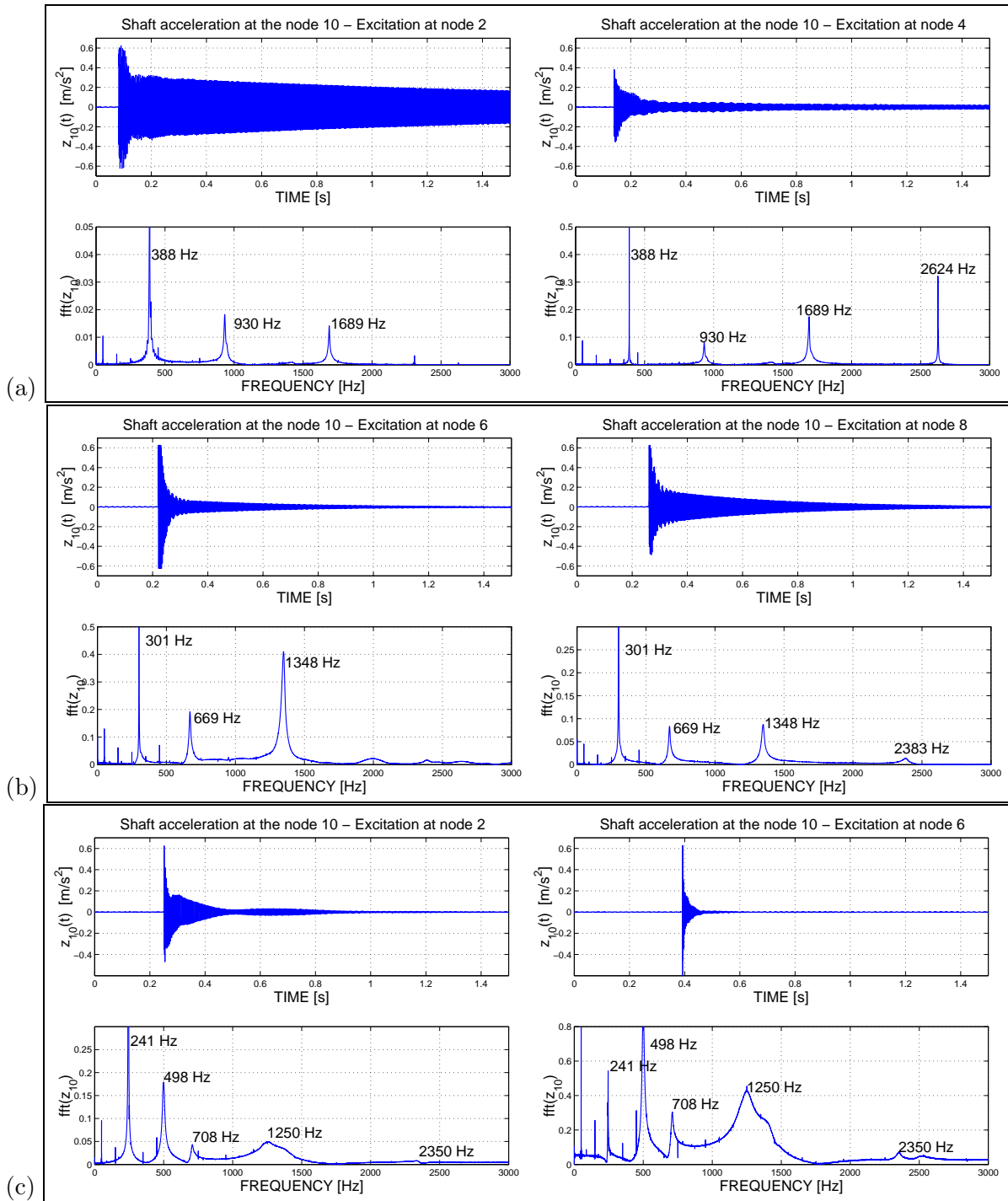


Figure 41: (a) Natural frequencies of the flexible shaft in a free-free condition – (b) Natural frequencies of the flexible shaft with one disc in a free-free condition – (c) Natural frequencies of the flexible shaft with two discs in a free-free condition.



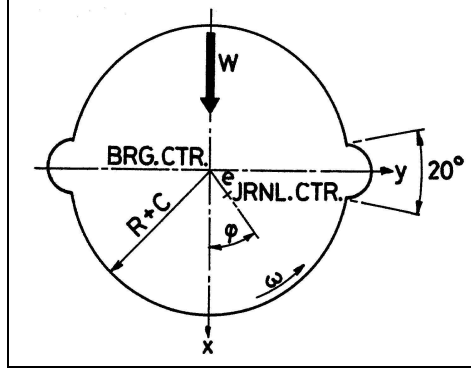


Figure 42: Two-axial groove journal bearing,  $L/D=0.5$ .

$S$	$\epsilon$	$\Phi$	$K_{vv}$	$K_{vw}$	$K_{wv}$	$K_{ww}$	$C_{vv}$	$C_{vw}$	$C_{wv}$	$C_{ww}$
6.430	0.071	81.89	1.55	14.41	-6.60	1.88	28.75	1.89	1.89	13.31
3.937	0.114	77.32	1.57	9.27	-4.20	1.89	18.44	1.93	1.93	8.58
2.634	0.165	72.36	1.61	6.74	-3.01	1.91	13.36	2.00	2.00	6.28
2.030	0.207	68.75	1.65	5.67	-2.50	1.93	11.18	2.07	2.07	5.33
1.656	0.244	65.85	1.69	5.06	-2.20	1.95	9.93	2.15	2.15	4.80
0.917	0.372	57.45	2.12	4.01	-1.30	1.85	7.70	2.06	2.06	3.23
0.580	0.477	51.01	2.67	3.70	-0.78	1.75	6.96	1.94	1.94	2.40
0.378	0.570	45.43	3.33	3.64	-0.43	1.68	6.76	1.87	1.87	1.89
0.244	0.655	40.25	4.21	3.74	-0.13	1.64	6.87	1.82	1.82	1.54
0.194	0.695	37.72	4.78	3.84	0.01	1.62	7.03	1.80	1.80	1.40
0.151	0.734	35.20	5.48	3.98	0.15	1.61	7.26	1.79	1.79	1.27
0.133	0.753	33.93	5.89	4.07	0.22	1.60	7.41	1.79	1.79	1.20
0.126	0.761	33.42	6.07	4.11	0.25	1.60	7.48	1.79	1.79	1.18
0.116	0.772	32.65	6.36	4.17	0.30	1.60	7.59	1.79	1.79	1.15
0.086	0.809	30.04	7.51	4.42	0.47	1.59	8.03	1.79	1.79	1.03
0.042	0.879	24.41	11.45	5.23	0.92	1.60	9.48	1.80	1.80	0.82

Table 3: Static and dynamic properties of a two-axial-groove journal bearing as a function of the bearing parameters:  $D$  - rotor diameter [m];  $L$  - bearing width [m];  $R = D/2$  - rotor radius [m];  $C$  - bearing clearance [m];  $W$  - external load [N];  $\eta$  - oil viscosity [ $N \cdot s/m^2$ ];  $N$  - rotor angular velocity [1/s];  $\omega = 2 * \pi * N$  - rotor angular velocity [rad/s];  $S = \eta * N * L * D/W * (R/C)^2$  - Sommerfeld number;  $\epsilon = e/C$  - eccentricity;  $\Phi$  - attitude angle;  $K_{ij} = (C/W) * k_{ij}$  ( $i, j = x, y$ ) - dimensionless stiffness coefficients;  $B_{ij} = (C * w/W) * k_{ij}$  ( $i, j = x, y$ ) - dimensionless damping coefficients. OBS: This values can only be used when  $L/D = 0.5$ .

## **2 Diagnosis of Rotating Machinery Malfunctions & Condition Monitoring**

### **2.1 Introduction**

Since the late 1960s have experimental and analytical techniques for assessing vibration levels been used routinely for diagnosis faults in operational rotating machinery. Until that time these techniques were used almost exclusively in the course of development by designers and developers to detect and correct design features causing excessive vibration. The diagnosis of vibration problems in machines depends on good measurements to obtain data from transducers during machine operation as well as diagnostic tests, parameter identification tests, and knowledge of the machine itself. Because the foundation of diagnostics is frequency information, analyzers used to process data must have adequate resolution. Successful implementation of most diagnostic techniques requires familiarity with the frequencies of the components of the machine as well as its dynamic properties. Parameter identification techniques are used to quantify natural frequencies, mode shapes, damping, stability and frequency-response characteristics. Time-domain analysis – the study of signatures directly from a transducer – and orbital analysis are used to diagnose faults when motions of a machine or a rotor provide direct information about dynamic behavior. Modern diagnostic techniques and the identification of specific malfunctions of rotating machines and their components are described in this section. (Eshleman, R. and Jackson, C. P. E., 1992)

### **2.2 Measurement Procedures and Locations**

The procedure used to achieve data for fault diagnosis depends on the equipment type and, to some extent, the nature of the problem. Data from the machine during operation are essential. The distance travelled by a vibration signal from its source to a transducer should be as short as possible to avoid signal amplification or attenuation, introduction of excessive noise, and waveform distortion. Diagnosis of vibration in a structure requires information about panels, structural supports, pedestals, and foundations during operation. Identification of faults that require phase data, e.g. misalignment, is dependent on the simultaneous recording or analysis of data from two sensors.

### **2.3 Diagnostic Techniques**

The techniques used to diagnose machinery listed in table 4 depend on processed and unprocessed vibration signals. These signals are examined principally for frequency information that can be related to a machine fault.

#### **2.3.1 Time-Domain or Waveform Analysis**

The time domain contains information about the physical behavior of a machine but is limited to viewing a single plane of motion and by the fact that it can be too complex for analysis if excessive noise, signal modification, or several frequencies are present; in such cases processing is necessary.

Technique	Use	Description	Instrument type
Time-domain analysis	modulation, pulses, phase, truncation, glitch	amplitude $\times$ time	analog oscilloscope digital oscilloscope FFT spectrum analyzer
Orbital Analysis	shaft motion, sub-synchronous, whirl	relative displacement of rotor bearing in XY direction	digital vector filter, oscilloscope
Spectrum analysis	direct frequencies, natural frequencies, sidebands, beats, sub-harmonics, sum and difference freq.	amplitude $\times$ frequency	FFT spectrum analyzer
Cepstrum analysis	Sideband and harmonic frequency measurement; accurate quantification of sideband and harmonic severity	inverse Fourier transform of the logarithmic power spectrum	FFT spectrum analyzer

Table 4: Diagnostic Techniques for Rotating Machinery (Eshleman, R. and Jackson, C. P. E., 1992)

### 2.3.2 Orbital Analysis

The x and y motions of the rotor with respect to a sensor mounted in the journal bearing are simultaneously displayed on the horizontal and vertical axes of an oscilloscope. The information about rotor motion provided by an orbit is similar to that obtained from a time domain. Both indicate rotor performance directly. The orbit can be used to assess oil whirl and other asynchronous motion as well as synchronous phenomena such as mass unbalance and misalignment. Orbital misalignment, both of which cause once-per-revolution forces. Note the elliptical shape of the orbit from mass unbalance as opposed to the flat and double-looped shape of the orbit from misalignment.

For synchronous rotor whirling in a symmetric bearing or casing or foundation machine that is generated by unbalance or misalignment, the orbit will be a circle with a single once-per-revolution time marker. The radius of the circle increases with speed to a maximum value at the first critical speed and then declines and increases again as successive critical speeds are passed. For an asymmetric machine (i.e., in which the natural frequency of the system on one principal axis is dissimilar to the natural frequency of the system on the orthogonal principal axis) the orbit will be an elongated ellipse as it passes through each natural frequency. The major axis of the ellipse will be along the principal axis associated with the critical natural frequency being encountered. It is possible to encounter backward synchronous whirl in the speed region between the pair of critical speeds.

Most asynchronous phenomena occur at a speed above the critical speed and result in whirling at the critical frequency. The whirl speed is then a fraction (less than 1) of the rotor speed. The whirling motion may be in the same direction as rotation, i.e., forward whirl, as is encountered in oil whip, hysteretic whirl, and whirl caused by fluid trapped in the rotor. Backward whirl caused by a dry friction rub between rotating and static parts occurs less frequently. In most real

situations the asynchronous whirling motion is accompanied by synchronous whirling associated with residual unbalance or misalignment. The orbit of such motion is a more complex pattern.

Some instances of asynchronous whirl occur at a nonrational fraction of rotation speed, so that the orbit is not a simple closed regular pattern, as for example a typical orbit for oil whip, in which the whirl direction is forward and whirl speed is less than one-half the speed (0.47 for example).

Orbital analysis in combination with dc gap measurement is perhaps the best way to distinguish between mass unbalance and misalignment. Note the elliptical shape for mass unbalance and misalignment in its early stages. After more severe misalignment occurs, the bearing restrains the rotor so that it cannot make a complete elliptical orbit. The generated orbit can have a bean form or a 8-form, providing a 2X vibration component in the spectrum.

### **2.3.3 Spectrum Analysis**

A spectrum analysis is conducted with an FFT algorithm or filters; the processed signal is an amplitude-versus-frequency display. Frequencies of vibration response can be related to direct excitation frequencies or their orders, natural frequencies, sidebands, sub-harmonics, and sum and difference frequencies. Frequencies can be identified directly in a linear system because the frequencies of the measured vibration response are equal to those of the forces causing the vibration.

Vibration at frequencies that are orders of the operating speed is an example typically resulting from truncation of the signal. Truncation can be attributed either to nonlinear behavior of the machine or to modification of the signal at interfaces (bolted joints) within the machine during transmission from the source to the measurement point. Amplification can occur if a natural frequency happens to be located at an order frequency. Orders can also result from shaft asymmetry and at universal joints and couplings when forces are generated that are exact multiples of the shaft speed.

Relative amplitudes of orders are important in the diagnostic process. The shape of the spectrum is different from displacement, velocity and acceleration. Low frequencies are emphasized when displacement is measured. High frequencies are emphasized in an acceleration spectrum.

Sub-harmonic excitations are vibration components that occur at exactly one-fourth, one-third, and one-half the operating speed. They result from forced vibration of a nonlinear system, e.g., fans mounted on nonlinear springs, rotors on nonlinear pedestals, rolling-element bearings, loose supports, or base-plates. If the natural frequency of a system coincides with a subharmonic excitation, subharmonic resonance occurs.

Beats are caused by a period pulsation of vibration amplitude resulting from the addition and subtraction of two signals with excitation frequencies close to each other. If the amplitudes of the two signals are equal, pure amplitude modulation occurs. If the components of vibration are not equal, both frequency and amplitude modulation occur simultaneously. Beat problems can be identified in either the time domain or the frequency domain. The length of the period of the beat is inversely related to the closeness of the frequencies of the components; i.e., the closer the frequencies, the longer the period.

### 2.3.4 Cepstrum Analysis

The cepstrum is defined as the inverse Fourier transform of the logarithmic power spectrum commonly used in vibration analysis. The complex cepstrum is reversible to a time signal. A cepstrum domain consists of data processed one step further than the frequency domain. A cepstrum is effective for accurately measuring frequency spacing – harmonic and sideband patterns – in the power spectrum. One component of a cepstrum represents the global power content of an entire family of harmonics or sidebands. The severity of a defect such as that in a rolling-element bearing is provided by one component of the cepstrum display. In the power spectrum, the severity is represented by a number of harmonics or sidebands for which the total power is not easily obtained.

## 2.4 Theoretical and Experimental Example

The goal of this study is to show some experimental examples to facilitate the understanding of the physical meaning of the main topics and definitions used when one speaks about diagnosis of rotating machinery malfunctions. Experimental studies are led step-by-step, clarifying the definitions of natural frequency, damping factor, logarithmic decrement, resonance, unbalance response, critical speeds, forwards and backward orbits, super-harmonic components etc.

### 2.4.1 Description of the Test Facilities

Figures 43 and 44 show the simple elements used during the experimental investigations: a flexible rotor with concentrated masses and inertias (discs) attached to a foundation and driven by an electric motor. Displacement sensors, signal amplifiers and a signal analyzer with 4 channels are used to demonstrate the different phenomena mentioned above.

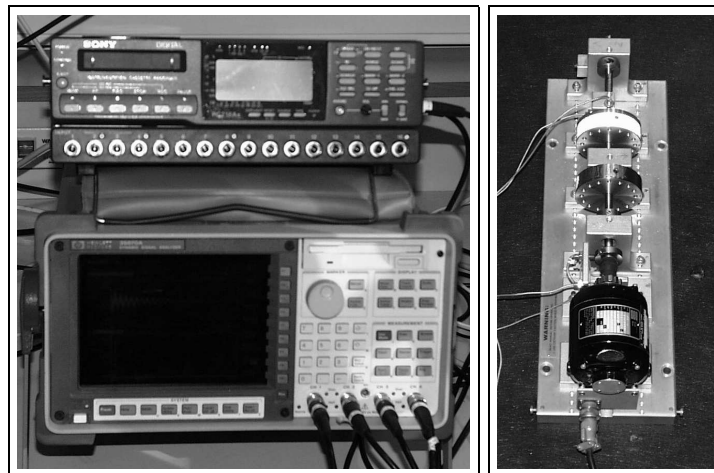


Figure 43: *Signal analyzer and rotor kit (flexible shaft, two rigid discs, two ball bearings, electrical motor and displacement probes).*

### 2.4.2 Mechanical Model of the Rotor Test Rig

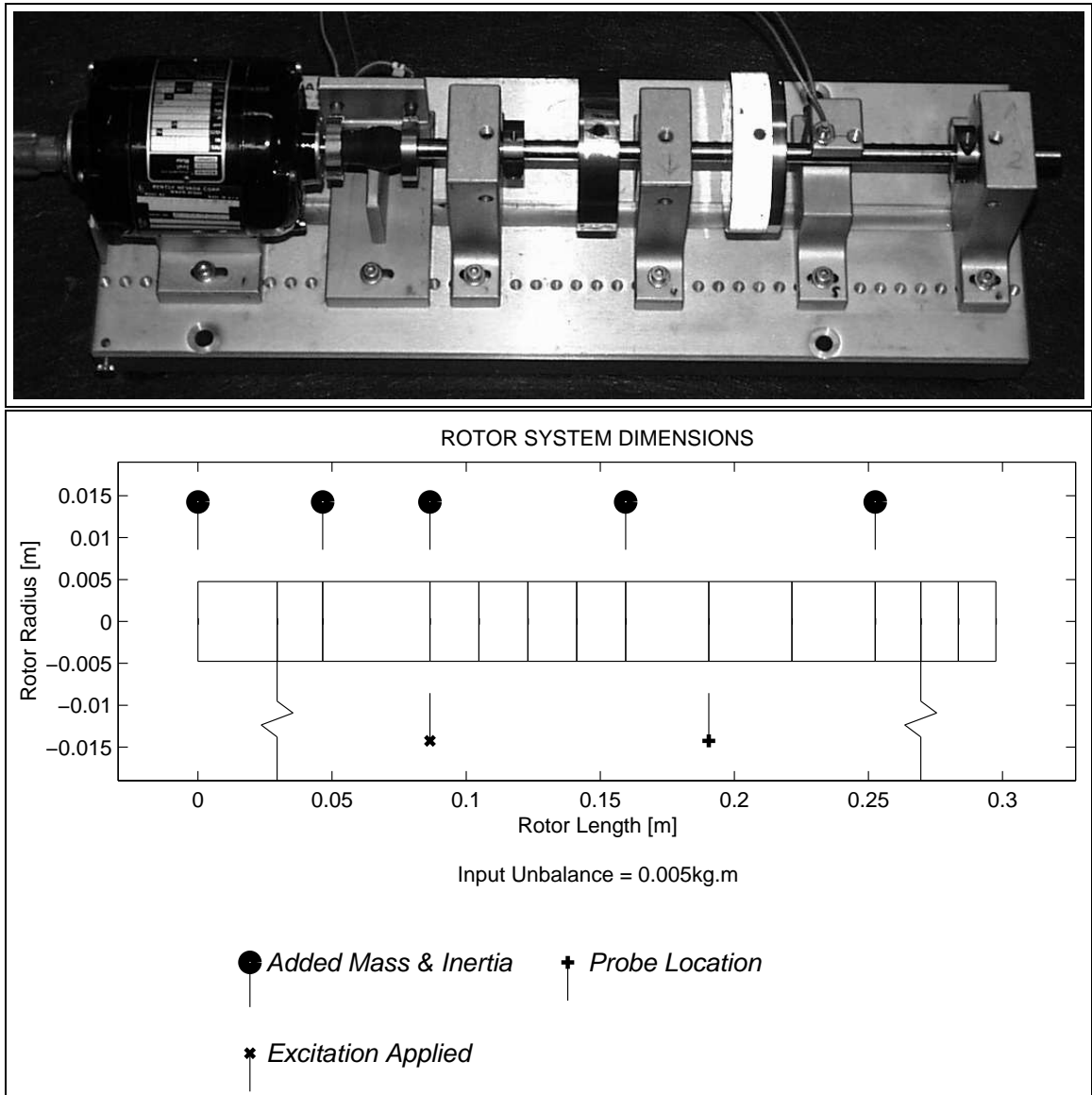


Figure 44: (a) Rotor Kit ((flexible shaft, two rigid discs, two ball bearings, electrical motor and displacement probes)used for visualization of natural frequencies in orthogonal directions, damping factor and logarithmic decrement (log dec), resonances, phase, beating, unbalance, critical speeds, forwards and backward motions; (b) Discrete Mechanical Model of the Rotor Test Rig, built by flexible shaft elements, rigid disks and flexible bearings.

### 2.4.3 Theoretical Natural Frequencies and Mode Shapes

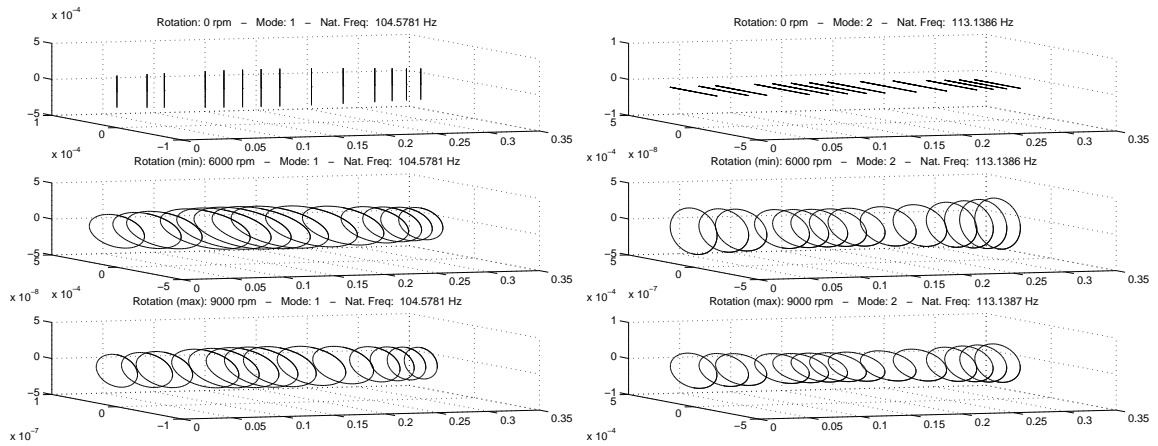


Figure 45: *First and Second Mode Shapes of the Rotor Rig – Vertical Direction (theoretical natural frequencies: 104 Hz and 113 Hz.)*

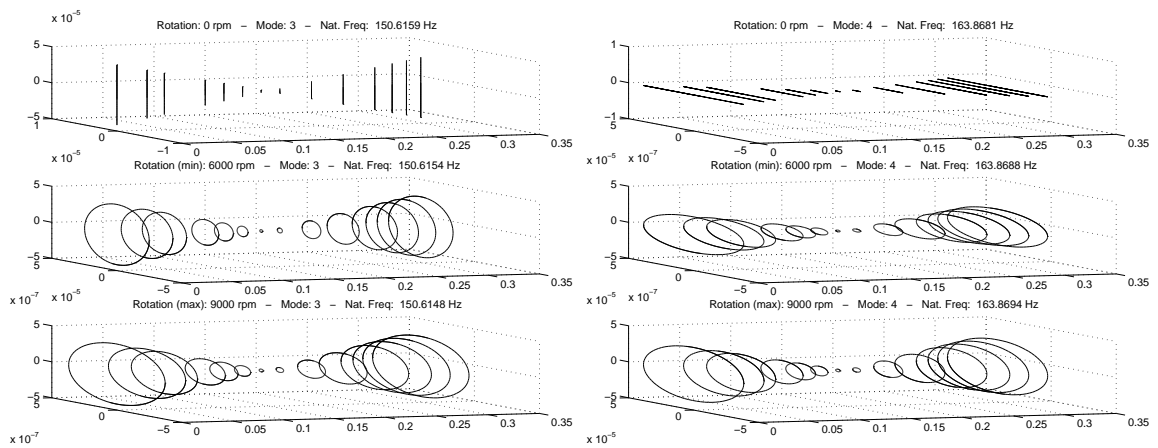


Figure 46: *Third and Fourth Mode Shapes of the Rotor Rig – Vertical Direction (theoretical natural frequencies: 150 Hz and 163 Hz.)*

## 2.4.4 Experimental Natural Frequencies of the Rotating Components

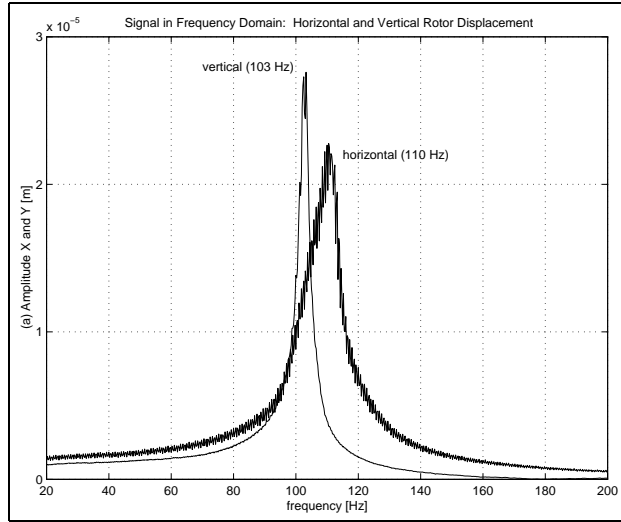


Figure 47: Natural frequencies of the flexible rotor in orthogonal directions eliminating the dynamical behavior of the foundation.

## 2.4.5 Measuring the Damping Factor ( $\xi$ ) and the Log Dec ( $\beta$ ) of the Rotor Kit.

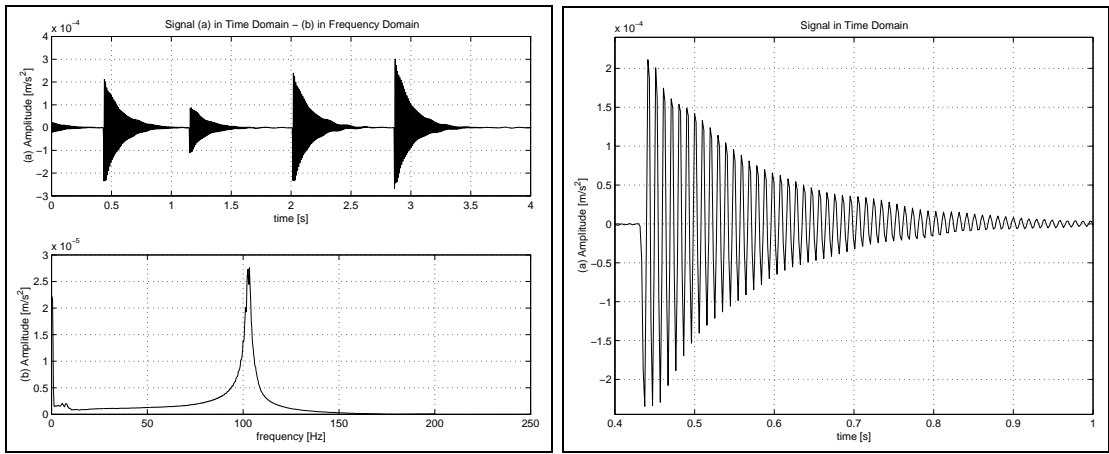


Figure 48: (I) Rotor displacement signal in vertical direction in (a) time and (b) frequency domains, while excited by a sequence of impulses; (II) Rotor displacement signal in vertical direction, plotted in a range of time of 0.4 to 1 second, while the rotor is excited by an impulse. Signal used for calculating the damping factor of the rotor kit.

- Damping Factor ( $\xi$ )

$$\xi = \frac{\frac{1}{2\pi 17} \ln \left( \frac{2.0 \cdot 10^{-4}}{0.5 \cdot 10^{-4}} \right)}{\sqrt{1 + \left[ \frac{1}{2\pi 17} \ln \left( \frac{2.0 \cdot 10^{-4}}{0.5 \cdot 10^{-4}} \right) \right]^2}} = \frac{0.012978}{1.000168} = 0.013$$



## 2.4.6 Experimental Natural Frequencies taking into account the Foundation

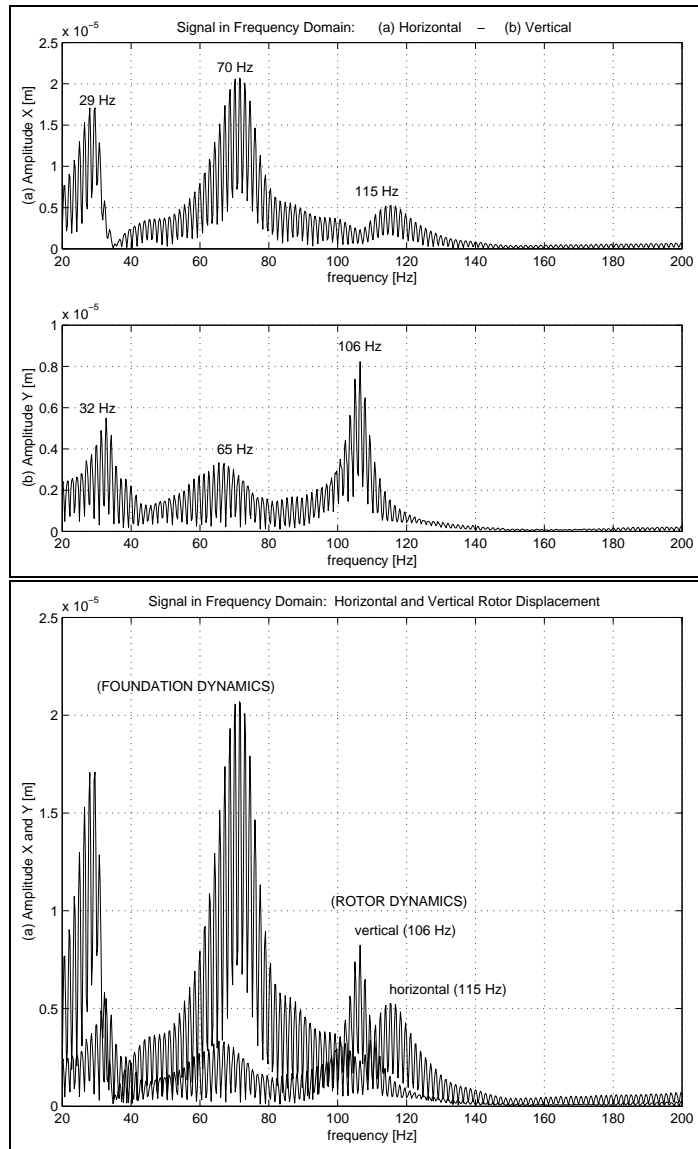


Figure 49: *Natural frequencies of the flexible rotor in orthogonal directions taking into account the dynamical behavior of the foundation.*

## 2.4.7 Experimental Forward and Backward Orbits

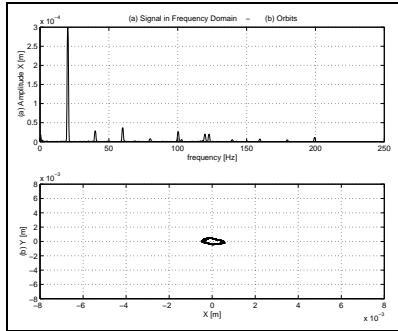


Figure 50: (a) FFT of the displacement signal mounted in the horizontal direction and (b) Orbits described by the rotor at the speed of 20 Hz.

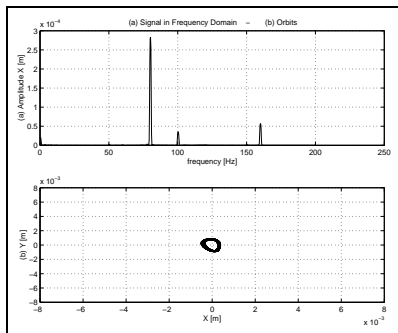


Figure 51: (a) FFT of the displacement signal mounted in the horizontal direction and (b) Orbits described by the rotor at the speed of 80 Hz.

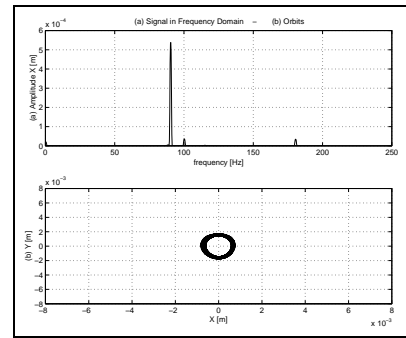


Figure 52: (a) FFT of the displacement signal mounted in the horizontal direction and (b) Orbits described by the rotor at the speed of 90 Hz.

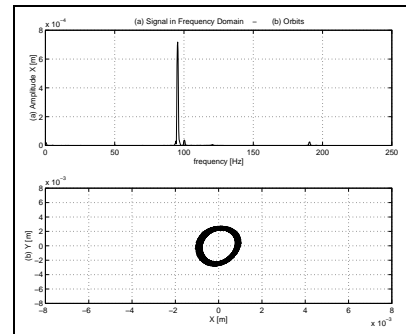


Figure 53: (a) FFT of the displacement signal mounted in the horizontal direction and (b) Orbits described by the rotor at the speed of 95 Hz.

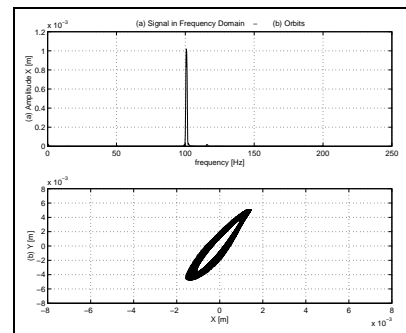


Figure 54: (a) FFT of the displacement signal mounted in the horizontal direction and (b) Orbits described by the rotor at the speed of 100 Hz.

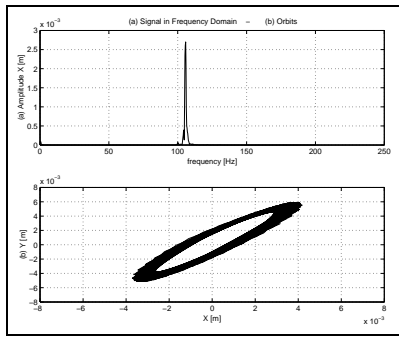


Figure 55: (a) FFT of the displacement signal mounted in the horizontal direction and (b) Orbits described by the rotor at the speed of 105 Hz.

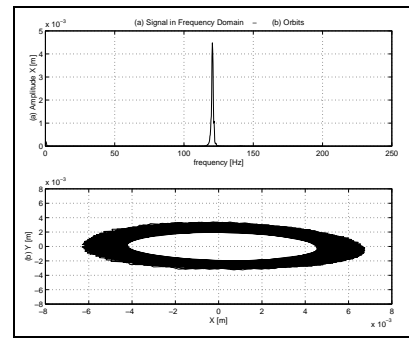


Figure 58: (a) FFT of the displacement signal mounted in the horizontal direction and (b) Orbits described by the rotor at the speed of 120 Hz.

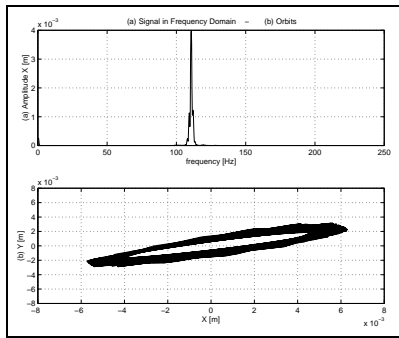


Figure 56: (a) FFT of the displacement signal mounted in the horizontal direction and (b) Orbits described by the rotor at the speed of 110 Hz.

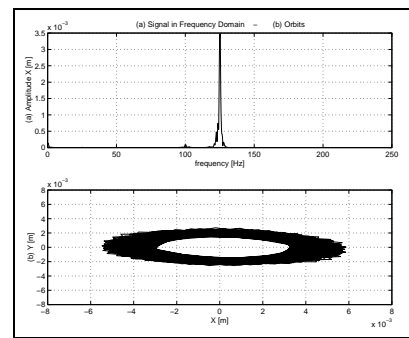


Figure 59: (a) FFT of the displacement signal mounted in the horizontal direction and (b) Orbits described by the rotor at the speed of 125 Hz.

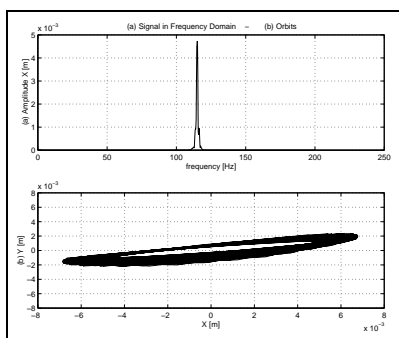


Figure 57: (a) FFT of the displacement signal mounted in the horizontal direction and (b) Orbits described by the rotor at the speed of 115 Hz.

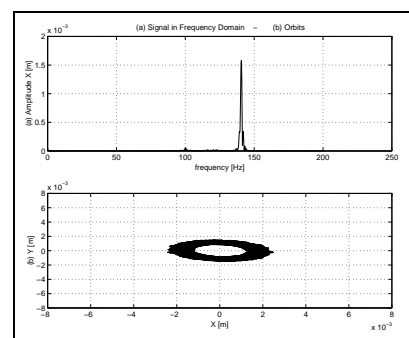


Figure 60: (a) FFT of the displacement signal mounted in the horizontal direction and (b) Orbits described by the rotor at the speed of 140 Hz.

### 2.4.8 Detecting Experimentally Super-Harmonic Vibrations

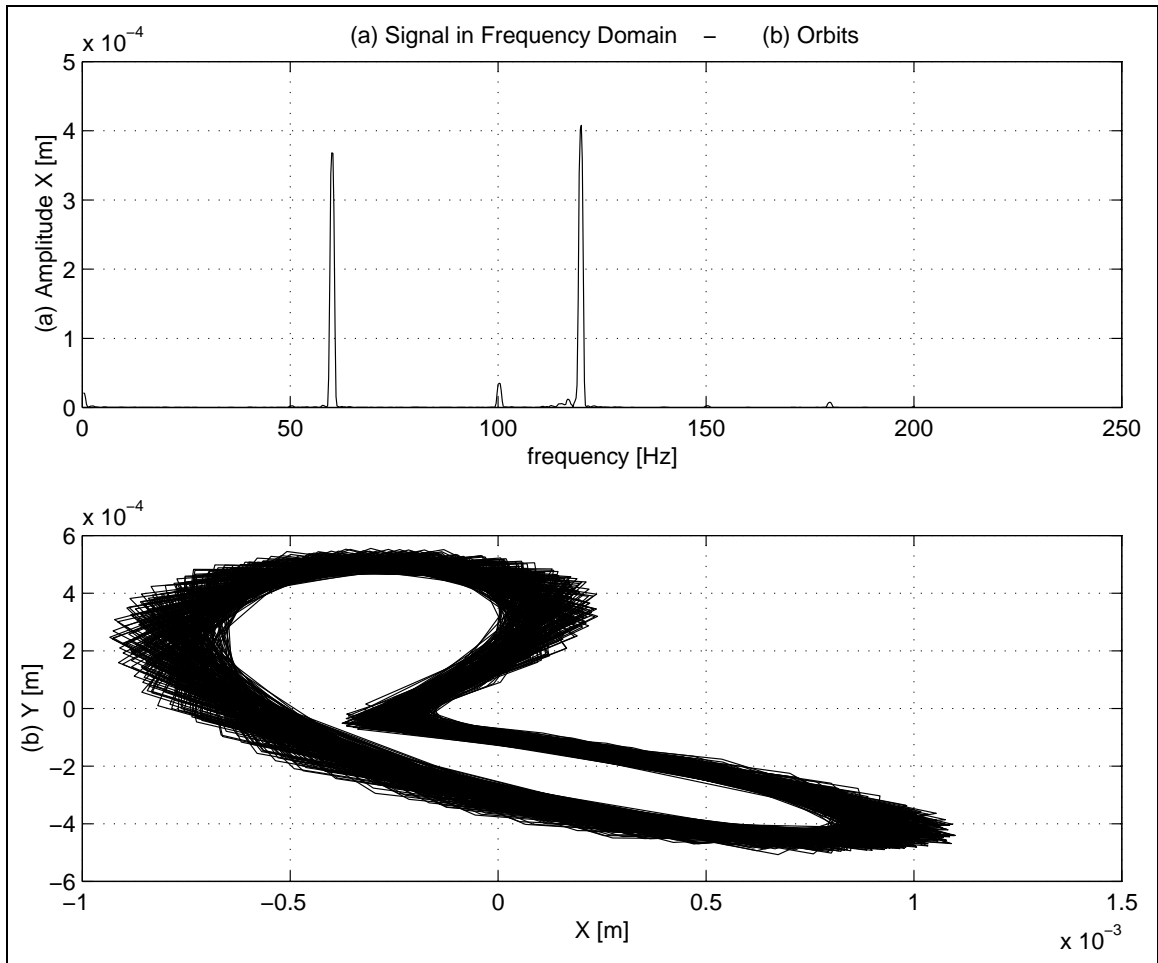


Figure 61: (a) *FFT of the displacement signal mounted in the horizontal direction and (b) Orbits described by the rotor at the speed of 60 Hz, exciting the super harmonic of 120 Hz (close to the shaft natural frequency).*

## 2.5 Identification of Malfunctions

The ease with which a fault can be identified from good test data is directly proportional to the information available on the design of a machine and its working mechanisms. This is especially true when similar frequencies are obtained for different faults, e.g., mass unbalance and misalignment. The operating speed is usually the reference frequency for diagnostic techniques. Other frequencies are either related to the operating speed or shown to be unrelated.

Fault	Frequency	Spectrum, time domain, orbit shape	Correction
Mass unbalance	1X	distinct 1X with much lower values of 2X, 3X etc., elliptical and circular orbits	field or shop balancing
Misalignment	1X, 2X, etc.	distinct 1x with equal or higher values of 2X, 3X, etc., figure 8-orbit	perform hot and/or cold alignment
Shaft bow	1X	dropout of vibration around critical speed in Bode plot	Heating or peening to straighten rotor
Steam loading	1X	load-sensitivity	modify admission sequence; repair diaphragms; install nozzle blocks properly
Bearing wear	1X, sub-harmonics, orders	high 1X and 0.5X, sometimes 1.5X or orders; can not be balanced	replace bearing
Gravity excitation	2X	0.5 critical speed appears on Bode plot (unfiltered)	reduce eccentricity by balancing
Asymmetric rotor	2X	0.5 critical speed appears on Bode plot (unfiltered)	eliminate asymmetry
Cracked rotor	1X, 2X	high 1X, 0.5 critical speed may show up on coast-down	remove rotor
Looseness	1X plus large number of orders, 0.5X may show up	high 1X with lower-level orders, large 0.5 order	shim and tighten bolts to obtain rigidity
Coupling lockup	1X, 2X, 3X, etc.	1X with high 2X similar to misalignment; start and stops may yield different vibration patterns	replace coupling or remove sludge
Thermal instability	1X	1X has varying phase angle and amplitude	compromise balance or remove problem
Oil whirl	0.35X to 0.47X	sub-synchronous component less than 0.5 order informal loop in orbit	temporary: load bearing heavier, correct misalignment; long term: change bearing type
Sub-harmonic resonance	1/2X, 1/3X, 1/4X, and higher	sub-synchronous vibration depending on natural frequency	remove looseness, excessive flexibility; change natural frequency so it does not match fractional frequencies
Rubs	1/4X, 1/3X, 1/2X or orders	external loops in orbits	eliminate condition such as thermal bow and mass unbalance that causes rub

## 2.6 Condition Monitoring – Steam Turbines<sup>1</sup>

Condition monitoring for machine protection and condition analysis has been available for more than 30 years. With the increasing use of digital electronic data collectors and processors, predictive maintenance programs based on periodic monitoring of machine vibrations become cost-effective and practical in most operational installations. Condition monitoring of critical equipment requires hard-wired permanently mounted sensors. They protect the equipment from unexpected sudden failure and provide the capability for condition analysis and diagnosis. The expense of continuous monitors is often more than justified by avoidance of repair costs and loss of production after failures. It is a fact that unexpected failures are much more serious and costly than parts replacement on a scheduled basis as a result of condition monitoring.

The primary goal of a good predictive maintenance program is efficient establishment of the mechanical condition of a machine so that decisions about repairs can be made. The electronic data collector has become the cornerstone of efficient data acquisition.

The objective of any condition monitoring program is to maintain or increase the availability of production equipment and avoid costs of failures. The cost of instrumentation and personnel involved in such a program must be justified by savings in machinery repair costs and decreases in lost production time. Savings must be documented so that management is aware that the investment has been worthwhile. The return on investment in protective monitoring is significant.

Management must establish an operational philosophy and be willing to make a commitment in test equipment and personnel that allows for development and operation of a program. Moreover, after a program has proved successful, commitment to it must continue or the program will falter. Those responsible for condition monitoring programs must thus continuously document savings and returns on money invested.

The development of a condition monitoring program requires careful planning. Criteria and goals must be established for the program. Criticality of equipment must be established, and equipment ranked accordingly. The ranking will determine the resources, e.g., work force and instrumentation, that can be devoted to any one machine. Critical equipment for which no backup exists, such as large turbines, should be monitored continuously; two levels of alarms – alert and shutdown – should be used.

Critical equipment and those items for which no spares are available such as turbine generators, turbine compressors, and mechanical drive turbines and motors must be permanently monitored. Good monitoring design involves good sensor locations and access for predictive monitoring or troubleshooting.

Steam turbines should have dual thrust probes at the axial position of the rotor mounted close to the thrust bearing. The probe should monitor an integral part of the rotor – usually the shaft end or a fixed collar close to the shaft end. The probes should be in a dual voting logic; 15-mil movement in either the active thrust direction (toward the exhaust) or the inactive direction (toward nozzles) should activate the warning alarm. An increase in movement to 25 mils should activate the shutdown alarm. The limits should be recorded on a data-managing system. Movement is measured from a reference such as the rotor reference mark, active-to-inactive thrust float at the bearings – usually 12 to 14 mils – or the setup positions or the first commissioning load position.

A position reference is necessary for the steam inlet and exhaust valves. It can be the cam lift, bar lift, or a controlled stroke. A local indicator can be used, or the position can be transmitted

to the control room or be part of the electro-hydraulic feedback signal in the speed-control scheme.

Dual-tip RTD or thermocouple sensors should be placed in the backing metal of the bearings but no in contact with the babbitt, in accordance with the API 670. Fifty percent of the active self-leveling articulating thrust pads should be monitored. A minimum of two probes (top and bottom) should be used; three probes 120° apart are preferred. The maximum number is four probes 90° apart.

Two proximity probes should be placed in each bearing region to sense shaft-related vibration. The probes should be 90° apart, straddle the vertical centerline of the rotor or bearing, and be held in retractable non-resonant probe holders.

Many utilities used the dual-probe assembly for large steam turbine-generator trains and gas turbine-generation drives. Two probes are involved, and three measurements are taken. The assembly is usually mounted to the structure – typically the bearing housing. One probe senses shaft motion relative to the bearing. The second probe is seismically mounted to detect the absolute bearing vibration relative to space. The absolute vibration can be determined by vector addition of the measurements.

A probe can be installed in the axial position at the exhaust end of a rotor to measure growth with temperature. The transient increase in heat in the rotor or casing can thus be monitored. Two additional sensors can be installed to measure bearing pedestal. The movement can exceed 0.5 in and requires a long-range sensor, vernier scales, or a linear variable differential transformer (LVDT) or its equivalent mounted on each side of the high-pressure pedestal.

It is also wise to record the first-stage pressure of the steam turbine relative to total steam flow or load on a condensing turbine. The pressure is a good indicator of blade fouling due to deposits of salt or silica. These data in combination with the positions of the steam inlet valves, thrust movement of the rotor, and temperatures of the thrust bearings in the active thrust bearing pads can be used to confirm that a turbine is dirty and that thrust overload exists.

1. Ehrich, F. F. (1992) "Handbook of Rotordynamics", Chapter 4, McGraw-Hill, Inc., New York. (in English)

## 2.7 Research & Development – Bearings with Electronic Oil Injection

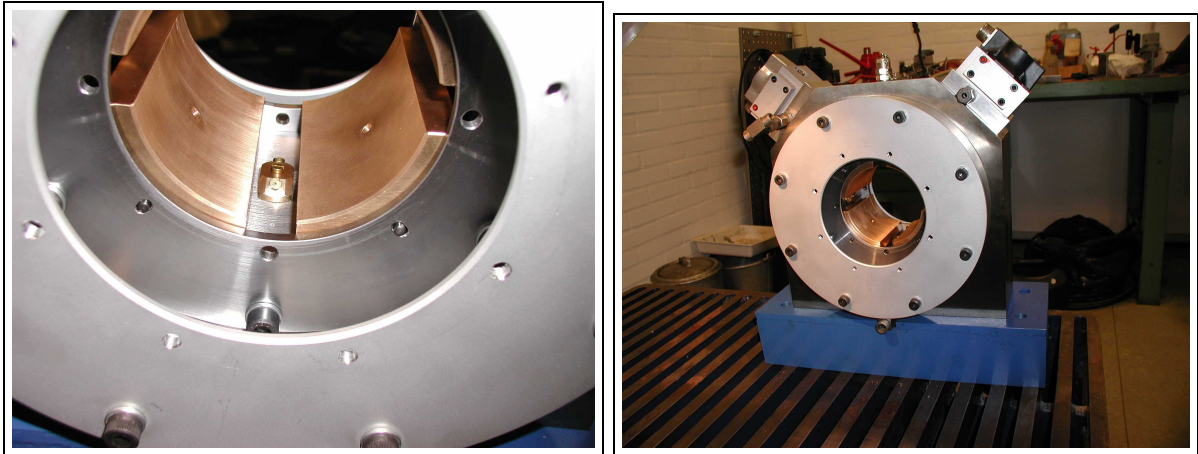


Figure 62: *New Test Rig built at MEK-DTU with financial support of Myhrwolds Foundation – Interior of the active lubricated tilting-pad bearing illustrating the orifice machined on the pad surface (active lubrication) and the conventional lubrication between pads (hydrodynamic lubrication).*

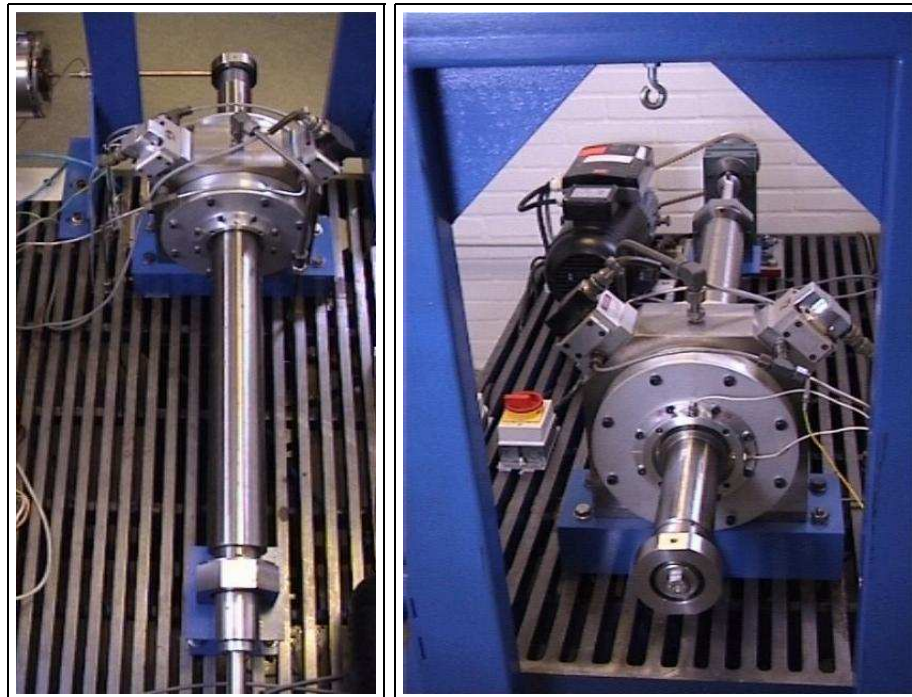


Figure 63: *Lateral dynamics and tests of a rotor-journal bearing – Electromagnetic shaker attached to the shaft extremity, journal bearing, displacement sensors mounted in orthogonal directions (horizontal and vertical) and motor connected to the shaft by belt.*